VIBRATIONAL MANY-BODY METHODS FOR MOLECULES AND EXTENDED SYSTEMS

BY

MURAT KEÇELI

DISSERTATION

Submitted in partial fulfillment of the requirements
for the degree of Doctor of Philosophy in Chemical Physics
in the Graduate College of the
University of Illinois at Urbana-Champaign, 2012

Urbana, Illinois

Doctoral Committee:

Professor So Hirata, Chair
Professor Alexander Scheeline
Professor Benjamin J. McCall
Professor Gregory S. Girolami

Abstract

Vibrational many-body methods for molecules and extended systems have been developed that can account for the effects of anharmonicity in the potential energy surfaces (PESs) on energies and other observable properties. For molecules, we present a general scheme to calculate anharmonic vibrational frequencies and vibrationally-averaged structures along with applications to some key species in hydrocarbon combustion chemistry: HCO^+, HCO, HNO, HOO, HOO^-, CH_3^+, and CH_3. We propose a hybrid, compact representation of PESs that combines the merits of two existing representations, which are a quartic force field (QFF) and numerical values on a rectilinear grid. We employed a combination of coupled-cluster singles and doubles (CCSD), CCSD with a second-order perturbation correction in the space of triples [CCSD(2)$_T$] and in the space of triples and quadruples [CCSD(2)$_{TQ}$], and a correlation-consistent basis set series to achieve the complete-correlation, complete-basis-set limits of the potential energy surfaces. The mean absolute deviation between the predicted and the observed frequencies is 11 cm^{-1}.

For extended systems, we generalized the formulations of the vibrational self-consistent field (VSCF), vibrational Møller–Plesset perturbation (VMP), and vibrational coupled-cluster (VCC) methods on the basis of a QFF in normal coordinates. We have identified algebraically and eliminated several terms in the formalisms of VSCF that have nonphysical size dependence, leading to compact and strictly size-extensive equations. This size-extensive VSCF method (XVSCF) thus defined has no contributions from cubic force constants and alters only the transition energies of the underlying harmonic-oscillator reference from a subset of quartic force constants. The mean-field potential of XVSCF felt by each mode is shown to be effectively harmonic, making the XVSCF equations subject to a self-consistent analytical solution without a basis-set expansion and matrix diagonalization, which are necessary in VSCF. We implemented the XVSCF method for finite systems, and applied it to polyacenes up to tetracene as well as to a model system of a linear chain of masses interacting through a quartic force field. We showed that the results of XVSCF and VSCF approach each other as the size of the system is increased, implicating the inclusion of unnecessary, nonphysical terms in VSCF. We have also shown that apart from reducing the scaling of the VSCF calculation from quartic to quadratic, XVSCF is nearly three orders of magnitude faster than VSCF implemented with a reduced set of force constants. The second-order VMP and VCC methods based on the XVSCF reference are shown to account for anharmonic effects due to all cubic and quartic force constants in a size-extensive fashion.

We also presented the Γ approximation for extended systems, which amounts to including only in-phase phonons throughout the generation of PES and solution of the vibrational Schrödinger equation. We computed the frequencies of the infrared- and/or Raman-active vibrations of polyethylene and polyacetylene using this approximation and we have shown that accounting for both electron correlation and anharmonicity is essential in achieving good agreement between computed and observed frequencies.

To Sevnur and my family.

Acknowledgments

First of all, I would like to gratefully acknowledge my advisor, So Hirata, without whom this thesis would certainly not be possible. I cannot thank him enough for his support and patience especially in the last two years. Apart from his scientific excellence, his kindness and thoughtfulness made me always feel very lucky to be in his group.

I am indebted to Kiyoshi Yagi who was the unseen co-advisor of this thesis on the other side of the world. I was also lucky that he decided to come to our side last year and taught me more on vibrational methods. He has the wisdom of explaining even the hardest concepts in a very neat and elegant fashion.

I would like to also thank Ben McCall and the S5 group members for including me in the most enjoyable and enlightening meetings. I learned from them a lot on the theory of spectroscopy, though, I guess it was not the initial idea of these meetings.

I am grateful to Gregory Girolami for being a member of my committee.

My special thanks go to Alexander Scheeline who agreed to be in my committee on a short notice.

I am thankful to Nancy Makri for the great meeting in Berkeley, and for letting me audit her class. I was always trying to learn more on dynamics and I think I could not be in a better place.

I would like to acknowledge professors Hai-Ping Cheng, Rod Bartlett, Adrian Roitberg, Nick Polfer, David Reitze and Yoonseok Lee for their help and support at the University of Florida.

I would like to thank all current and past members of the Hirata group. I will always be indebted to Olaseni Sode who was always there when I needed help. I cannot imagine our group without him. I would like to thank Toru Shiozaki from whom I have learned a lot and always enjoyed his friendship. I am also thankful to Yu-ya Ohnishi and Muneaki Kamiya. They were always very helpful and friendly. I would like to thank recent members of our group, Matt Hermes, Xiao He, and Kandis Abdul-Aziz for their valuable comments at the group meetings. When Matt joined the group, I was supposed to teach him on what I have been doing, he quickly came to a level such that I started to learn from him.

I am grateful to the late İhsan Doğramacı, the founder of Bilkent University where I got my BS and MS degrees. I am also thankful to many professors in Bilkent University, especially: Igor Kulik, Mehmet Özgür Oktel, Bilal Tanatar, Fatih Ömer İlday, and Azer Kerimov.

I would like to also acknowledge my teachers in my early education whom I owe much: Zeynep Keçeli, Fazilet Özkara, Kenan Kavak, Mustafa Kıymaç, Gülfidan Tece, Aynur Köksal, Müjgan Arslan, and Emel Albayram.

Finally, I would like to thank my family for their endless support. My wife, Sevnur, probably suffered most during my studies. It is very hard to express my gratefulness to her, for her love and patience.

I would like to also leave a note here for my niece, Demir, and my daughter, Asya, who joined our life recently. You brought the sunlight to us, I hope we can prepare a brighter future for you.

Table of Contents

Chapter 1

Introduction

Vibrational spectroscopy is one of the primary experimental sources for information on the composition and the structural and dynamical properties of molecular and condensed phase systems. Understanding the spectrum using some approximate physical models and assigning the vibrational band-origins to specific vibrational modes predicted by these models is a task in theoretical chemistry.[1] Predictive theoretical simulations based purely on ab initio methods became possible in the past 20 years. This owes much to the development of predictive electronic structure methods[2] which can be used to produce potential energy surfaces (PESs), without any empirical models. These PESs become a part of the equation of motion of nuclei within the Born-Oppenheimer framework.[3]

Wave function based ab initio methods for electronic structure calculations have come to a level that chemical accuracy (1 kcal/mol) can be attained for total electronic energies of small molecules composed of main group elements.[4,5] Even higher accuracy can be expected for properties that depend on relative energies like vibrational transition energies. With such high accuracy in electronic energies, the usual harmonic treatment of vibrations became inadequate and wave function based ab initio methods for vibrations that can account for anharmonic effects must be developed and applied.[6–9] Apart from quantitative failure, the harmonic approximation cannot explain bond dissociation, intensity borrowing, Fermi resonance[10] and vibrationally averaged properties including thermal expansion of solids.[11]

The overarching goal of this thesis is to develop a predictive computational capability to perform vibrational analyses for molecules and extended systems. Our analyses consist in (1) the converging electronic structure methods that generate accurate potential energy surfaces, (2) the compact and systematic representations of the PESs, and (3) the hierarchical vibrational many-body methods that can include the effects of anharmonicity on energies and other observable properties to any desired extent.

Step (1) is further divided into three parts. The first one is to find the equilibrium geometry, and then the second is to perform a normal mode analysis to generate the normal coordinates and harmonic frequencies. The third part is to run the electronic energy calculations to generate the PES expressed in a mathematical form which depends on the choice in step (2).

For the PES representation, step (2), the common choice is to either use a Taylor expansion or tabulated values

of energies on a grid. Both have certain advantages and disadvantages that are discussed in Section 1.5.2 and 1.5.3. We also propose a new, compact representation of PESs (Section 2.2.2) that combines the merits of two existing representations, while minimizing their shortcomings.

For step (3), the vibrational self-consistent field (VSCF),[12] second-order Møller–Plesset perturbation (VMP),,[13] configuration-interaction (VCI)[14] and coupled-cluster (VCC)[15] methods have been developed in complete analogy to the corresponding methods for electronic structures. Just as electronic counterparts, these systematic methods can in principle solve the vibrational Schrödinger equation of a given PES essentially exactly if the rank of these methods is raised to a sufficiently high level.

1.1 Outline

We propose our predictive scheme for gas phase molecules, and introduce a new type of PES representation in Chapter 2. Derivations of the size-extensive generalizations of the vibrational many-body methods are given in Chapter 3. It is followed by Chapter 4 where we present the definition and implementation of the size-extensive VSCF (XVSCF) method for finite systems and show applications on a linear atomic chain and a series of polyacenes. In Chapter 5, we introduce the Γ approximation which considers only in-phase vibrations and present applications on polyethylene and polyacetelyne. Finally, we give a brief summary of the thesis in Chapter 6. In the rest of this chapter, we explain the basic concepts and methods that are used throughout the thesis.

1.2 Molecular Hamiltonian

In the non-relativistic regime, the molecular Hamiltonian can be written as:

$$H = -\sum_{I=1}^{N} \frac{1}{2m_I}\nabla_I^2 + \sum_{I=1}^{N}\sum_{J>I}^{N} \frac{Z_I Z_J}{R_{IJ}} - \sum_{i=1}^{n} \frac{1}{2}\nabla_i^2 + \sum_{i=1}^{n}\sum_{j>i}^{n} \frac{1}{r_{ij}} - \sum_{I=1}^{N}\sum_{i=1}^{n} \frac{Z_I}{r_{iI}} \tag{1.1}$$

where N and n refers to total number of nuclei and electrons, respectively, and atomic units are used throughout this thesis. The analytical solutions of the time-independent Schrödinger equation for this Hamiltonian cannot be obtained except for the special case of $N = n = 1$, which corresponds to the hydrogen-like atoms. However, as the system gets larger, even numerical solutions become difficult without using effective approximations.

1.3 Born-Oppenheimer approximation

Within this approximation, one can write the electronic-only Hamiltonian as,

$$H_{\mathrm{e}} = -\sum_{i=1}^{n} \frac{1}{2}\nabla_i^2 + \sum_{i=1}^{n}\sum_{j>i}^{n} \frac{1}{r_{ij}} - \sum_{I=1}^{N}\sum_{i=1}^{n} \frac{Z_I}{r_{iI}} \tag{1.2}$$

where nuclear coordinates are considered as parameters. The eigenvalue E_{e} of this Hamiltonian enters to the nuclear Hamiltonian,

$$H_{\mathrm{N}} = -\sum_{I=1}^{N} \frac{1}{2m_I}\nabla_I^2 + \sum_{I=1}^{N}\sum_{J>I}^{N} \frac{Z_I Z_J}{R_{IJ}} + E_{\mathrm{e}}(R_{\mathrm{N}}). \tag{1.3}$$

Sum of the last two terms is the total energy for fixed nuclei and can be represented by $V(R_{\mathrm{N}})$. The latter is generally referred to as the PES. Once the electronic and nuclear Schrödinger equations are solved, the total wave function can be written as a product of the eigenfunctions of the electronic and nuclear Hamiltonians:

$$\Psi = \Psi_{\mathrm{e}}(r_{\mathrm{e}}; R_{\mathrm{N}})\Psi_{\mathrm{N}}(R_{\mathrm{N}}), \tag{1.4}$$

where Psi_{e} is the electronic wave function, Psi_{N} is the nuclear wave function, and the semicolon separates variables from parameters.

1.4 Vibrational Hamiltonian and normal coordinates

The nuclear problem differs from the electronic one in many ways. One difference is that the nuclear problem is closer to the classical regime, so we can make use of classical mechanics to simplify some aspects of the problem. Another difference is that, indistinguishability of the particles is much less a concern in small-amplitude vibrations and can be relatively easily taken into account in rotations. For vibrational problems we are concerned with, the nuclear Schrödinger equation serves as the sole equation of motion with no constraint imposed on the wave function with respect to particle interchanges.

The nuclear Hamiltonian given in Equation (1.3) is invariant under translation and rotation of the molecule as a rigid body. By using a space-fixed frame where the origin is at the center of mass of the molecule, translational motion can easily be taken out. To separate rotational degrees of freedom, one needs to use a body-fixed frame which rotates with the molecule. This part is the most complicated part in the derivation of the vibrational Hamiltonian[16] for two reasons: there is no unique way of choosing the body-fixed frame, and the kinetic energy term in the vibrational Hamiltonian becomes very complicated. One of the most common choices for the body-fixed frame is the one Eckart suggested[17] which requires minimization of the angular momentum with respect to this frame. Such a choice also

minimizes the coupling between rotation and vibration. It should be noted that there is no possible transformation to completely get rid of this coupling.[18]

We can introduce the normal coordinates using the classical harmonic theory of small vibrations. There exists a set of coordinates, Q_k, that reduces the kinetic and potential energy terms (without anharmonic terms) in this simple form:

$$T = \frac{1}{2}\sum_{k=1}^{3N}\dot{Q}_k^2, \quad V = \frac{1}{2}\sum_{k=1}^{3N}\lambda_k Q_k^2 \tag{1.5}$$

where the potential energy term has no cross term and λ_k are the square of harmonic frequencies. Such coordinates are known as normal coordinates and they can be obtained from the eigenvectors of the Hessian (mass-weighted second-order energy derivatives with respect to nuclear displacements) matrix at the equilibrium geometry of the molecule. They are orthogonal to each other, and each represents simultaneous linear motion of nuclei with the same frequencies and phases, but with different amplitudes. Therefore, these coordinates are non-local and rectilinear. It has been shown that[19] normal coordinates satisfy the Eckart condition and harmonic frequencies corresponding to translational and rotational modes are identically zero. Given the classical form by Wilson and Howard,[20] the derivation of the quantum mechanical Hamiltonian in terms of normal coordinates was first given by Darling and Deninson[21] and later put in simpler forms for nonlinear[22] and linear[23] molecules by Watson.

For nonlinear reference configurations, the vibration-only part of the Watson Hamiltonian in normal coordinates is

$$\hat{H} = -\frac{1}{2}\sum_{i=1}^{M}\frac{\partial^2}{\partial Q_i^2} + V(Q_1,\ldots,Q_M) + \frac{1}{2}\sum_{\alpha\beta}\hat{\pi}_\alpha\mu_{\alpha\beta}\hat{\pi}_\beta - \frac{1}{8}\sum_{\alpha}\mu_{\alpha\alpha}, \tag{1.6}$$

where M is the total vibrational degrees of freedom, and V represents the Born-Oppenheimer PES. The last two terms involve $\mu_{\alpha\beta}$ which is the generalized inverse inertia tensor. The third term represents the Coriolis coupling and contains the so-called *vibrational* angular momenta operator, $\hat{\pi}_\alpha$. These terms cause singularities in the Watson Hamiltonian for linear geometries, thereby greatly complicating a robust computer implementation. In principle, these terms are important only for the molecules that have large rotational constants (small moments of inertia) like the water molecule. Studies on the water molecule[6,24,25] show that although the errors (relative to the full Watson Hamiltonian results) can be severe for high-lying vibrational states, they are only around 10 cm^{-1} for the fundamentals. While an implementation of the Watson Hamiltonian is mandatory to obtain spectroscopic accuracy (<1 cm^{-1}) for light molecules and successful applications for small molecules exist in the literature,[26] we neglect the last two terms in Equation (1.6) which is justifiable for the target accuracy of a few 10 cm^{-1} for general polyatomic molecules. This is consistent with our neglect of core-correlation corrections, relativistic effects, non-Born–Oppenheimer effects, etc. It should be also noted that the effect of these terms decreases as the size of the molecule increases and vanishes

completely for extended systems. The Watson Hamiltonian without the rovibrational coupling terms reads as

$$H = -\frac{1}{2}\sum_{i=1}^{M}\frac{\partial^2}{\partial Q_i^2} + V\left(Q_1, \ldots, Q_M\right). \tag{1.7}$$

This form of the Hamiltonian is valid for both linear and nonlinear molecules without any forms of singularity. All the vibrational calculations presented in this thesis are based on this Hamiltonian.

1.5 Potential energy surface representations

There are two main challenges in finding compact mathematical representations of the Born–Oppenheimer PES in the vibrational Hamiltonian: the presence of higher-order coupling of all the modes (contrary to the electronic Hamiltonian which has only up to two-body interactions) and lack of a closed analytical form (again, contrary to the electronic Hamiltonian where particle-particle interactions are Coulombic).

1.5.1 *n*-Mode representation

The *n*-mode representation (*n*MR) addresses the first issue by using a many-body expansion for the PES. A restricted two-mode representation has been initially proposed by Jung and Gerber[27] and extensively used in many studies. A general solution to this problem has been developed by Carter, Culik, and Bowman,[28] who represent the M-mode PES as a sum of one-, two-, up to n-mode coupling terms. *n*MR-PES is given as,

$$V(Q_1, \ldots, Q_M) = V_{\text{ref}} + \sum_i V_i(Q_i) + \sum_{i<j} V_{ij}(Q_i, Q_j) + \sum_{i<j<k} V_{ijk}(Q_i, Q_j, Q_k) + \ldots \tag{1.8}$$

and truncated after the n-mode coupling term. Such an expansion is exact when all the couplings are included ($n = M$). The crucial point is that each coupling term in the expansion should be zero if any of the coordinates is zero to ensure that there is no over counting of the terms. The advantage of this representation is its rather quick and easily testable convergence. Wu *et al.*[29] demonstrated the convergence of the *n*MR expansion on CH_4 and its isotopomers which have nine-dimensional PESs. All fundamentals are found to be converged within 5 cm^{-1} at 3MR-PESs. The *n*MR expansion also allows for the multi-resolution approach,[30,31] where each term in the expansion can be obtained with different electronic structure methods allowing a considerable saving in computational time without a significant loss of accuracy.

1.5.2 Grid

In the grid representation, the second problem is partially addressed. It discretizes the PES on a grid, such as a rectilinear grid with P points along each normal coordinate.[32,33] This approach would require P^M points to represent a global PES, and due to this exponential scaling, grid based PESs are not practical for large molecules. Grid PESs are thus ideally suited to a combination with the nMR scheme which reduces the scaling to $\binom{M}{n}P^n$.[34–36] The most common choice of grid along each normal coordinate is the one associated with a Gauss-Hermite quadrature that would give very accurate integrations to solve the vibrational Schrödinger equation. Ten points in each normal coordinate has been shown to be sufficient[35] for several low-lying vibrational states of small molecules.

1.5.3 Taylor expansion

An inexpensive alternative to grid based representation is a low-order truncation of the multinomial Taylor expansion of PES around a reference geometry.

$$V = V_{\text{ref}} + \sum_i F_i Q_i + \frac{1}{2}\sum_{i,j} F_{ij} Q_i Q_j + \frac{1}{6}\sum_{i,j,k} F_{ijk} Q_i Q_j Q_k + \frac{1}{24}\sum_{i,j,k,l} F_{ijkl} Q_i Q_j Q_k Q_l + \ldots, \tag{1.9}$$

where the summation indices i, j, k, and l run from 1 through M. The force constants, F, are the derivatives of the PES at some judiciously chosen reference geometry, typically, the equilibrium geometry, with respect to the normal coordinates. The quartic force fields (QFFs), Taylor expansions truncated at the fourth order, are among the most efficient and compact PES representations for low-lying vibrational states. Expanded by normal coordinates around the equilibrium geometry, the gradients (F_i) and the cross terms in the Hessian (F_{ij} with $i \neq j$) vanish. With this assumption and also organizing terms according to the number of different modes involved, we can rewrite Equation (1.9) as

$$\begin{aligned} V = {} & V_{\text{ref}} + \sum_i \left(\frac{1}{2}F_{ii}Q_i^2 + \frac{1}{6}F_{iii}Q_i^3 + \frac{1}{24}F_{iiii}Q_i^4\right) \\ & + \sum_{i,j}\left(\frac{1}{2}F_{iij}Q_i^2 Q_j + \frac{1}{8}F_{iijj}Q_i^2 Q_j^2 + \frac{1}{6}F_{iiij}Q_i^3 Q_j\right) \\ & + \sum_{i,j,k}\left(\frac{1}{6}F_{ijk}Q_i Q_j Q_k + \frac{1}{4}F_{iijk}Q_i^2 Q_j Q_k\right) \\ & + \sum_{i,j,k,l}\frac{1}{24}F_{ijkl}Q_i Q_j Q_k Q_l. \end{aligned} \tag{1.10}$$

Truncation of Equation (1.10) after the second, third, and fourth term amounts to using the nMR approximation with n = 1, 2, and 3, respectively, within the framework of the QFF.

The number of single point energy calculations for a QFF scales as M^4 but that can be reduced to M^n when the nMR approximation is used. Despite its lower cost and analytical expression for the PESs, QFFs cannot describe strong Morse-like anharmonicity and tend to exhibit fortuitous minima in the regions away from the equilibrium geometries.[8,37] Errors (with respect to accurate grid PESs) in the frequencies of stretching modes involving hydrogen motions can be as large as 20 cm^{-1} (see Section 2.2.2) and nonphysical states supported by the fortuitous minima can appear. Another possible source of error in QFFs is the difficulty in evaluating accurately the coefficients of the expansion by numerical (finite-difference) differentiation. Analytical derivatives can improve this accuracy and reduce the number of single point energy calculations considerably.

1.6 Vibrational many-body methods

Once the PES is expressed in an appropriate mathematical function, the remaining task is to solve the vibrational Schrödinger equation for the PES. This is carried out with one or more of the following vibrational many-body methods.

1.6.1 Vibrational self-consistent field theory

In the vibrational self-consistent field (VSCF) method, we seek variationally the best wave function of the Hartree product form for a molecule whose equilibrium structure belong to an Abelian point group,

$$\Phi_{\mathbf{s}}(Q_1,\ldots,Q_M) = \prod_{m=1}^{M} \phi_{s_m}(Q_m), \tag{1.11}$$

where ϕ_{s_m} is a one-mode function (modal) of normal coordinate Q_m and $\mathbf{s}$ is a string of quantum numbers $s_1,\ldots,s_m,\ldots,s_M$ specifying the vibrational state with M modes. We vary modals such that the expectation value of the vibrational Hamiltonian $\hat{H}$ in $\Phi_{\mathbf{s}}$ reaches a minimum with the constraint that each modal remains normalized. This results in a set of coupled one-dimensional eigenvalue equations:

$$\hat{G}_{m,\mathbf{s}}|\phi_{s_m}\rangle = \epsilon_{s_m}|\phi_{s_m}\rangle, \qquad m = 1,\ldots,M, \tag{1.12}$$

where ϵ_{s_m} is the energy of the modal and the mean-field operator $\hat{G}$ has the form,

$$\hat{G}_{m,\mathbf{s}} = \langle\Psi_{m,\mathbf{s}}|\hat{H}|\Psi_{m,\mathbf{s}}\rangle, \tag{1.13}$$

with

$$\Psi_{m,\mathbf{s}} = \prod_{i \neq m} \phi_{s_i}(Q_i). \tag{1.14}$$

By multiplying Equation (1.12) with $\phi^*_{s_i}$ and integrating, one can see that ϵ_{s_m} also gives the total VSCF energy of the state **s**,

$$\epsilon_{s_m} = \langle \Phi_{\mathbf{s}} | \hat{H} | \Phi_{\mathbf{s}} \rangle \equiv E^{\mathrm{VSCF}}_{\mathbf{s}}. \tag{1.15}$$

Since the mean-field operator $\hat{G}_{m,\mathbf{s}}$ for a specific mode requires the knowledge of all the other modals, each equation is coupled to all the others. A standard way to solve this coupled system of equations is the self-consistent iterative procedure that starts with an initial guess of the VSCF wave function and ends when the subsequent iterations yield essentially the same result for the energies and/or the wave functions. One needs to perform an (M–1)-dimensional integration in Equation (1.13), which becomes computationally the most demanding part of the method as the number of modes increases.

Introducing the explicit form of the vibrational Hamiltonian given in Equation (1.7), the mean-field operator assumes the form,

$$\hat{G}_{m,\mathbf{s}} = -\frac{1}{2}\frac{\partial^2}{\partial Q_m^2} + U_{m,\mathbf{s}}(Q_m), \tag{1.16}$$

where the one-mode function, $U_{m,\mathbf{s}}(Q_m)$, is the mean-field potential felt by mode m in the presence of others. For a QFF PES [Equation (1.10)], the mean-field potential is given by

$$U_{m,\mathbf{s}}(Q_m) = U^{(0)}_{m,\mathbf{s}} + U^{(1)}_{m,\mathbf{s}} Q_m + \frac{1}{2} U^{(2)}_{m,\mathbf{s}} Q_m^2 + \frac{1}{6} U^{(3)}_{m,\mathbf{s}} Q_m^3 + \frac{1}{24} U^{(4)}_{m,\mathbf{s}} Q_m^4 \tag{1.17}$$

with

$$\begin{aligned} U^{(0)}_{m,\mathbf{s}} = {} & V_{\mathrm{ref}} + \sum_i{}' \left(-\frac{1}{2} \left\langle \frac{\partial^2}{\partial Q_i^2} \right\rangle + \frac{1}{2} F_{ii} \langle Q_i^2 \rangle + \frac{1}{6} F_{iii} \langle Q_i^3 \rangle + \frac{1}{24} F_{iiii} \langle Q_i^4 \rangle \right) \\ & + \sum_{i,j}{}' \left(\frac{1}{2} F_{iij} \langle Q_i^2 \rangle \langle Q_j \rangle + \frac{1}{8} F_{iijj} \langle Q_i^2 \rangle \langle Q_j^2 \rangle + \frac{1}{6} F_{iiij} \langle Q_i^3 \rangle \langle Q_j \rangle \right) \\ & + \sum_{i,j,k}{}' \left(\frac{1}{6} F_{ijk} \langle Q_i \rangle \langle Q_j \rangle \langle Q_k \rangle + \frac{1}{4} F_{iijk} \langle Q_i^2 \rangle \langle Q_j \rangle \langle Q_k \rangle \right) \\ & + \sum_{i,j,k,l}{}' \frac{1}{24} F_{ijkl} \langle Q_i \rangle \langle Q_j \rangle \langle Q_k \rangle \langle Q_l \rangle, \end{aligned} \tag{1.18}$$

$$
\begin{aligned}
U^{(1)}_{m,\mathbf{s}} &= \sum_i{}' \left(\frac{1}{2} F_{iim} \langle Q_i^2 \rangle + \frac{1}{6} F_{iiim} \langle Q_i^3 \rangle \right) + \sum_{i,j}{}' \left(\frac{1}{2} F_{ijm} \langle Q_i \rangle \langle Q_j \rangle + \frac{1}{2} F_{iijm} \langle Q_i^2 \rangle \langle Q_j \rangle \right) \\
&\quad + \sum_{i,j,k}{}' \frac{1}{6} F_{ijkm} \langle Q_i \rangle \langle Q_j \rangle \langle Q_k \rangle, \qquad (1.19) \\
U^{(2)}_{m,\mathbf{s}} &= F_{mm} + \sum_i{}' \left(F_{imm} \langle Q_i \rangle + \frac{1}{2} F_{iimm} \langle Q_i^2 \rangle \right) + \sum_{i,j}{}' \frac{1}{2} F_{ijmm} \langle Q_i \rangle \langle Q_j \rangle, \qquad (1.20) \\
U^{(3)}_{m,\mathbf{s}} &= F_{mmm} + \sum_i{}' F_{immm} \langle Q_i \rangle, \qquad (1.21) \\
U^{(4)}_{m,\mathbf{s}} &= F_{mmmm}, \qquad (1.22)
\end{aligned}
$$

where $\langle f(Q_i) \rangle$ is a shorthand notation for $\langle \phi_{s_i} | f(Q_i) | \phi_{s_i} \rangle$ and the primes on the summation symbols indicate that the mth mode is excluded from the sums.

The set of coupled eigenvalue equations, Equation (1.12), does not have an analytical solution. We must, therefore, resort to a numerical solution by expanding each modal in the basis of, typically, the harmonic oscillator (HO) wave functions,

$$
\phi_{s_m}(Q_m) = \sum_{n=0}^{N_m - 1} C_{n,s_m} \chi_{n,m}(Q_m), \qquad (1.23)
$$

where N_m is the number of the HO basis functions and C_{n,s_m} is an expansion coefficient. The nth-order HO basis function is given by

$$
\chi_{n,m}(Q_m) = \mathcal{N}_{n,m} \mathcal{H}_n(\sqrt{\omega_m} Q_m) \exp\left(-\omega_m Q_m^2 / 2\right), \qquad (1.24)
$$

where $\mathcal{N}_{n,m}$ is the normalization constant, $\mathcal{H}_n$ is an Hermite polynomial of order n, and ω_m is the harmonic frequency for mode m. The expansion coefficients are determined by solving the matrix eigenvalue equation,

$$
\sum_{n=0}^{N_m - 1} G_{n'n} C_{n,s_m} = C_{n',s_m} \epsilon_{s_m}, \qquad (1.25)
$$

where $G_{n'n} = \langle \chi_{n',m} | \hat{G}_{m,\mathbf{s}} | \chi_{n,m} \rangle$. Hence, the algorithm of VSCF involves repeated diagonalization of the G matrix for each mode until self consistency across all the modes is attained. These matrix elements can be evaluated analytically and those that are necessary to implement VSCF with a QFF are given explicitly in Table 1.1.

VSCF method captures a significant portion of anharmonicity, $E_{\mathbf{s}}^{\text{Anharm}}$, which can be defined as the difference of the total energy, $E_{\mathbf{s}}$, from that in the harmonic approximation,

$$
E_{\mathbf{s}}^{\text{Anharm}} = E_{\mathbf{s}} - \sum_m (s_m + 1/2) \omega_m. \qquad (1.26)
$$

If all the modes were uncoupled as the 1MR approximation, VSCF method would give the exact energies, $E_{\mathbf{s}} = E_{\mathbf{s}}^{\mathrm{VSCF}}$. Anharmonic terms beyond 1MR (also known as off-diagonal anharmonic terms), give rise to coupling between the modes and VSCF describes this coupling in a mean-field approximation. To capture the rest of the anharmonicity, one needs anharmonic many-body methods that go beyond VSCF. Such methods are better known as vibrational correlation methods and are built upon the VSCF wave function. In this context, the vibrational correlation energy can be defined as,

$$E_{\mathbf{s}}^{\mathrm{Corr}} = E_{\mathbf{s}} - E_{\mathbf{s}}^{\mathrm{VSCF}}. \tag{1.27}$$

1.6.2 Vibrational perturbation theories

Rayleigh-Schrödinger perturbation theory is a standard method to address many-body problems. It partitions the Hamiltonian into an exactly solvable part, $\hat{H}^{(0)}$, and a smaller perturbation term, $\hat{H}'$. Eigenfunctions and eigenvalues are expanded in a Taylor series in λ, which is used as an ordering parameter and set to one when perturbation series are defined at each order.

$$\hat{H} = \hat{H}^{(0)} + \lambda \hat{H}' \tag{1.28}$$

$$\Psi_{\mathbf{s}} = \Psi_{\mathbf{s}}^{(0)} + \lambda \Psi_{\mathbf{s}}^{(1)} + \lambda^2 \Psi_{\mathbf{s}}^{(2)} + \dots \tag{1.29}$$

$$E_{\mathbf{s}} = E_{\mathbf{s}}^{(0)} + \lambda E_{\mathbf{s}}^{(1)} + \lambda^2 E_{\mathbf{s}}^{(2)} + \dots \tag{1.30}$$

The zeroth, first and second order energies are given, respectively, as,

$$E_{\mathbf{s}}^{(0)} = \langle \Psi_{\mathbf{s}}^{(0)} | \hat{H}^{(0)} | \Psi_{\mathbf{s}}^{(0)} \rangle, \tag{1.31}$$

$$E_{\mathbf{s}}^{(1)} = \langle \Psi_{\mathbf{s}}^{(0)} | \hat{H}' | \Psi_{\mathbf{s}}^{(0)} \rangle, \tag{1.32}$$

$$E_{\mathbf{s}}^{(2)} = \sum_{\mathbf{s}' \neq \mathbf{s}} \frac{|\langle \Psi_{\mathbf{s}}^{(0)} | \hat{H}' | \Psi_{\mathbf{s}'}^{(0)} \rangle|^2}{E_{\mathbf{s}}^{(0)} - E_{\mathbf{s}'}^{(0)}}. \tag{1.33}$$

For anharmonic vibrational problems, there are two ways of partitioning the Hamiltonian. In the first one, known as vibrational perturbation theory (VPT), the zeroth order Hamiltonian is the Hamiltonian in the harmonic approximation, which has analytical solutions.

$$\hat{H}^{(0)} = -\frac{1}{2} \sum_i \frac{\partial^2}{\partial Q_i^2} + \frac{1}{2} \sum_i F_{ii} Q_i^2 \tag{1.34}$$

If the full Hamiltonian has a QFF PES, the perturbation has the form

$$\begin{aligned}\hat{H}' &= \sum_i \left(\frac{1}{6}F_{iii}Q_i^3 + \frac{1}{24}F_{iiii}Q_i^4\right) \\ &+ \sum_{i,j}\left(\frac{1}{2}F_{iij}Q_i^2Q_j + \frac{1}{8}F_{iijj}Q_i^2Q_j^2 + \frac{1}{6}F_{iiij}Q_i^3Q_j\right) \\ &+ \sum_{i,j,k}\left(\frac{1}{6}F_{ijk}Q_iQ_jQ_k + \frac{1}{4}F_{iijk}Q_i^2Q_jQ_k\right) \\ &+ \sum_{i,j,k,l}\frac{1}{24}F_{ijkl}Q_iQ_jQ_kQ_l. \end{aligned} \tag{1.35}$$

Since harmonic oscillator eigenfunctions are either even or odd, expectation values of an odd power of normal coordinate in a harmonic oscillator wave function vanish identically. Therefore the first order correction has contributions from only certain types of quartic force constants.

$$E_{\mathbf{s}}^{(1)} = \langle\Psi_{\mathbf{s}}^{(0)}|\sum_i \frac{1}{24}F_{iiii}Q_i^4 + \sum_{i,j}\frac{1}{8}F_{iijj}Q_i^2Q_j^2|\Psi_{\mathbf{s}}^{(0)}\rangle \tag{1.36}$$

Since the above expression has at most a double summation, the cost of the calculation scales with M^2. The second order correction to the energy [Equation (1.33)] has contributions from all the force constants. The summation over the states can be classified according to the number of modes that differ from the target state $\mathbf{s}$. Nonvanishing integrals in the denominator, that differs by a single mode (singles) have the form:

$$\langle\mathbf{s}|\frac{1}{6}F_{iii}Q_i^3 + \sum_{j\neq i}\frac{1}{2}F_{ijj}Q_iQ_j^2|\mathbf{s}\pm 1_i\rangle, \tag{1.37}$$

$$\langle\mathbf{s}|\frac{1}{24}F_{iiii}Q_i^4 + \sum_{j\neq i}\frac{1}{4}F_{iijj}Q_i^2{Q_j}^2|\mathbf{s}\pm 2_i\rangle, \tag{1.38}$$

$$\langle\mathbf{s}|\frac{1}{6}F_{iii}Q_i^3|\mathbf{s}\pm 3_i\rangle, \tag{1.39}$$

$$\langle\mathbf{s}|\frac{1}{24}F_{iiii}Q_i^4|\mathbf{s}\pm 4_i\rangle, \tag{1.40}$$

Doubles:

$$\langle \mathbf{s}|\frac{1}{6}F_{iiij}Q_iQ_j^3+\frac{1}{6}F_{iiij}Q_i^3Q_j+\sum_{k\neq i,j}\frac{1}{4}F_{ijkk}Q_iQ_jQ_k^2|\mathbf{s}\pm 1_i\pm 1_j\rangle, \tag{1.41}$$

$$\langle \mathbf{s}|\frac{1}{2}F_{ijj}Q_iQ_j^2|\mathbf{s}\pm 1_i\pm 2_j\rangle, \tag{1.42}$$

$$\langle \mathbf{s}|\frac{1}{8}F_{iijj}Q_i^2Q_j^2|\mathbf{s}\pm 2_i\pm 2_j\rangle, \tag{1.43}$$

$$\langle \mathbf{s}|\frac{1}{6}F_{iiij}Q_iQ_j^3+\frac{1}{6}F_{iiij}Q_i^3Q_j|\mathbf{s}\pm 1_i\pm 3_j\rangle. \tag{1.44}$$

Triples:

$$\langle \mathbf{s}|\frac{1}{6}F_{ijk}Q_iQ_jQ_k|\mathbf{s}\pm 1_i\pm 1_j\pm 1_k\rangle, \tag{1.45}$$

$$\langle \mathbf{s}|\frac{1}{4}F_{ijkk}Q_iQ_jQ_k^2|\mathbf{s}\pm 1_i\pm 1_j\pm 2_k\rangle, \tag{1.46}$$

Quadruples:

$$\langle \mathbf{s}|\frac{1}{24}F_{ijkl}Q_iQ_jQ_kQ_l|\mathbf{s}\pm 1_i\pm 1_j\pm 1_k\pm 1_l\rangle, \tag{1.47}$$

where $|\mathbf{s}'\rangle = |\mathbf{s}\pm 1_i\rangle$ denotes the state of which the, ith mode has quantum number s_i+1 while all the other quantum numbers in the state $\mathbf{s}'$ are identical to those of the state $\mathbf{s}$. For a QFF PES there is at most quadruples contribution to the second order energy and due to the four-fold summations, the cost of the calculations grow as M^4.

The second choice for partitioning the Hamiltonian is based on the VSCF solution and analogous to the Møller-Plesset (MP) perturbation[38] in electronic structure theory. VMP was initially proposed by Norris *et al.*[13] in 1996. The zeroth-order Hamiltonian and the perturbation in VMP is

$$\hat{H}^{(0)}_{\mathbf{r}} = \sum_m \hat{G}_{m,\mathbf{r}} = \sum_m \left(-\frac{1}{2}\frac{\partial^2}{\partial Q_m^2}+U_{m,\mathbf{r}}(Q_m)\right), \tag{1.48}$$

$$\hat{H}'_{\mathbf{r}} = V(Q_1,\ldots,Q_M)-\sum_m U_{m,\mathbf{r}}(Q_m), \tag{1.49}$$

where **r** refers to the reference state for which the VSCF calculation is performed. Based on the choice of **r**, there are two types of VMP calculations for excited states: one is based on an excited-state Hartree wave function constructed with the virtual states of the ground state VSCF solution, and the other uses the excited-state VSCF wave function optimized for each target state. The former is referred to as ground-state VMP (gsVMP) while the latter is referred to as state-specific VMP (ssVMP). It should be noted that for ssVMP, the partition of the Hamiltonian changes with states of interest.

The zeroth order wave function is identical to the VSCF solution (see Section 1.6.1),

$$\Psi_{\mathbf{s}}^{(0)} = \Phi_{\mathbf{s}}, \tag{1.50}$$

and the zeroth order energy is given by,

$$E_{\mathbf{s}}^{(0)} = \langle \Phi_{\mathbf{s}} | \sum_{m} \hat{G}_{m,\mathbf{r}} | \Phi_{\mathbf{s}} \rangle = M E_{\mathbf{s}}^{\mathrm{VSCF}}, \tag{1.51}$$

The first order correction to the energy is,

$$E_{\mathbf{s}}^{(1)} = \langle \Phi_{\mathbf{s}} | \hat{H} - \hat{H}^{(0)} | \Phi_{\mathbf{s}} \rangle = (1 - M) E_{\mathbf{s}}^{\mathrm{VSCF}}. \tag{1.52}$$

Therefore, the energy up to first order is the same as the VSCF energy:

$$E_{\mathbf{s}}^{(0)} + E_{\mathbf{s}}^{(1)} = E_{\mathbf{s}}^{\mathrm{VSCF}} \tag{1.53}$$

The second order energy has contributions from all the anharmonic force constants except the diagonal ones (anharmonic terms in 1MR PES); the latter are already accounted completely in the VSCF solution.

The VMP method has been successful for problems with only moderate mode-mode coupling. However, if there is a strong coupling or degeneracy, then VMP2 fails due to the form of the denominator in Equation (1.33). A quasi-degenerate version of VMP2 has been developed by Yagi *et al.*[39] based on van Vleck perturbation theory. It is also found that[40] higher order corrections (VMP3 and further) are more prone to divergences and generally VMP2 often gives the most reasonable result in the perturbation series.

1.6.3 Vibrational configuration-interaction theory

Variational calculations for anharmonic vibrations date back to 1975 when Whitehead and Handy's work on triatomic molecules was published.[32] A formalism analogous to the configuration-interaction method in electronic structure

theory[41] was later developed by Tobin and Bowman *et al.* in 1980.[14] The basic idea of the configuration-interaction methods is to diagonalize the Hamiltonian in a basis of M-mode Hartree-product functions, to obtain variationally the best wave function within the basis set. One-mode functions from which the Hartree product is formed, typically VSCF modals, are also expanded in a basis-set formed by suitable one-dimensional functions, e.g. the HO eigenfunctions (see Section 1.6.1).

The form of the VCI wave function is,

$$\Psi_{\mathbf{s}}^{\mathrm{VCI}}(Q_1, \ldots, Q_M) = \sum_{\mathbf{s}'}^{K} C_{\mathbf{s}}^{\mathbf{s}'} \Phi_{\mathbf{s}'}(Q_1, \ldots, Q_M) \tag{1.54}$$

where K is the total number of Hartree products (or configurations). VCI coeffients, $C_{\mathbf{s}}^{\mathbf{s}'}$ are obtained by variationally minimizing the energy,

$$E_{\mathbf{s}}^{\mathrm{VCI}} = \langle \Psi_{\mathbf{s}}^{\mathrm{VCI}} | \hat{H} | \Psi_{\mathbf{s}}^{\mathrm{VCI}} \rangle. \tag{1.55}$$

Computationally, this is done by forming the Hamiltonian matrix in the basis of modals, $\Phi_{\mathbf{s}'}$, and diagonalizing. The eigenvectors give the VCI coefficients, and the eigenvalues give the energies. If we could have a complete basis set and a full configuration space, we would have the exact energies for all the states. With a finite basis set and configuration space, we would get an upper bound for the energies.

One can either use a HO basis set, or eigenfunctions of a ground state VSCF solutions to form the configuration space. The latter is expected to converge more rapidly since VSCF solutions already includes a significant portion of anharmonicity.

One of the practical disadvantages of the VCI method is its cost, since the order of the full Hamiltonian matrix scales as N^M, where N is the number of basis functions for each mode. Therefore, except for the smallest molecules, a full VCI calculation is not feasible and one needs to select the important configurations to reduce the size of the matrix and carefully check for the convergence of the solution.

There are several criteria that one can use to restrict the size of the configuration space. The most effective one is to arrange the configuration space according to the number of excited-state HO or VSCF modals in the Hartree product basis. With this arrangement, Equation (1.54) takes the form,

$$\Psi_{\mathbf{s}}^{\mathrm{VCI}} = C_0 \Phi_0 + \sum_i \sum_r C_i^r \Phi_i^r + \frac{1}{2} \sum_{i,j} \sum_{r,t} C_{ij}^{rt} \Phi_{ij}^{rt} + \ldots, \tag{1.56}$$

where indices $i, j, \ldots$ denote which mode(s) are excited and $s, t, \ldots$ denotes the level of excitation for the corresponding mode. The first summation corresponds to single excitations and a VCI calculation truncated at this level is referred as VCI singles or VCIS and similarly, including two-mode excitations, doubles, one has VCISD, and so on. For a

three-mode system VCI with singles, doubles and triples (VCISDT) amounts to full VCI. Additional criteria can be used to restrict the level of excitation. That is, one can set a maximum value of excitation for each mode and/or restrict the total excitation by using a cut-off for $s+t+\ldots < S_{\text{sum-max}}$. Alternatively, an energy based cut-off value can also be used to restrict the configuration space. There are various other techniques to increase the speed of VCI calculations as implemented by different groups.[8,15,42]

Apart from the practical limitations of the VCI method, it has a more fundamental shortcoming of not being size consistent and its accuracy is known to deteriorate with system size, giving no anharmonic correction beyond the reference method in the bulk limit. A detailed discussion on this issue is given in Section 3.3.6.

1.7 Tables

Table 1.1: The elements of the matrix representation of various operators ($f(Q_m) = \partial^2/\partial Q_m^2, Q_m, Q_m^2, Q_m^3, Q_m^4$) in the harmonic oscillator basis functions, $\langle\chi_{n',m}|f(Q_m)|\chi_{n,m}\rangle$. Only $n > n'$ cases are shown, since the operators considered are Hermitian. All matrix elements vanish when $n > n' + 4$.

$n-n'$	$\partial^2/\partial Q_m^2$	Q_m	Q_m^2	Q_m^3	Q_m^4
0	$-\omega_m(n+1/2)$	0	$(n+1/2)/\omega_m$	0	$\{6n(n+1)+3\}/4\omega_m^2$
1	0	$\sqrt{n/2\omega_m}$	0	$3(n/2\omega_m)^{3/2}$	0
2	$\omega_m\sqrt{n(n-1)}/2$	0	$\sqrt{n(n-1)}/2\omega_m$	0	$(n-1/2)\sqrt{n(n-1)}/\omega_m^2$
3	0	0	0	$\sqrt{n(n-1)(n-2)}/(2\omega_m)^{3/2}$	0
4	0	0	0	0	$\sqrt{n(n-1)(n-2)(n-3)}/4\omega_m^2$

Chapter 2

Anharmonic calculations for small molecules

2.1 Introduction

Predictive chemical computing[2] based on converging electron-correlation methods combined with systematic basis sets[43,44] have come to a stage that it is now possible to routinely predict the electronic properties of small but general polyatomic molecules within controlled accuracy.

The objective of this chapter* as well as several other recent studies in our group[2,46–48] is to extend the domain of predictive computing to bound nuclear motions, i.e., anharmonic molecular vibrations, vibrationally-averaged properties, and various molecular spectra. In addition to providing computed properties and spectra that can be directly compared with the observed, they can serve as an independent and reliable source of chemical information of which direct experimental measurements may be technically difficult, expensive, and/or dangerous.

As described in Chapter 1, the predictive vibrational analyses consist in (1) converging electronic structure methods for generating accurate potential energy surfaces (PESs), (2) compact and systematic representations of the PESs, and (3) hierarchical vibrational many-body methods that can include vibrational anharmonicity and anharmonic mode-mode coupling to any desired extent.

For (1), we employ the converging series of combined coupled-cluster (CC) and perturbation theories, i.e., coupled-cluster singles and doubles (CCSD),[49,50] CCSD with a second-order triples correction abbreviated as CCSD(2)$_T$,[51] and CCSD with a second-order triples and quadruples correction or CCSD(2)$_{TQ}$[51] in this chapter. For stable molecules near their equilibrium geometries, this is perhaps among the most rapidly converging series of electron-correlation methods. The complete-basis-set (CBS) limits are reached by extrapolation with the correlation-consistent basis sets,[52] although an effort to eliminate this step with the aid of the so-called R12 or F12 methods[53] is underway in our group.[5,54,55]

For (2), we propose a new hybrid representation of PESs, which combines a Taylor expansion truncated at the fourth order (a quartic force field or QFF) and numerical energy values on a rectilinear quadrature grid (a grid PES) both in the so-called *n*MR (*n*-mode representation) approximation.[27,28] The QFFs are among the most accurate and compact PES representations for low-lying vibrational states[35,56–62] . However, they cannot describe strong Morse-like

*The work in this chapter has been published in Ref. 45. Reprint permission is granted by Taylor & Francis.

anharmonicity and tend to exhibit fortuitous minima in the regions away from the equilibrium geometries.[8,37] When VCI is applied to these QFFs, errors (with respect to grid PESs) in the frequencies of stretching modes involving hydrogen motions can be as large as 20 cm^{-1} (see below) and nonphysical states supported by the fortuitous minima can appear. Such nonphysical states can be easily identified by an inspection of wave functions or, alternatively, a Morse-like[63] or similar coordinate transformations[37] can be applied before the VCI step to avoid both problems. In this chapter, however, we circumvent them by improving the global representation of a PES qualitatively by combining a QFF and a grid PES[35,36,64] while further improving the local representation near the equilibrium geometry quantitatively. Grid PESs maintain an equal accuracy (subject to errors in electronic structure methods used) in the entire geometry domain covered by the grids, but they are exponentially expensive to compute (without *n*MR approximation) as the number of atoms increases. The new hybrid representation combines a QFF obtained by high-rank electronic structure methods in the CBS limits and a grid PES obtained by low-rank methods and smaller basis sets. The proposed hybrid QFF/grid PESs are expected to be most meritorious when applied to large-amplitude motions and highly excited vibrational states. The QFFs, grid PESs, and hybrid QFF/grid PESs are defined in normal coordinates.[19] Although local coordinates may be more suitable for large-amplitude motions or highly excited vibrational states, we adopt normal coordinates for their unambiguousness, convenience, and generality[8,19,36,63–65] .

Vibrational many-body problems in these PESs are solved by vibrational self-consistent-field (VSCF)[66–69] , second-order Møller–Plesset perturbation (VMP2),[13,27,31,64] and general-order configuration-interaction (VCI)[12] methods implemented in the SINDO program developed by Yagi.[70] See Section 1.6, or a recent review[8] for the details of these methods as well as the vibrational coupled-cluster methods (VCC)[15] added recently to the repertory of vibrational many-body methods. Although this method is not used in this chapter, it is a promising method for its size-extensivity which makes it the right tool for larger systems where a full VCI is not applicable. The necessary molecular integrals are computed over the harmonic oscillator basis functions along the normal coordinates. Together, our composite vibrational method can attain complete-correlation, CBS (CC-CBS) limits in anharmonic frequencies and vibrationally-averaged properties in a cost-effective fashion (although its applicability to large molecules is still limited).

We apply the method to seven key species in hydrocarbon combustion: the formyl cation (HCO^+), the formyl radical (HCO), the nitrosyl hydride (HNO), the hydroperoxy radical (HOO), the hydroperoxy anion (HOO^-), the methyl cation (CH_3^+), and the methyl radical (CH_3). Some are important in atmospheric and/or interstellar chemistry also. There is a considerable lack of experimental data of molecular constants of these species, since most of them are unstable under typical laboratory conditions and, therefore, their characterization calls for a predictive theory. For instance, the transition frequencies of one of the fundamentals of CH_3 and CH_3^+ as well as all of the fundamentals of HOO^- are unknown, in spite of the significance of these species and their vibrational spectra as a source of information about hydrocarbon combustion processes. Furthermore, the comparison of predicted frequencies and rotational constants

with the observed values, when available, serves as a rigorous test of the validity and accuracy of the computational scheme, including the hybrid QFF/grid PESs proposed in this chapter.

There has been a considerable body of work[26,58–62,71,72] reporting high accuracy anharmonic frequencies of fundamental vibrations of small molecules. Some of these works are based on QFF in tailored coordinates, vibrational perturbation theories including Coriolis coupling, and various CBS extrapolations of electronic energies, including small electronic effects such as core correlation and relativistic effects as well as diagonal Born–Oppenheimer corrections. In contrast to these previous high-accuracy studies, this chapter and a few previous studies[2,46,47] from our group aim at establishing blackbox computational procedures for low-lying anharmonic vibrational frequency calculations applicable generally and unambiguously to various polyatomic molecules in the same sense of "model chemistry" advocated by Pople (see, e.g.,[73]) in electronic structure theory. The reliance on normal modes, the mixed use of QFF, grid, and hybrid QFF/grid PES representations, and the open-ended combinations of systematic electronic and vibrational many-body methods in this work are to achieve good balance between general applicability of the theories, robustness and availability of the implementations, and high (if not the highest) accuracy. A wider range of molecules (seven species) that are studied in one place is also to show the generality of our model chemistry, its uniform accuracy, and affordability of computations both in terms of computational cost and the ease of use for non-experts of computational chemistry.

It will be shown that the hybrid PESs constitute a uniform and inexpensive improvement over both QFFs and grid PESs. When combined with the CC-CBS electronic structure method and VCI, it reproduces the frequencies of the fundamentals within the mean absolute deviation of 11 cm^{-1} and the maximum deviation of 41 cm^{-1}. Our calculated results are reliable predictions (within ca. 20 cm^{-1}) for the hitherto-undetermined fundamental frequencies of HOO^-, CH_3^+, and CH_3. The predicted rotational constants also serve as an additional basis for correct band assignments, although in some instances they are found to be unreliable because of strong centrifugal distortion and Coriolis coupling, which are neglected in this work. The vibrationally-averaged structural parameters are expected to be accurate to within several thousandths of 1 Å and are possibly more accurate than experimentally derived values. While our computational scheme is still severely limited in its applicability to large molecules, it is a general, predictive, blackbox method applicable to any polyatomic molecule.

2.2 Theory and computational procedure

2.2.1 Electronic part

Geometry optimization and normal coordinate calculations were performed with CCSD(2)$_T$ with the aug-cc-pVDZ basis set. All PESs of a molecule were represented in this single set of coordinates to facilitate the CC-CBS extrap-

olation. Three different CBS extrapolation schemes [Equations 2.1-2.3] were examined on the basis of the CCSD energies obtained with the aug-cc-pVXZ basis sets in the range of X = D, T, and Q (abbreviated hereafter as "aXZ"). The first of these is the exponential–Gaussian three-point extrapolation formula advocated by Peterson, Woon, and Dunning,[74] which assumes the energy obtained with the l-th basis set (l = 2, 3, and 4 correspond to X = D, T, and Q, respectively) satisfy the following equation,

$$E(l) = E_{\mathrm{CBS}} + A\exp[-(l-1)] + B\exp\left[-(l-1)^2\right], \tag{2.1}$$

where A, B, and E_{CBS} are constants (the last quantity corresponds to the CBS total energy). The second is the power law three-point formula proposed by Martin and Lee,[75] which can be written as

$$E(l) = E_{\mathrm{CBS}} + A(l+1/2)^{-4} + B(l+1/2)^{-6}, \tag{2.2}$$

where the meaning of the variable l and the constants are the same as in Eq 2.1. The third is the two-point formula of Helgaker *et al*:[76]

$$\Delta E(l) = \Delta E_{\mathrm{CBS}} + Al^{-3} \tag{2.3}$$

where $\Delta E(l)$ and ΔE_{CBS}represent the correlation energy of the l-th basis set (with l = 3 and 4) and at the CBS limit, respectively. The CBS correlation energies obtained with the third extrapolation formula was combined with the Hartree–Fock (HF) energies in the CBS limit obtained by Eq 2.1 or 2.2. Table 2.1 shows that there is no significant difference in anharmonic vibrational frequencies among these formulas for the purpose of this chapter. This result also indicates the robustness of our final predictions with respect to the arbitrary choice of empirical extrapolation formulas. We elected to use Eq 2.1 for the rest of the calculations without assuming any superiority of this formula over the others. The CC-CBS limits ($E_{\mathrm{CC-CBS}}$) were obtained by the following formula:[77]

$$E_{\mathrm{CC-CBS}} = (E_{\mathrm{CCSD/CBS}} - E_{\mathrm{CCSD/aDZ}})\frac{E_{\mathrm{CCSD(2)}_T\mathrm{/aTZ}} - E_{\mathrm{CCSD(2)}_T\mathrm{/aDZ}}}{E_{\mathrm{CCSD/aTZ}} - E_{\mathrm{CCSD/aDZ}}} + E_{\mathrm{CCSD(2)}_{TQ}\mathrm{/aDZ}}. \tag{2.4}$$

This procedure will not yield the absolute energies accurately but is expected to minimize the errors in the energy differences, i.e., the shape of the PESs. To obtain a CC-CBS energy, one must execute only three single-point energy calculations at the CCSD/aQZ, CCSD(2)$_T$/aTZ, and CCSD(2)$_{TQ}$/aDZ levels. The CCSD/aTZ energy is obtained as a byproduct of the CCSD(2)$_T$/aTZ calculation and the CCSD/aDZ and CCSD(2)$_T$/aDZ energies from CCSD(2)$_{TQ}$/aDZ. These were carried out within the frozen core approximation using the NWCHEM[78] and ACES II[79] programs.

2.2.2 Hybrid potential energy surface

The simplified vibrational Hamiltonian is given as,

$$\hat{H} = -\frac{1}{2}\sum_{i=1}^{m}\frac{\partial^2}{\partial Q_i^2} + \hat{V}(Q_1, \ldots, Q_m) \tag{2.5}$$

for both linear and nonlinear molecules without any forms of singularity. The motivation behind neglecting the rotation-vibration coupling terms is given in Section 1.4. This is also consistent with our neglect of core-correlation corrections, relativistic effects, non-Born–Oppenheimer effects, higher-order correlation effects, etc. However, as we shall show in the following, the approximate Hamiltonian used in this chapter is likely responsible for some pronounced errors in predicted vibrationally averaged rotational constants.

For the PES, we adopted the nMR approximation (See Section 1.5.1 for more details) that expressed $\hat{V}$ as a sum of one-, two-, up to m-mode coupling terms and truncated the sum after the n-mode coupling terms. We used $n = 3$ or the 3MR approximation, which amounted to a non-truncated PES for nonlinear triatomic molecules. We defined a rectilinear grid along the CCSD(2)$_T$/aDZ normal coordinates centered at the CCSD(2)$_T$/aDZ optimized geometry. Eleven grid points were placed along each normal coordinate according to the Gauss–Hermite quadrature rule and single-point electronic structure calculations were performed on the geometries of these points. In the 3MR approximation, there were $\binom{m}{3}11^3$ grid points in total, if we disregard symmetry advantages. This number has been shown to be sufficient[35] for several low-lying vibrational states of the molecules studied here. Grid-based algorithms for anharmonic vibrational problems are quite old,[32,33] but they became routine[35,36,64] only after they were combined with the nMR approximation. An inexpensive alternative is the QFFs, which are computed by a finite difference method described in Refs.,[56,57] requiring only a few tens of single-point energy calculations to compute. We used both representations in this work with SINDO that took advantage of the Abelian sub-group of the symmetry group of a molecule. While highly accurate near the equilibrium geometries, the QFFs become progressively unrealistic as the geometries are more distorted. They also cannot dissociate bonds and often deflect downwards away from the equilibrium geometries, often causing artificial minima in a PES. The grid PESs do not share these shortcomings, but they are exponentially expensive to compute. Here, we propose a new hybrid representation, which combines the merits of the grid and QFF representations, while keeping the overall computational cost manageable. It involves a grid and QFF obtained at the same low electronic structure level and another QFF at a higher electronic structure level and adds the difference between high- and low-level QFFs to the low-level grid PESs:

$$E_{\text{hybrid}} = E_{\text{QFF/high}} - E_{\text{QFF/low}} + E_{\text{grid/low}}, \tag{2.6}$$

where $E_{\text{QFF/high}}$ and $E_{\text{QFF/low}}$ are the energies at a given grid point obtained by evaluating the quartic polynomial

functions of high- and low-level QFFs, respectively, and $E_{\mathrm{grid/low}}$ is the energy value directly computed at the grid point at the low-level method. The left-hand side is the hybrid QFF/grid PES defined numerically on the same grid and approximates the grid PES obtained at the high-level method.

The remarkable performance of this hybrid representation can be seen in Table 2.2 in which anharmonic vibrational frequencies of HOO^- obtained with five different PESs are compared. Relative to the grid PES obtained by CCSD(2)$_T$/aTZ, which serves as the accurate and very expensive reference, the two PESs obtained by CCSD/aDZ suffer from large errors in excess of 30 cm^{-1} in the vibrational energies. These are clearly due to the inherent errors in the CCSD/aDZ regardless of the representation (grid or QFF). If we raise the electronic structure level to CCSD(2)$_T$/aTZ (the same as the reference), however, the QFF representation is still responsible for an error of –22 cm^{-1} in the O–H stretching frequency. When these three PESs (the bottom three rows) are combined and the hybrid QFF/grid PES is formed, the errors become uniformly small (within 3.1 cm^{-1}). They are much smaller than those obtained with any of the three constituent PESs. Note also that forming the hybrid PES is an order of magnitude less expensive than generating the corresponding grid PES and, furthermore, the advantage of the former is expected to grow as molecules become larger. We adopted the hybrid representation for all the molecules studied here. We chose CCSD/aDZ as the low electronic structure level to obtain the grid PES and the CC-CBS composite defined by Eq 2.4 for the QFFs. Four PES scans (three QFF calculations for CC-CBS and one grid PES calculation for forming the hybrid PES) were run for each molecule, apart from the geometry optimization and normal coordinate determination.

2.2.3 Vibrational part

With the accurate PESs thus obtained, we solved the vibrational Schrödinger equation with the VSCF, VMP2 and VCI methods (the VSCF and VMP2 results are not shown, for more details on these methods see Section 1.6), using SINDO. The full VCI method was applied to the nonlinear and linear triatomic molecules (involving 1331 and 14641 excited VSCF configurations, respectively). For tetratomic molecules, we examined two configuration selection schemes. In one, all VSCF configurations that involved simultaneous excitations of up to three modals (21561 configurations) were included. In the other, simultaneous excitations of up to four modals were allowed but the sum of vibrational quanta was limited to 15. There were 30011 VSCF configurations in the latter. It was confirmed that the fundamental frequencies obtained in either of these schemes were converged within 1 cm^{-1} of the limits with respect to the configuration space size. The vibrationally-averaged structural parameters (at zero temperature) were obtained by using the VCI wave functions. The expectation values of the relative nuclear positions in the normal mode coordinates were calculated and then they were transformed into the Cartesian coordinates. The vibrationally-averaged rotational constants were computed by evaluating the rigid-rotor formulae of the rotational constants with the vibrationally-averaged nuclear coordinates. Note that there are at least two approximations in this treatment. First,

they do not correspond to the expectation values that are observed as rotational constants. Second, they neglect rovibrational coupling such as centrifugal distortion and Coriolis coupling. As a result, the computed rotational constants can deviate, sometimes significantly, from experimental values and are at best of a semi-quantitative value.

2.3 Combustion chemistry applications

2.3.1 HCO^+ ($\tilde{X}^1\Sigma^+$)

The formyl cation (HCO^+) in its $\tilde{X}^1\Sigma^+$ state is a linear molecule ubiquitous in interstellar medium[80] and also in hydrocarbon flames.[81] Buhl and Snyder[82] observed an interstellar transition which was identified computationally by Klemperer[83] as a rotational transition of HCO^+. Klemperer's computational assignment was supported theoretically[84] and subsequently confirmed experimentally.[85] Its rotational and vibrational transitions have been thoroughly characterized by microwave[86–94] and infrared laser spectroscopy.[95–104] There have been many computational studies on the structure, PES,[105–110] and rovibrational spectra[111–114] of HCO^+. Some[111,113,114] are based on CCSD with noniterative triples [CCSD(T)] while Ref. 112 on the multireference configuration interaction (MRCI) and their results on anharmonic vibrational frequencies agree with one another, attesting to the limited multireference character of the wave function of HCO^+.

Table 2.4 compiles the experimental frequency of the fundamental transitions and four of the most accurate computed frequencies by other groups as well as our computed frequencies. Mladenovi and Schmatz[113] computed energies at 842 geometries with CCSD(T)/cc-pVQZ and obtained anharmonic fundamental frequencies by a variational method. They are within 5 cm^{-1} of the observed. The authors state the fitting of the PES by analytical functions has an inherent error of 9 cm^{-1} (the standard deviation), but the error may be mostly due to geometries with high energies and it is possible that the fundamental frequencies can have higher accuracy than the fitting error. However, the result obtained by van Mourik, Dunning, and Peterson[114] using CCSD(T) and a larger basis set (aug-cc-pVQZ) has slightly greater errors, suggesting that the accurate agreement of Mladenovic and Schmatz is likely due to some error cancellation between residual basis set effects and other small electronic effects neglected in their work.

Puzzarini *et al.*[112] used MRCI/cc-pVQZ to obtain a sextic force field, and evaluated spectroscopic parameters by second-order perturbation theory. They also scaled this force field empirically and used variational methods to solve for rovibrational energy levels, which yielded the fundamental frequencies within 2 cm^{-1} of the experimental values. An earlier work of Martin *et al.*[111] was based on CCSD(T)/cc-pVTZ QFF and, because of the smallness of the basis set, had slightly greater errors.

The harmonic frequencies obtained at the CCSD(2)$_T$/aDZ level, which serve as the basis of our subsequent anharmonic calculations, indicate small anharmonicity in the ν_2 (bend) and ν_3 (C–O stretch). The CC-CBS extrapolation of

the PES in the QFF representation and a full VCI calculation indeed increases the error in the ν_2 frequency from 7 to 24 cm^{-1}, while they bring the computed frequency of ν_1 (C–H stretch) in much better accord with experiment (3072 and 3089 cm^{-1}, respectively). This error in the ν_2 frequency is largely due to the QFF and can be removed effectively by switching to the hybrid QFF/grid PES. With the latter, the VCI method places the fundamental frequencies at 3083, 823, and 2175 cm^{-1}, which agree with the corresponding experimental values (3089, 830, and 2184 cm^{-1}) within 9 cm^{-1}. While similar or more accurate agreement has been reported by the previous studies, we note that our proposed method is a black-box approach applicable to general polyatomic molecules with minimum molecule-specific adjustments of coordinates, PES representations, etc. Accuracy higher than this (9 cm^{-1}) cannot be expected without a CC-CBS extrapolation and inclusion of rovibrational couplings, non-Born–Oppenheimer effects, and small electronic effects such as core correlation and relativistic effects.[26,72] The frequencies obtained by the individual methods that lead to the CC-CBS limit (see Section 2.2) are listed in Table S-1. These results reveal that the error arising from basis set truncation and that from the higher-order excitations tend to have opposite signs. Similar pattern was observed for all the molecules studied here. The success of the previous results,[111,113,114] therefore, may be partly because of the cancellation of the errors between them, especially for the C–O stretching mode due to its slower convergence in both limits.

Table 2.5 compares the vibrationally-averaged rotational constants (B's) with the observed[88,96–98] for four low-lying states. While the absolute values of the calculated constants have errors on the order of 1%, their variation with vibrational states is remarkably accurately reproduced by our scheme. Note that the harmonic approximation is incapable of describing such variation. These computed state-specific rotational constants can, therefore, serve as a useful, independent source of information for correct band assignments, when the assignments based on calculated and observed frequencies alone are inconclusive (which is, however, not the case with HCO^+). The potential curves along the C–H and C–O stretches are Morse-like and the corresponding vibrations increase the average C–H and C–O bond lengths, respectively. They result in noticeable reductions in the rotational constants in the (1000) and (0001) states. The bending vibration in the linear molecule, in contrast, has a net effect of pulling the terminal H and O atoms closer, causing the rotational constant in the (0110) state to be slightly greater than the zero-point value. Judging from the computed and observed rotational constants, the predicted C–O and C–H bond lengths should be within several thousandths of 1 Å of the experimental values (unknown).

2.3.2 HCO ($\tilde{X}^2A'$)

Unlike its cationic counterpart, the formyl radical (HCO) in its $\tilde{X}^2A'$ state is bent. The radical was first identified in ethylene flame[115] and was found to be responsible for the blue emission bands known as the hydrocarbon flame

bands. It is also an intermediate in the formation of HCO^+ in hydrocarbon flames. A characterization of the radical was performed by electronic absorption spectroscopy during the flash photolysis of acetaldehyde and other aldehydes, identifying two additional absorption bands as the transitions from the ground state in the bent structure to excited states in linear configurations.[116,117] The vibrational frequencies for C–H stretching,[118–122] bending[117,122–126] and C–O stretching[121,126–128] of HCO were measured by several experimental groups.

There is a considerable amount of computational studies on the PES of HCO,[114,129–151] a significant proportion of which concerns with its anharmonic vibrations. Bowman, Bittman, and Harding[132] reported its PES obtained with the configuration-interaction singles and doubles (CISD) and a double-ζ basis set plus some empirical corrections. This PES (called BBH potential) was modified and used in many subsequent dynamics calculations.[135–137,141,143,146] Werner *et al.*[144] employed MRCI with a quadruple-ζ basis set and obtained the fundamental anharmonic frequencies that agreed with the experimental values accurately except for the ν_3 (C–O stretch), which was 24 cm^{-1} too low. Serrano-Andrs, Forsberg, and Malmqvist[148] obtained similar results using a 177-point PES obtained with the multireference second-order perturbation method (CASPT2). The CCSD(T)/aQZ work of van Mourik, Dunning, and Peterson,[114] in contrast, obtained quantitative agreement between the computed and observed ν_2 (bend) and ν_3 (C–O stretch) frequencies, but the predicted ν_1 (C–H stretch) frequency was too high by 26 cm^{-1}. Marenich and Boggs[150] performed all-electron CCSD(T) calculations in the CBS limits and observed similar overestimation of the ν_1 frequency, causing them to question the experiments. However, the same authors[151] subsequently improved their calculations by including fifth- and sixth-order force constants along the C–H stretch (133 single-point calculations in total) and obtained the computed ν_1 and ν_3 frequencies which were, nonetheless, still too low by 19 cm^{-1} and too high by 17 cm^{-1}, respectively.

The observed[120,121,124] and computed[114,144,148,151] anharmonic fundamental frequencies of HCO are compared in Table 2.5. Our VCI results based on the CC-CBS, hybrid QFF/grid PES are within 6 cm^{-1} of the experimental values. Again, the QFF representation of essentially the same PES leads to a much greater error of 30 cm^{-1} in ν_1 (C–H stretch), underscoring the utility of the hybrid representation, particularly, in this strongly anharmonic mode. Our variational method (VCI) indicates a small mode-mode coupling (ca. 5% in the wave function) between the first overtone of ν_2 and fundamental ν_1, which is in agreement with Bowman, Bittman, and Harding. While the previously computed frequencies listed in Table 2.7 generally agree well with the experiment, our CC-CBS values are in the most accurate and uniform agreement with the observed.

Table 2.8 compares the vibrationally-averaged structures and rotational constants with experimental values[123,152–154] for four low-lying states. The two sets of experimental zero-point structures differ from each other by hundredths of 1 Å or a few degrees. The computed and observed structures agree within this inherent ambiguity in the experimental structural parameters. The computed rotational constants B and C also agree well with the observed within a few

percent, whereas the computed rotational constant A suffers from a greater error of ca. 5%, which is likely due to the neglect of rovibrational coupling in our computation. In fact, there are large discrepancies between the values of A in the (010) state between our prediction and Ref. 151, the origin of which is unclear. The computed values of B and C in the (010) state are similar to those in the (000) state, which is supported by experiments.

2.3.3 HNO ($\tilde{X}^1A'$)

Nitrosyl hydride or nitroxyl (HNO) in its $\tilde{X}^1A'$ state is a bent molecule of considerable importance in combustion chemistry as an intermediate in the formation of the air pollutant NO.[155] It has also recently gained attention in biochemistry and pharmacology as possible endogenous signaling species.[156,157] The observation of HNO was made initially in a flash photolysis[158] and subsequently by infrared spectroscopy in an argon matrix.[159] It has been also observed in interstellar medium by radio detection.[160] Its fundamental vibrational frequencies were analyzed by electronic emission spectroscopy,[161] absorption spectroscopy[162] and by electronic and vibrational emission spectroscopy.[163] They were confirmed by matrix-isolation infrared spectroscopy[164] and then improved in accuracy by laser Stark spectroscopy[165] which allowed a complete analysis of bending and C–O stretching fundamentals. Accurate measurements of the C–H stretch frequency were made by infrared absorption[166] and emission spectroscopy.[167] A number of other experimental studies on its microwave absorption[168,169] were reported on this molecule.

Among numerous computational studies on the PES of HNO,[170–179] the anharmonic vibrational analysis by Dateo, Lee, and Schwenke[177] is the most pertinent to our work. They established a QFF in an internal coordinate using the CCSD(T)/cc-pVQZ method. The frequencies with the QFF were in good agreement with the observed, although the frequency of ν_1 (N–H stretch) was somewhat too low (by 17 cm^{-1}). Mordaunt *et al.* [179] employed MRCI with a triple-ζ basis set to scan the three lowest-lying PESs, which were subsequently scaled empirically to yield accurate fundamental frequencies. Also, HNO has the longest known N–H (equilibrium) bond length of 1.053 Å and its accurate structure has been under considerable scrutiny by Lee[180] and later by Demaison *et al.*[181,182]

Table 2.10 and Table 2.11 list the anharmonic vibrational frequencies and vibrationally-averaged structures and rotational constants of HNO and compare them with the observed. Our CC-CBS PES in the hybrid QFF/grid representation reproduces the frequencies within 7 cm^{-1} of the experimental values.[165,166] State-specific rotational constants were reported[154,158,165,166] for all four states considered in Table 2.11. While the computed absolute values of the rotational constants can have errors in excess of a few percents, their variation across states (i.e., vibration-rotation coupling) is semi-quantitatively reproduced by theory. For instance, the (010) state has slightly greater values of A and B than the (001) state and this trend is predicted correctly by our calculation. Note that the order of these two states can be reversed in the harmonic approximation,[180] causing an incorrect band assignment in the past. Our

ability to compute state-specific rotational constants with sufficient accuracy will be helpful to avoid such problems. The vibrationally-averaged structural parameters are expected to be an order of magnitude more accurate than the rotational constants and should be within several thousandths of 1 Å of the true values. Our calculation favors the experimental zero-point geometry of Dalby.[158]

2.3.4 HOO ($\tilde{X}^2A''$)

The hydroperoxy radical (HOO) is an intermediate in the reaction H + O2 → OH + O, which has been referred to as "the single most important chemical reaction in combustion" in Ref. 183. It also plays a key role in atmospheric chemistry because the reverse reaction of the above is responsible for ozone destruction.[184] The reaction involves a conical intersection on the PES of HOO and its characterization is a challenging theoretical problem. Hence, there is an extensive literature on the PES of HOO; for a recent survey, the reader is referred to Xie *et al.*[185] Several spectroscopic studies were performed to accurately measure the frequencies of the O–H stretch,[186] bend,[187,188] and C–O stretch.[187,189–191] Electron paramagnetic resonance measurements[192,193] also yielded ground state parameters.

Walch and Duchovic[194] employed MRCI to generate a PES expressed as a QFF and obtained the anharmonic frequencies of fundamentals, which deviated from the observed by up to 108 cm^{-1}. Xu *et al.*[195] computed energies at 15000 geometries by MRCI with the Davidson correction with the aug-cc-pVQZ basis set. They solved the vibrational Schrödinger equation by the Lanczos method[196] and obtained vibrational energies up to 7000 cm^{-1}. They subsequently improved their PES and achieved the vibrational state calculations up to the dissociation limit.[185,197,198] Their computed frequencies of the fundamentals[197] were in excellent agreement with the observed (within 8 cm^{-1}). Among the other computational studies, those that are closely related to this one are Refs.[199–209]

Our calculated anharmonic frequencies agree with experiment[186,188,190] within 23 cm^{-1}. The errors are small but somewhat larger (especially for ν_3 or the O–O stretch) than those in the other molecules studied in this work. Since the full VCI method is used for this radical and the differences between QFF and hybrid QFF/grid representations are no greater than the other cases, the electronic structure methods are likely the primary source of the errors. Although the CC-CBS limits are supposed to be reached, the extrapolation formulae assume the validity of perturbation treatments of triple and quadruple excitations. It is possible that this assumption is not entirely valid for this radical at certain geometries. Comparing our vibrational state energies with the results of Xu *et al.*,[185] we find that both studies are in perfect agreement in the assignments of the states up to 5500 cm^{-1}. Below this threshold, the experimental energies tend to fall in between our computed values and those of Xu *et al.*, the latter being always the lower bound. This suggests that our PES is slightly more strongly curved than the true PES.

Notwithstanding the slight increase in the errors in the anharmonic frequencies, our calculations reproduce the variation in the rotational constants with respect to vibrational states well. The variations of B and C are smaller but

their trends are accurately predicted. The computed $r_{O–O}$ and a_{HOO} are in agreement with the observed, whereas it is hard to gauge the accuracy of $r_{O–H}$ because the experimental values are scattered. We expect that our computed structures have uniform accuracy of a few tenths of 1% regardless of the types of atoms involved or vibrational states.

2.3.5 HOO^- ($\tilde{X}^1A'$)

In contrast to its neutral counterpart, the literature on the hydroperoxy anion (HOO^-) is scarce. There is only one report on its photoelectron spectrum,[210] which provides an approximate frequency of 775 ± 250 cm^{-1} for ν_3 (O–O stretch). On the theory side, Horn *et al.*[211] obtained a 144-point PES with the CCSD(T)/aug-cc-pVTZ method and predicted the anharmonic frequencies of the fundamentals listed in Table 2.16. Chan *et al.*[212] performed QCISD(T)/6-311++G(2df,pd) energy calculations at 1535 geometries and fitted the PES with a 120-parameter analytic function with a root mean square error of 223 cm^{-1}. The predicted frequencies of the fundamentals obtained with this PES differ from those of Horn *et al.* by up to 80 cm^{-1}. Botschwina and Horn[206] upgraded the previous results[211] by increasing the electronic structure theory level to CCSD(T)/aug-cc-pVQZ. The predicted frequencies were close (within 11 cm^{-1}) to the values of Horn *et al.* Computational simulations of their photoelectron spectra were also performed for this anion.[213–215]

Our predicted values of the fundamental frequencies display the same general trend observed for the other bent triatomic molecules: small anharmonicity in ν_2 and ν_3 frequencies and a slightly greater improvement in the ν_1 frequency by the hybrid QFF/grid representation. Our best theoretical predictions (CC-CBS/hybrid/VCI) agree with those of Botschwina and Horn[206] within 11 cm^{-1} and with those of Horn *et al.*[211] within 15 cm^{-1}. They differ from the values suggested by Chan and Hamilton[212] by 78 and 54 cm^{-1} in ν_1 and ν_3, respectively. As in the case with the neutral, the ν_3 (O–O stretch) frequency shows slightly slower convergence with respect to the electronic structure level and the basis set size (see Table S-5). We, therefore, expect that our predicted frequencies are approximately within 10, 10, and 20 cm^{-1} of the true ν_1, ν_2, and ν_3 frequencies, respectively. The uncertainty in the observed ν_3 frequency[210] appears to be much smaller than 250 cm^{-1}.

Our predicted zero-point bond lengths (Table 2.17) agree well with the observed values,[210] whereas the computed bond angle is considerably smaller than the observed. The disagreement is due the fact that the bond angle (and one of the bond lengths) was simply assumed rather than determined experimentally.[210] The values reported by other theoretical studies also favor our prediction.[206,211–215] Unlike the experimental determination of these parameters via the interpretation of the spectra, our computed values are expected to have uniform accuracy across different parameters. The predicted rotational constants will be helpful for band assignments, when state-specific rotational constants of HOO^- are observed.

2.3.6 CH_3^+ $(\tilde{X}^1A_1')$

The methyl cation is among the most important carbonium ions. It is highly reactive and commonly found in the discharges from hydrocarbon combustion. CH_3^+ in its $\tilde{X}^1A_1'$ state has a planar equilibrium geometry belonging to the $D3h$ group. Despite its importance, there is a lack of high resolution spectroscopic data for CH_3^+ primarily because of its polymerization in discharges.[216] Oka and co-workers[216–218] observed the accurate frequency of the degenerate C–H stretch (ν_3) by infrared spectroscopy. There have also been reports[219–222] on the frequencies of the umbrella (out-of-plane or OPLA) mode (ν_2) and deformation mode (ν_4) primarily with photoelectron spectroscopy. However, no observed frequency of the non-degenerate C–H stretch (ν_1) has been available yet.

Following earlier computational studies,[223–228] Yu and Sears[229] performed a CC-CBS extrapolation akin to ours in the PES scan of CH_3^+. They employed the approach of Halkier *et al.*[230] based on the CCSD(T)/cc-pVTZ and cc-pVQZ energies at 227 geometries. The PES was expressed as a QFF in an internal coordinate. The raw PES was found to overestimate the frequencies of some of the fundamentals by 30 cm^{-1} and a coordinate scaling was applied to achieve the best overall agreement. The frequencies of Yu and Sears in Table 2.19 correspond to the scaled PES and experimental frequencies are taken from Refs.[216–222]

Anti-symmetric C–H stretch (ν_3) and deformation (ν_4) modes of CH_3^+ are doubly degenerate due to the $D3h$ symmetry. The 3MR approximation and our use of $C2v$ computational symmetry throughout the calculations can cause these degenerate modes to be treated in a non-equivalent manner. However, the lifting of degeneracy still stays about 1 cm^{-1} for both modes with the grid and hybrid QFF/grid PES representations. On the other hand, in the QFF calculations, the degeneracy of the ν_3 mode is lifted by 10 cm^{-1}, while that of the deformation mode is hardly affected. This is probably due to inevitable errors in finite-difference numerical differentiation used to obtain the QFF that are particularly large for ν_3 which experiences a strongly anharmonic Morse-type potential. We simply report the average of the two frequencies for the QFF results. It should be noted that the hybrid QFF/grid method resists to such numerical errors and preserves the degeneracy within 1 cm^{-1}, which is another advantage of our proposed scheme.

Although our CC-CBS calculations do not involve any coordinate scaling, their frequencies are in generally good agreement with the predictions of Yu and Sears. Hence, 2940 ± 20 cm^{-1} serves as a reliable predicted value of the frequency of ν_1, the experimental value of which is still unknown. The frequencies of the two other modes (ν_2 and ν_4) are exceedingly close to each other and the correct assignment on the basis of the observed and calculated frequencies alone is difficult. Here, our vibrationally-averaged rotational constants (shown in Table 2.20) can be useful in assisting in experimental spectroscopic studies. The theory predicts the C–H bond length and hence the values of both B and C are noticeably different between (0100) and (0001) states, which can, therefore, be spectroscopically discernible by rotational constants. The vibrational state dependence of the measured values of B and C are consistent with our prediction, although the absolute computed values of B can be erroneous by 2%.

The wave functions of the (0010) and (0001) states transform as e' and are doubly degenerate. The vibrationally-averaged structures in these states belong to of the C2v group, which is the Abelian sub-group of the D3h and the computational symmetry used in our calculation. For instance, one of the degenerate (0010) states has the C–H bond lengths of 1.1020, 1.1187, and 1.1187 Å and the HCH bond angles of 120.17, 120.17, and 119.65 degrees, whereas the other has the bond lengths of 1.1245, 1.1079, and 1.1079 Å and the bond angles of 119.83, 119.83, and 120.34 degrees. Because the degenerate states can be rotated by an arbitrary unitary transformation, these structures by themselves do not have particular physical significance. However, the averages of the C–H bond lengths (1.113 Å) and bond angles (120.0 degree) are invariant to this rotation and it is meaningful to compare these averages with the structures of other states. In the (0010) state, the average C–H bond length experiences a net increase of 0.01 Å from the zero-point value, reflecting the Morse-like shape of the C–H stretch. In our rigid-rotor treatment, the rotational constants of a degenerate state can be computed either from the averaged and hence D3h structure or from two C2v structures and then averaged afterwards. The values in Table 2.20 were obtained in the latter procedure. Owing to this ambiguity in our rigid-rotor treatment, the computed rotational constants are expected to be less accurate than the vibrationally-averaged structures.

2.3.7 CH_3 ($\tilde{X}^2A_2''$)

As its cationic counterpart, the methyl radical (CH_3) in the $\tilde{X}^2A_2''$ state has a planar structure that belongs to the D3h group. The planarity was a subject of controversy partly because of the rather small frequency (606 cm^{-1}) of the umbrella (OPLA) vibration (ν_2) that had been viewed as an indication of non-planar geometry until the planarity was confirmed spectroscopically by Yamada, Hirota, and Kawaguchi.[231] The frequency of the symmetric C–H stretch fundamental (ν_1) was the subject of many spectroscopic studies.[232–236] Those of the umbrella (OPLA) (ν_2)[231,237,238] and anti-symmetric C–H stretch (ν_3)[239–244] were also measured accurately. For the deformation (ν_4), approximate values of its frequency were obtained[245–248] by the matrix isolation technique and they were in the range of 1396 to 1403 cm^{-1}. No gas-phase measurements have so far been reported for this mode.

A considerable number of computational studies on CH_3 were reported,[223–225,249–257] but most of them focused on its electronic structure, geometry, and frequencies in the harmonic approximation and only a few were concerned with anharmonic vibrations. Surratt and Goddard[224] solved the one-dimensional vibrational Schrödinger problem along the umbrella mode (ν_2), assuming the planar equilibrium geometry and obtained the frequency of 585 cm^{-1}, which was in good agreement with the observed (606 cm^{-1}). Botschwina, Flesch, and Meyer[252] obtained a QFF in just two vibrational degrees of freedom with the coupled electron pair approximation (CEPA) method. Their computed frequencies of ν_1 and ν_2 were 63 and 8 cm^{-1} too high and too low, respectively. More recently, Neto, Chakravorty, and

Machado[257] performed the CBS extrapolation of the calculated C–H bond length and harmonic frequencies calculated at the CCSD(T) level. According to their study, large anharmonic contributions of 80–150 cm^{-1} exist inν_1, ν_2, and ν_3.

Table 2.22 compares our computed frequencies with the observed[231,234,239,245,247] as well as the previous calculations.[224,252,257] Our CC-CBS/hybrid/VCI frequencies are in good agreement with the observed although the error in the frequency of ν_2 (42 cm^{-1}) appears to be slightly outside the usual range. This may be due to a vibronic coupling between the ground and excited electronic states, as suggested by Burdett[258] and Yamada *et al.*[231] Another possible source of the error is the neglect of the rovibrational coupling in this study, which is known to be generally greater in out-of-plane modes.[259] Our predicted frequency of ν_4 is somewhat smaller than those measured in the matrices. A part of the error might be ascribed to matrix shifts, which are positive and do not exceed ca. 20 cm^{-1} forν_4.

Table 2.23 compares the vibrationally-averaged bond lengths and rotational constants with the observed.[231,234,239,244] The latter is available for three of the low-lying vibrationally excited states as well as for the zero-point vibrational state. The computed values of C (corresponding to the rotations around the $C3$ axis) reproduce the observed trend across different states reasonably well, although the agreement cannot be said to be quantitative. The theory also correctly predicts the increase in the C–H bond lengths in the (1000) state, which is clearly due to the Morse-like shape of the C–H stretch potential. However, it completely fails in reproducing even the signs of variation in the C–H bond lengths upon excitation to the (0100) and (0010) states. Although the bending vibrations usually decrease the average bond lengths and our result for the (0100) state appears to follow this trend, the experimental result[234] indicates the opposite. The predicted values of B do not agree well with the observed for almost all states considered. This may underscore the significance of the rovibrational couplings and also possibly be related to the aforementioned vibronic coupling operating in this molecule.

2.4 Conclusion

An accurate and predictive scheme to compute low-lying vibrational wave functions and energies of polyatomic molecules is proposed with applications to the seven key species of hydrocarbon combustion. The results have been compared with experimental values, whenever the latter are available. The agreement between theory and experiment for fundamental frequencies is within 11 cm^{-1} (the mean absolute deviation) for all the molecules. When only the triatomic molecules are considered, this deviation reduces to 7 cm^{-1}; the agreement in CH_3^+ and CH_3 is slightly worse partly because of the 3MR approximation and larger rovibrational couplings. For HOO^-, CH_3^+, and CH_3, of which some or all of experimental data for the fundamental transition frequencies are unknown, our predicted frequencies are expected to be no more than 20 cm^{-1} away from the correct values. In most cases, the vibrationally-averaged structural parameters and rotational constants reproduce their trend observed across different vibrational states. However, there

have been cases where the vibrationally-averaged rotational constants obtained in the rigid-rotor approximation are qualitatively incorrect. The core of this scheme is the converged PESs in wide areas of the geometry space obtained by combining different electronic structure methods [CCSD, CCSD(2)$_T$, and CCSD(2)$_{TQ}$] and basis sets (aDZ, aTZ, and aQZ) to extrapolate the CC-CBS limit. The results of these individual calculations are also presented in corresponding tables. This CC-CBS extrapolation is feasible because a common set of normal coordinates is used. The PESs generated by this method are represented by QFFs and numerical values on rectilinear grids, but the new hybrid representation has also been proposed to avoid the shortcomings of the former. This hybrid representation has been shown to be a uniform and inexpensive improvement over QFFs or grid PESs. The vibrational Schrödinger equation has been solved by VCI, which is exact for the triatomic molecules (all configurations are included) and sufficiently converged for the tetratomic molecules.

The approximations involved in this scheme are the Born–Oppenheimer approximation, the neglect of rovibrational coupling (centrifugal distortion and Coriolis coupling), non-relativistic treatment, the neglect of core-correlation effects, the higher-order electron-correlation and mode-mode coupling, etc. This scheme is inadequate for highly-excited vibrations or very large-amplitude vibrations owing to our dependence on normal coordinates. Although the use of internal coordinates and keeping all the terms in Watson Hamiltonian can avoid such problems in triatomic molecules, our scheme is expected to be more widely and generally applicable to larger polyatomic molecules with small amplitude vibrations.

2.5 Tables

Table 2.1: Comparison of the fundamental vibrational transitions energies (in cm^{-1}) of HNO obtained with different CBS extrapolations. Correlation energy (ΔE) is obtained by CCSD method and aXZ basis sets are used where X = D, T, and Q.

HF CBS	ΔE CBS	(100)[a]	(010)[a]	(001)[a]
Eq (2.1)	Eq (2.1)	1542.5	1655.6	2760.8
Eq (2.2)	Eq (2.2)	1543.5	1658.8	2760.9
Eq (2.1)	Eq (2.3)[b]	1543.2	1657.0	2763.3
Eq (2.2)	Eq (2.3)[b]	1543.5	1658.5	2763.2

[a] The vibrational quanta of the N–H stretch, bend, and N–O stretch, respectively.

[b] The aTZ and aQZ basis sets are used.

Table 2.2: Comparison of the three fundamental vibrational transitions energies (in cm^{-1}) of HOO^- obtained with three PES representations (QFF, grid, and hybrid QFF/grid) and the full VCI. Except for the grid CCSD(2)$_T$/aTZ results (the top row), which serve as the accurate reference frequencies, the differences from the reference values are shown.

PES	(100)a	(010)[a]	(001)[a]
CCSD(2)$_T$/aTZ (grid)	3572.2	1082.2	747.7
Hybrid QFF/grid[b]	+3.1	+0.5	+0.2
CCSD(2)$_T$/aTZ (QFF)	–21.5	+1.2	–11.6
CCSD/aDZ (grid)	+2.0	+17.4	+0.3
CCSD/aDZ (QFF)	–19.3	+24.6	–5.0

[a] The vibrational quanta of the O–H stretch, bend, and O–O stretch, respectively.

[b] Combines the PESs in the last three rows.

Table 2.3: Fundamental vibrational transition energies (in cm^{-1}) of HCO^+.

Method	(1000)[a]	(0110)[a]	(0001)[a]
CCSD/aDZ/grid/VCI	3092	833	2200
CCSD/aDZ/QFF/VCI	3077	822	2199
$CCSD(2)_T$/aDZ/QFF/VCI	3053	801	2131
$CCSD(2)_{TQ}$/aDZ/QFF/VCI	3049	795	2114
CCSD/aTZ/QFF/VCI	3098	836	2236
$CCSD(2)_T$/aTZ/QFF/VCI	3071	813	2167
CCSD/aQZ/QFF/VCI	3101	837	2250

[a] The vibrational quanta of the C–H stretch, bend, and C–O stretch, respectively.

Table 2.4: Fundamental vibrational transition energies (in cm^{-1}) of HCO^+.

Method	(1000)[a]	(0110)[a]	(0001)[a]
Experiment	3088.74[b]	829.72[c]	2183.95[d]
CC-CBS/hybrid/VCI[e]	3083	823	2175
CC-CBS/QFF/VCI[e]	3072	806	2176
$CCSD(2)_T$/aDZ/harmonic[e]	3214	837	2160
Mladenovic and Schmatz[113]	3086	831	2179
Puzzarini *et al.*[112]	3090[f]	831[f]	2183[f]
Martin, Taylor and Lee[111]	3088	824	2166
van Mourik, Dunning, and Peterson[114]	3083	823	2177

[a] The vibrational quanta of the C–H stretch, bend, and C–O stretch, respectively.

[b] Amano.[96]

[c] Davies and Rothwell.[98]

[d] Foster, McKellar, and Sears.[99]

[e] This work. The CC-CBS results are based on the CCSD/(aDZ, aTZ, aQZ), $CCSD(2)_T$/(aDZ, aTZ) and $CCSD(2)_{TQ}$/aDZ energies.

[f] The PES was scaled empirically.

Table 2.5: Vibrationally-averaged bond lengths (in Å) and rotational constant (B) (in cm^{-1}) of HCO^+ computed by the CC-CBS/hybrid/VCI method (experimental values, when available, in parentheses).

State[a]	(0000)[a]	(1000)[a]	(0110)[a]	(0001)[a]
r_{C-O}[b]	1.112	1.113	1.112	1.118
r_{C-H}[b]	1.096	1.127	1.081	1.099
B	1.48 (1.49)[c]	1.46 (1.48)[d]	1.49 (1.49)[e]	1.46 (1.48)[f]

[a] The vibrational quanta of the C–H stretch, bend, and C–O stretch, respectively.

[b] The equilibrium bond lengths are 1.10474 (r_{C-O}) and 1.09725 Å(r_{C-H}) according to Woods.[91]

[c] Sastry, Herbst, and de Lucia.[88]

[d] Amano.[96]

[e] Davies and Rothwell.[98]

[f] Davies, Hamilton, and Rothwell.[97]

Table 2.6: Fundamental vibrational transition energies (in cm^{-1}) of HCO.

Method	(100)[a]	(010)[a]	(001)[a]
CCSD/aDZ/grid/VCI	2428	1069	1877
CCSD/aDZ/QFF/VCI	2402	1069	1872
CCSD(2)$_T$/aDZ/QFF/VCI	2363	1060	1829
CCSD(2)$_{TQ}$/aDZ/QFF/VCI	2358	1057	1813
CCSD/aTZ/QFF/VCI	2450	1088	1913
CCSD(2)$_T$/aTZ/QFF/VCI	2413	1077	1865
CCSD/aQZ/QFF/VCI	2449	1092	1927

[a] The vibrational quanta of the C–H stretch, bend, and C–O stretch,respectively.

Table 2.7: Fundamental vibrational transition energies (in cm^{-1}) of HCO.

Method	(100)[a]	(010)[a]	(001)[a]
Experiment	2434.48[b]	1080.76[c]	1868.17[c]
CC-CBS/hybrid/VCI[d]	2432	1079	1874
CC-CBS/QFF/VCI[d]	2403	1081	1870
CCSD(2)$_T$/aDZ/harmonic[d]	2683	1100	1848
Werner *et al.*[144]	2446	1081	1844
Serrano-Andrs, Forsberg, and Malmqvist[148]	2443	1072	1851
van Mourik, Dunning, and Peterson[114]	2461	1079	1866
Marenich and Boggs[151]	2416	1076	1885

[a] The vibrational quanta of the C–H stretch, bend, and C–O stretch, respectively.

[b] Dane *et al.*[120]

[c] Johns, McKellar, and Riggin.[124]

[d] This work. The CC-CBS results are based on the CCSD/(aDZ, aTZ, aQZ), CCSD(2)$_T$/(aDZ, aTZ) and CCSD(2)$_{TQ}$/aDZ energies.

Table 2.8: Vibrationally-averaged bond lengths (in Å) and angle (in degrees) and rotational constants (A, B, and C) (in cm^{-1}) of HCO computed by the CC-CBS/hybrid/VCI method (experimental values, when available, in parentheses).

State[a]	(000)[a]	(100)[a]	(010)[a]	(001)[a]
$r_{C–H}$	1.141 (1.151[b], 1.125[c])	1.199	1.133	1.140
$r_{C–O}$	1.180 (1.178[b], 1.175[c])	1.176	1.180	1.188
a_{HCO}	124.3 (123.0[b], 125.0[c])	123.7	124.5	124.1
A	23.2 (24.3[d], 24.3[e])	20.9	23.6	23.1
B	1.48 (1.47[d], 1.49[e])	1.48	1.48 (1.50)[c]	1.47
C	1.39 (1.37[d], 1.40[e])	1.38	1.40 (1.39)[c]	1.38

[a] The vibrational quanta of the C–H stretch, bend, and C–O stretch, respectively.

[b] Ogilvie.[154]

[c] Brown and Ramsay.[123]

[d] Hirota.[153]

[e] Brown, Radford, and Sears.[152]

Table 2.9: Fundamental vibrational transition energies (in cm^{-1}) of HNO.

Method	(100)[a]	(010)[a]	(001)[a]
CCSD/aDZ/grid/VCI	2701	1518	1616
CCSD/aDZ/QFF/VCI	2701	1512	1613
$CCSD(2)_T$/aDZ/QFF/VCI	2637	1480	1553
$CCSD(2)_{TQ}$/aDZ/QFF/VCI	2627	1467	1532
CCSD/aTZ/QFF/VCI	2749	1531	1629
$CCSD(2)_T$/aTZ/QFF/VCI	2681	1496	1565
CCSD/aQZ/QFF/VCI	2757	1538	1645

[a] The vibrational quanta of the N–H stretch, bend, and N–O stretch, respectively.

Table 2.10: Fundamental vibrational transition energies (in cm^{-1}) of HNO.

Method	(100)[a]	(010)[a]	(001)[a]
Experiment	2683.95[b]	1500.82[c]	1565.35[c]
CC-CBS/hybrid/VCI[d]	2683	1503	1572
CC-CBS/QFF/VCI[d]	2679	1499	1568
$CCSD(2)_T$/aDZ/harmonic[d]	2909	1531	1590
Dateo, Lee, and Schwenke[177]	2667	1507	1571
Mordaunt *et al.*[179]	2682[e]	1502[e]	1563[e]

[a] The vibrational quanta of the N–H stretch, bend, and N–O stretch, respectively.

[b] Johns, McKellar, and Weinberger.[166]

[c] Johns and McKellar.[165]

[d] This work. The CC-CBS results are based on the CCSD/(aDZ, aTZ, aQZ), $CCSD(2)_T$/(aDZ, aTZ) and $CCSD(2)_{TQ}$/aDZ energies.

[e] The PES was scaled empirically.

Table 2.11: Vibrationally-averaged bond lengths (in Å) and angle (in degrees) and rotational constants (A, B, and C) (in cm^{-1}) of HNO computed by the CC-CBS/hybrid/VCI method (experimental values, when available, in parentheses).

State[a]	(000)[a]	(100)[a]	(010)[a]	(001)[a]
$r_{N–H}$	1.075 (1.09[b], 1.063[c])	1.124	1.071	1.075
$r_{N–O}$	1.213 (1.209[b], 1.212[c])	1.208	1.217	1.221
a_{HNO}	108.4 (108.0[b], 108.6[c])	108.7	108.4	108.5
A	18.2 (18.5)[d,e]	16.8 (17.7)[d]	18.3 (18.8)[d,e]	18.2 (18.6)[d,e]
B	1.40 (1.41)[d,e]	1.41(1.42[d])	1.39 (1.41)[d,e]	1.38 (1.40)[d,e]
C	1.30 (1.31)[d,e]	1.30 (1.31[d])	1.30 (1.29[d], 1.30[e])	1.29 (1.30[d], 1.29[e])

[a] The vibrational quanta of the N–H stretch, bend, and N–O stretch, respectively.

[b] Ogilvie.[154]

[c] Dalby.[158]

[d] Johns, McKellar, and Weinberger.[166]

[e] Johns and McKellar.[165]

Table 2.12: Fundamental vibrational transition energies (in cm^{-1}) of HOO.

Method	(100)[a]	(010)[a]	(001)[a]
CCSD/aDZ/grid/VCI	3447	1409	1090
CCSD/aDZ/QFF/VCI	3426	1410	1088
$CCSD(2)_T$/aDZ/QFF/VCI	3380	1383	1054
$CCSD(2)_{TQ}$/aDZ/QFF/VCI	3366	1374	1045
CCSD/aTZ/QFF/VCI	3476	1420	1136
$CCSD(2)_T$/aTZ/QFF/VCI	3422	1390	1101
CCSD/aQZ/QFF/VCI	3489	1431	1154

[a] The vibrational quanta of the O–H stretch, bend, and O–O stretch, respectively.

Table 2.13: Fundamental vibrational transition energies (in cm^{-1}) of HOO.

Method	(100)[a]	(010)[a]	(001)[a]
Experiment	3436.20[b]	1391.75[c]	1097.63[d]
CC-CBS/hybrid/VCI[e]	3447	1399	1121
CC-CBS/QFF/VCI[e]	3424	1400	1118
$CCSD(2)_T$/aDZ/harmonic[e]	3628	1428	1080
Walch and Duchovic[194]	3356	1415	1206
Xu *et al.*[197]	3433	1389	1090

[a] The vibrational quanta of the O–H stretch, bend, and O–O stretch, respectively.

[b] Yamada, Endo, and Hirota.[186]

[c] Nagai, Endo, and Hirota.[188]

[d] Johns, McKellar, and Riggin.[190]

[e] This work. The CC-CBS results are based on the CCSD/(aDZ, aTZ, aQZ), $CCSD(2)_T$/(aDZ, aTZ) and $CCSD(2)_{TQ}$/aDZ energies.

Table 2.14: Vibrationally-averaged bond lengths (in Å) and angle (in degrees) and rotational constants (A, B, and C) (in cm^{-1}) of HOO computed by the CC-CBS/hybrid/VCI method (experimental values, when available, in parentheses).

State[a]	(000)[a]	(100)[a]	(010)[a]	(001)[a]
$r_{O–H}$	0.984 (1.006[b], 0.977[c])	1.022	0.977	0.983
$r_{O–O}$	1.333 (1.333[b], 1.334[c])	1.330	1.337	1.345
a_{HOO}	104.6 (104.4[b], 104.1[c])	105.0	104.9	104.0
A	20.2 (20.4)[d]	18.8 (19.6)[e]	20.5 (21.0)[f]	20.1 (20.3)[g]
B	1.12 (1.12)[d]	1.12 (1.12)[e]	1.11 (1.12)[f]	1.10 (1.11)[g]
C	1.06 (1.06)[d]	1.06 (1.06)[e]	1.05 (1.05)[f]	1.04 (1.04)[g]

[a] The vibrational quanta of the O–H stretch, bend, and O–O stretch, respectively.

[b] Ogilvie.[154]

[c] Barnes, Brown, and Radford.[193]

[d] Barnes *et al.*[192]

[e] Yamada, Endo, and Hirota.[186]

[f] Nagai, Endo, and Hirota.[188]

[g] Johns, McKellar, and Riggin.[190]

Table 2.15: Fundamental vibrational transition energies (in cm^{-1}) of HOO^-.

Method	(100)[a]	(010)[a]	(001)[a]
CCSD/aDZ/grid/VCI	3574	1100	748
CCSD/aDZ/QFF/VCI	3553	1107	743
CCSD$(2)_T$/aDZ/QFF/VCI	3516	1090	688
CCSD$(2)_{TQ}$/aDZ/QFF/VCI	3503	1060	648
CCSD/aTZ/QFF/VCI	3591	1118	796
CCSD$(2)_T$/aTZ/QFF/VCI	3551	1083	736
CCSD/aQZ/QFF/VCI	3610	1129	802

[a] The vibrational quanta of the O–H stretch, bend, and O–O stretch, respectively.

Table 2.16: Fundamental vibrational transition energies (in cm^{-1}) of HOO^-.

Method	(100)[a]	(010)[a]	(001)[a]
Experiment			775 ± 250[b]
CC-CBS/hybrid/VCI[c]	3587	1088	739
CC-CBS/QFF/VCI[c]	3561	1084	742
CCSD$(2)_T$/aDZ/harmonic[c]	3768	1109	725
Horn *et al.*[211]	3585	1073	728
Chan and Hamilton[212]	3665	1079	685
Botschwina and Horn[206]	3581	1084	728

[a] The vibrational quanta of the O–H stretch, bend, and O–O stretch, respectively.

[b] Oakes, Harding, and Ellison.[210]

[c] This work. The CC-CBS results are based on the CCSD/(aDZ, aTZ, aQZ), CCSD$(2)_T$/(aDZ, aTZ) and CCSD$(2)_{TQ}$/aDZ energies.

Table 2.17: Vibrationally-averaged bond lengths (in Å) and angle (in degrees) and rotational constants (A, B, and C) (in cm^{-1}) of HOO^- computed by the CC-CBS/hybrid/VCI method (experimental values, when available, in parentheses).

State[a]	(000)[a]	(100)[a]	(010)[a]	(001)[a]
r_{O-H}	0.969 (0.97[b,c])	1.006	0.958	0.967
r_{O-O}	1.525 (1.50)[b]	1.520	1.535	1.541
a_{HOO^-}	97.7 (104[b,c])	98.5	97.2	96.7
A	19.5	18.2	19.9	19.5
B	0.87	0.87	0.86	0.85
C	0.83	0.83	0.82	0.82

[a] The vibrational quanta of the O–H stretch, bend, and O–O stretch, respectively.

[b] Oakes, Harding, and Ellison.[210]

[c] Assumed values.[210]

Table 2.18: Fundamental vibrational transition energies (in cm^{-1}) of CH_3^+.

Method	(1000)[a]	(0100)[a]	(0010)[a]	(0001)[a]
CCSD/aDZ/grid/VCI	2935	1385	3099	1375
CCSD/aDZ/QFF/VCI	2930	1381	3106	1371
$CCSD(2)_T$/aDZ/QFF/VCI	2919	1376	3096	1365
$CCSD(2)_{TQ}$/aDZ/QFF/VCI	2917	1375	3095	1365
CCSD/aTZ/QFF/VCI	2945	1390	3106	1389
$CCSD(2)_T$/aTZ/QFF/VCI	2931	1384	3094	1381
CCSD/aQZ/QFF/VCI	2948	1391	3110	1392

[a] The vibrational quanta of the symmetric C–H stretch (a_1'), umbrella (a_2''), anti-symmetric C–H stretch (e'), and deformation (e'), respectively.

Table 2.19: Fundamental vibrational transition energies (in cm^{-1}) of CH_3^+.

Method	(1000)[a]	(0100)[a]	(0010)[a]	(0001)[a]
Experiment		1359 ± 7[b]	3108.38[c]	1370 ± 7[b]
CC-CBS/hybrid/VCI[d]	2940	1383	3096	1384
CC-CBS/QFF/VCI[d]	2933	1383	3099[e]	1385
$CCSD(2)_T$/aDZ/harmonic[d]	3037	1418	3247	1429
Yu and Sears[229]	2942[f]	1378[f]	3108[f]	1387[f]

[a] The vibrational quanta of the symmetric C–H stretch (a_1'), umbrella (a_2''), anti-symmetric C–H stretch (e'), and deformation (e'), respectively.

[b] Liu, Gross, and Suits.[222]

[c] Crofton *et al.*[216]

[d] This work. The CC-CBS results are based on the CCSD/(aDZ, aTZ, aQZ), $CCSD(2)_T$/(aDZ, aTZ) and $CCSD(2)_{TQ}$/aDZ energies.

[e] The average of 3094 and 3105 cm^{-1} (see text).

[f] The PES was scaled empirically.

Table 2.20: Vibrationally-averaged C–H bond length (in Å) and rotational constants (B and C) (in cm^{-1}) of CH_3^+ computed by the CC-CBS/hybrid/VCI method (experimental values, when available, in parentheses).

State[a]	(0000)[a]	(1000)[a]	(0100)[a]	(0010)[a]	(0001)[a]
r_{C-H}	1.102 (1.1)[b]	1.112	1.100	1.113[c]	1.101[d]
B	9.18 (9.36)[e]	9.02	9.21 (9.1)[f]	9.00[g]	9.20[h](9.1)[f]
C	4.59 (4.61)[b]	4.51	4.61	4.50	4.60

[a] The vibrational quanta of the symmetric C–H stretch (a_1'), umbrella (a_2''), anti-symmetric C–H

[b] Crofton *et al.*[216]

[c] One of the degenerate states has the bond lengths of 1.1245, 1.1079 and 1.1079 Å and bond angles of 119.83, 119.83, and 120.33 degrees. The other has the bond lengths of 1.1020, 1.1187 and 1.1187 Å and bond angles of 120.17, 120.17, and 119.65 degrees.

[d] One of the degenerate states has the bond lengths of 1.1030, 1.0997 and 1.0997 Å and bond angles of 119.67, 119.67, and 120.67 degrees. The other has the bond lengths of 1.0983, 1.1020 and 1.1020Å and bond angles of 120.33, 120.33, and 119.35 degrees.

[e] Jagod *et al.*[218]

[f] Liu, Gross, and Suits.[222]

[g] The average of 9.06 and 8.94 cm^{-1}.

[h] The average of 9.24 and 9.16 cm^{-1}.

Table 2.21: Fundamental vibrational transition energies (in cm^{-1}) of CH_3.

Method	(1000)[a]	(0100)[a]	(0010)[a]	(0001)[a]
CCSD/aDZ/grid/VCI	2992	546	3132	1369
CCSD/aDZ/QFF/VCI	2987	559	3130	1365
$CCSD(2)_T$/aDZ/QFF/VCI	2972	556	3116	1358
$CCSD(2)_{TQ}$/aDZ/QFF/VCI	2970	556	3114	1357
CCSD/aTZ/QFF/VCI	3011	579	3146	1386
$CCSD(2)_T$/aTZ/QFF/VCI	2995	576	3131	1377
CCSD/aQZ/QFF/VCI	3015	581	3153	1387

[a] The vibrational quanta of the symmetric C–H stretch (a_1'), umbrella (a_2''), anti-symmetric C–H stretch (e'), and deformation (e'), respectively.

Table 2.22: Fundamental vibrational transition energies (in cm^{-1}) of CH_3.

Method	(1000)[a]	(0100)[a]	(0010)[a]	(0001)[a]
Experiment	3004.4[b]	606.45[c]	3160.82[d]	(1396[e], 1403[f])
CC-CBS/hybrid/VCI[g]	3002	565	3139	1377
CC-CBS/QFF/VCI[g]	2998	580	3139[h]	1375
CCSD(2)$_T$/aDZ/harmonic[g]	3103	498	3292	1407
Surratt and Goddard[224]		585		
Botschwina, Flesch, and Meyer[252]	3067	598		
Roberto-Neto, Chakravorty, and Machado[257]	3129[i]	524[i]	3313[i]	1424[i]

[a] The vibrational quanta of the symmetric C–H stretch (a_1'), umbrella (a_2''), anti-symmetric C–H stretch (e'), and deformation (e'), respectively.

[b] Triggs *et al.*[234]

[c] Yamada, Hirota, and Kawaguchi.[231]

[d] Amano *et al.*[239]

[e] A matrix-isolation study by Snelson.[245]

[f] A matrix-isolation study by Momose *et al.*[247]

[g] This work. The CC-CBS results are based on the CCSD/(aDZ, aTZ, aQZ), CCSD(2)$_T$/(aDZ, aTZ) and CCSD(2)$_{TQ}$/aDZ energies.

[h] The average of 3133 and 3144 cm^{-1} (see text).

[i] CCSD(T)/CBS in the harmonic approximation.

Table 2.23: Vibrationally-averaged C–H bond length (in Å) and rotational constants (B and C) (in cm^{-1}) of CH_3 computed by the CC-CBS/hybrid/VCI method (experimental values, when available, in parentheses).

State[a]	(0000)[a]	(1000)[a]	(0100)[a]	(0010)[a]	(0001)[a]
$r_{C–H}$	1.087 (1.079)[b]	1.097 (1.084)[b]	1.080 (1.097)[b]	1.098[c](1.085)[b]	1.086[d]
B	9.43 (9.58)[e]	9.26 (9.49)[b]	9.56 (9.26)[e]	9.26[f](9.47)[e,g,h]	9.47[i]
C	4.72 (4.74)[e]	4.63 (4.69)[b]	4.78 (4.81)[e]	4.63 (4.70)[g,h]	4.73

[a] The vibrational quanta of the symmetric C–H stretch (a_1'), umbrella (a_2''), anti-symmetric C–H stretch (e'), and deformation (e'), respectively.

[b] Triggs *et al.*[234]

[c] One of the degenerate states has the bond lengths of 1.0864, 1.1031 and 1.1031 Å and bond angles of 120.27, 120.27, and 119.47 degrees. The other has the bond lengths of 1.1086, 1.0925, and 1.0925 Å and bond angles of 119.75, 119.75, and 120.49 degrees.

[d] One of the degenerate states has the bond lengths of 1.0882, 1.0843 and 1.0843 Å and bond angles of 119.68, 119.68, and 120.65 degrees. The other has the bond lengths of 1.0826, 1.0870, and 1.0870 Å and bond angles of 120.32, 120.32, and 119.36 degrees.

[e] Yamada, Hirota, and Kawaguchi.[231]

[f] The average of 9.30 and 9.21 cm^{-1}.

[g] Amano *et al.*[239]

[h] The average of 9.50 and 9.43 cm^{-1}.

[i] Kawaguchi.[244]

Chapter 3

First-principles methods for anharmonic lattice vibrations

3.1 Introduction

Electronic structures of infinitely extended systems with one-dimensional periodicity (e.g. crystalline polymers) can be characterized accurately by crystalline orbital (CO) theory.[260–262] They are based on size-extensive approximations such as the Hartree–Fock (HF),[263–265] second- and third-order Møller–Plesset perturbation (MP2 and MP3),[266–268] and coupled-cluster singles and doubles (CCSD) methods.[51,268] The corresponding methods for vibrational structures have also been established[8,269–271] presently for molecules only as the vibrational self-consistent field (VSCF),[67–69,272] vibrational Møller–Plesset perturbation (VMP),[13,40,273] vibrational configuration-interaction (VCI),[12] and vibrational coupled-cluster (VCC) methods (for more details see Section 1.6).[274–277] They allow anharmonicity in potential energy surfaces (PES) and resulting mode-mode coupling to be accounted for in vibrational spectra[46,47] and vibrationally averaged properties.[2,45] However, these vibrational methods have not thus far been applied to anharmonic lattice vibrations in solids apart from a few notable exceptions;[278–280] nor have their formalisms been shown rigorously to have the correct size dependence and be safely applicable to extended systems. For a pioneering analysis of this issue, the reader is referred to Christiansen.[15]

The objective of this chapter* is to present size-extensive generalizations of the VSCF, first- and second-order VMP (VMP1 and VMP2), and VCC methods for extended systems of one-dimensional periodicity in delocalized normal coordinates. The conclusion drawn should be applicable to extended systems of two- and three-dimensional periodicity. The size dependence of the methods is determined by inspecting the asymptotic functional dependence of various quantities that enter their formalisms upon the number (K) of k vectors in the first Brillouin zone (BZ).[262,282] The analysis has revealed that copious terms in the formalisms of VSCF have nonphysical size dependence. These terms have been identified algebraically and eliminated so that compact and strictly size-extensive equations are obtained for a quartic force field (QFF), defining the size-extensive VSCF method (XVSCF) as well as the VMP and VCC methods in a QFF (XVMP and XVCC) based on a XVSCF reference. The XVSCF method has no contributions from cubic force constants and alters only the frequencies of the underlying harmonic-oscillator reference from a sub-

*The work in this chapter has been published in Ref. 281. Reprint permission is granted by American Institute of Physics.

set of quartic force constants. It also provides a way to evaluate an anharmonic correction to the lattice structure due to cubic force constants of a certain type. The VMP2 and VCC methods include the anharmonic effects due to all cubic and quartic force constants in a size-extensive fashion. It is also shown algebraically that VCI lacks size-extensivity. This chapter reports only the equations defining these methods and a formal analysis of size-extensivity.

3.2 Electronic structures

This section briefly reviews the established formalism of the MP2 CO method to illustrate the algebraic method of analyzing size-extensivity. In the periodic boundary conditions, a one-dimensional extended system is viewed as a ring of K identical repeat units. A symmetry-adapted orbital such as a canonical Hartree–Fock (HF) orbital is then delocalized over the entire ring and has the Bloch form:

$$\varphi_{pk_p} = K^{-1/2} \sum_{\mu} \sum_{m} c^{\mu}_{pk_p} \exp(-imk_p a) \chi_{\mu}(\mathbf{r} - m\mathbf{a}), \tag{3.1}$$

where $c^{\mu}_{pk_p}$ is an expansion coefficient, m is the unit cell index and runs over all K unit cells in the system, $\mathbf{a}$ is the lattice vector, and $\chi_{\mu}(\mathbf{r} - m\mathbf{a})$ is the μth atomic orbital (AO) centered in the mth unit cell. Each orbital is characterized by the linear quasi-momentum k_p, which can take one of the following K distinct values:

$$k_p = \frac{2n}{K}, \{n \in \mathbb{Z} | 0 \leq n < K\}, \tag{3.2}$$

where the unit of length is adopted in which $|\mathbf{a}| = \pi$. Notice the dual role played by K in the periodic boundary conditions: K is the nominal size of the extended system and also the number of distinct k vectors in the first BZ. We use this knowledge to establish whether a method is size-extensive and, therefore, applicable to extended systems.[262,282]

Take the MP2 theory[51] as an example. The correlation energy of the entire ring is given by

$$E_{\mathrm{MP2}} = \sum_{i,j,a,b} \sum_{k_i,k_j,k_a} \frac{v^{ik_i jk_j}_{ak_a bk_b} \left(2v^{ik_i jk_j}_{ak_a bk_b} - v^{ik_i jk_j}_{bk_b ak_a}\right)^*}{e_{ik_i} + e_{jk_j} - e_{ak_a} - e_{bk_b}}, \tag{3.3}$$

where the CO-based one- and two-electron integrals are related to the AO-based counterparts defined elsewhere[51] by

$$e_{pk_p} = K^0 \sum_{\mu,\nu} \sum_{m} c^{\mu *}_{pk_p} c^{\nu}_{pk_p} \exp(-imk_p a) f^{\mu(0)}_{\nu(m)}, \tag{3.4}$$

$$v^{pk_p qk_q}_{rk_r sk_s} = K^{-1} \sum_{\kappa,\lambda,\mu,\nu} \sum_{m_1} \sum_{m_2} \sum_{m_3} c^{\kappa *}_{pk_p} c^{\lambda}_{rk_r} c^{\mu *}_{qk_q} c^{\nu}_{sk_s} \exp\left\{i(-m_1 k_r + m_2 k_q - m_3 k_s)a\right\} v^{\kappa(0)\mu(m_2)}_{\lambda(m_1)\nu(m_3)}. \tag{3.5}$$

The k summation (BZ integration) in Equation (3.3) is only three-fold although there are four distinct k vectors in the

summand. This is because the v integrals vanish identically unless the following momentum conservation condition is satisfied:

$$k_i + k_j - k_a - k_b = 2n, \{n \in \mathbb{Z}\}. \tag{3.6}$$

We can establish[262] the size-extensivity of MP2 by inspecting the K dependence of the quantities entering Equation (3.3). The numerator in the equation displays K^{-2} dependence as v is inversely proportional to K [Equation (3.5)]. The denominator does not depend on K because of Equation (3.4). The three-fold k summation gives rise to the factor of K^3. Together they make E_{MP2} exhibit asymptotic K^1 dependence and thus proportional to size, as expected for a size-extensive theory.

3.3 Vibrational structures

3.3.1 Normal coordinates

The normal coordinates and harmonic-oscillator wave functions[283,284] form the basis of our theories. Harmonic force constants of an extended system of one-dimensional periodicity may be obtained in Cartesian coordinates as

$$F_{\mu(0)\nu(m)} = \frac{\partial^2 V}{\partial X_{\mu(0)} \partial X_{\nu(m)}}, \tag{3.7}$$

where V is an electronic energy of the whole system and $X_{\nu(m)}$ is the νth Cartesian coordinate in the mth unit cell. While V is size-extensive, the force constants are size-intensive because they are associated with spatially local coordinates. Its discrete Fourier transform defines the dynamical force-constant matrix,

$$F_k^{\mu\nu} = \sum_m F_{\mu(0)\nu(m)} \exp(-imka), \tag{3.8}$$

and the dynamical mass-weighted force-constant matrix,

$$\tilde{F}_k^{\mu\nu} = m_\mu^{-1/2} F_k^{\mu\nu} m_\nu^{-1/2}, \tag{3.9}$$

where m_ν is the atomic mass associated with the νth Cartesian coordinate. The diagonalization of the latter yields squared harmonic frequencies ($\omega^2_{pk_p}$) and normal-mode vectors ($C^\mu_{pk_p}$) as eigenvalues and eigenvectors, respectively:

$$\sum_\nu \tilde{F}^{\mu\nu}_{k_p} C^\nu_{pk_p} = \omega^2_{pk_p} C^\mu_{pk_p}. \tag{3.10}$$

The pth branch of the phonon dispersion curves can be obtained by plotting the frequency ω_{pk_p} as a function of the linear quasi-momentum k_p. There are $3N$ such branches (N is the number of atoms in a unit cell) and they are categorized into $3N-4$ ($3N-3$) optical and 4 (3) acoustic phonon branches (the values in parentheses are for a linelike polymer).

A complex normal coordinate is defined as the orthonormal linear combination of mass-weighted Cartesian coordinates,[285]

$$Q_{pk_p} = K^{-1/2} \sum_{\nu} \sum_{m} m_{\nu}^{1/2} C_{pk_p}^{\nu} \exp(-imk_p a) X_{\nu(m)}, \tag{3.11}$$

which satisfies $Q_{pk_p}^{*} = Q_{p-k_p}$. In the BO approximation, the vibrational Hamiltonian is

$$\hat{H}_{\mathrm{n}} = -\frac{1}{2} \sum_{p} \sum_{k_p} \frac{\partial^2}{\partial Q_{pk_p}^{*} \partial Q_{pk_p}} + V, \tag{3.12}$$

where V (the potential energy surface or PES) is an electronic energy of the whole system (not an energy per unit cell). In the harmonic approximation,

$$V = V_{\mathrm{HRM}} \equiv \frac{1}{2} \sum_{p} \sum_{k_p} \omega_{pk_p}^2 Q_{pk_p}^{*} Q_{pk_p}. \tag{3.13}$$

The normal coordinates of the first kind,[285] which are real, can be defined by

$$Q_{pk_p} = 2^{-1/2} \left(q_{pk_p} + i\bar{q}_{pk_p} \right), \tag{3.14}$$

$$Q_{pk_p}^{*} = 2^{-1/2} \left(q_{pk_p} - i\bar{q}_{pk_p} \right), \tag{3.15}$$

except when $k_p = 0$ in which case $Q_{p0} = Q_{p0}^{*} = q_{p0}$ ($\bar{q}_{p0}$ is not defined). They satisfy the relations, $q_{p-k_p} = q_{pk_p}$ and $\bar{q}_{p-k_p} = -\bar{q}_{pk_p}$, and, therefore, the nonredundant set of independent k vectors in these coordinates spans just one half BZ. In these coordinates, the Hamiltonian in the harmonic approximation reduces to the sum of the Hamiltonians of independent harmonic oscillators,

$$\hat{H}_{\mathrm{HRM}} = -\frac{1}{2} \sum_{p} {\sum_{k_p}}' \frac{\partial^2}{\partial q_{pk_p}^2} - \frac{1}{2} \sum_{p} {\sum_{k_p}}' \frac{\partial^2}{\partial \bar{q}_{pk_p}^2} + \frac{1}{2} \sum_{p} {\sum_{k_p}}' \omega_{pk_p}^2 q_{pk_p}^2 + \frac{1}{2} \sum_{p} {\sum_{k_p}}' \omega_{pk_p}^2 \bar{q}_{pk_p}^2, \tag{3.16}$$

where the primes indicate that the summations are taken over only the nonredundant set of k vectors. The vibrational Schrödinger equation of this Hamiltonian is subject to complete separation of variables and can thus be solved exactly. For a state characterized by a string of quantum numbers $\mathbf{v} \equiv v_{1k_0} \ldots v_{(3N)k_{K/2}} \bar{v}_{1k_1} \ldots \bar{v}_{(3N)k_{K/2}}$, the wave function and

energy of the whole system are given by

$$\Phi^{\mathbf{v}}_{\mathrm{HRM}} = \prod_{p}\prod_{k_p}{}' \eta^{v_{pk_p}}_{pk_p}(q_{pk_p}) \prod_{p}\prod_{k_p}{}' \eta^{\bar{v}_{pk_p}}_{pk_p}(\bar{q}_{pk_p}), \tag{3.17}$$

$$E^{\mathbf{v}}_{\mathrm{HRM}} = \sum_{p}\sum_{k_p}{}' \omega_{pk_p}\left(v_{pk_p}+1/2\right) + \sum_{p}\sum_{k_p}{}' \omega_{pk_p}\left(\bar{v}_{pk_p}+1/2\right), \tag{3.18}$$

where the symbols with overbars are associated with $\bar{q}_{pk_p}$ and those without overbars with q_{pk_p}. The one-mode wave function with the quantum number v_{pk_p} is

$$\eta^{v_{pk_p}}_{pk_p}(q_{pk_p}) = N_{v_{pk_p}} H_{v_{pk_p}}(\omega^{1/2}_{pk_p} q_{pk_p}) \exp(-\omega_{pk_p} q^2_{pk_p}/2). \tag{3.19}$$

The explicit expressions of the normalization coefficients $N_{v_{pk_p}}$ and the Hermite polynomials $H_{v_{pk_p}}$ are found in many places.[19] The functional forms of $\eta^{v_{pk_p}}_{pk_p}$ and $\eta^{\bar{v}_{pk_p}}_{pk_p}$ are identical to each other when $v_{pk_p} = \bar{v}_{pk_p}$. It is evident that ω_{pk_p} and $E^{\mathbf{v}}_{\mathrm{HRM}}$ are K^0 (size-intensive) and K^1 (size-extensive) quantities, respectively.

3.3.2 Anharmonic potential energy functions

There are a number of ways to approximate V.[286] In view of the enormous dynamical degrees of freedom in an extended system, one practical way will be to expand V in a Taylor series and truncate it after a finite order. A QFF (Refs.[56] and[57]) in the normal coordinates is written as

$$\begin{aligned} V &= \sum_{p} F_{p0} Q_{p0} + \frac{1}{2!}\sum_{p,q}\sum_{k_p} F_{pk_pqk_q} Q_{pk_p} Q_{qk_q} + \frac{1}{3!}\sum_{p,q,r}\sum_{k_p,k_q} F_{pk_pqk_qrk_r} Q_{pk_p} Q_{qk_q} Q_{rk_r} \\ &\quad + \frac{1}{4!}\sum_{p,q,r,s}\sum_{k_p,k_q,k_r} F_{pk_pqk_qrk_rsk_s} Q_{pk_p} Q_{qk_q} Q_{rk_r} Q_{sk_s} \qquad (3.20) \\ &= \sum_{p} F_{p0} q_{p0} + \frac{1}{2!2}\sum_{p,q}\sum_{k_p} F_{pk_pqk_q}\left(q_{pk_p} q_{qk_q} + 2i q_{pk_p}\bar{q}_{qk_q} - \bar{q}_{pk_p}\bar{q}_{qk_q}\right) \\ &\quad + \frac{1}{3!2^{3/2}}\sum_{p,q,r}\sum_{k_p,k_q} F_{pk_pqk_qrk_r}\left(q_{pk_p} q_{qk_q} q_{rk_r} + 3i q_{pk_p} q_{qk_q}\bar{q}_{rk_r} - 3 q_{pk_p}\bar{q}_{qk_q}\bar{q}_{rk_r} - i\bar{q}_{pk_p}\bar{q}_{qk_q}\bar{q}_{rk_r}\right) \\ &\quad + \frac{1}{4!2^2}\sum_{p,q,r,s}\sum_{k_p,k_q,k_r} F_{pk_pqk_qrk_rsk_s}\left(q_{pk_p} q_{qk_q} q_{rk_r} q_{sk_s} + 4i q_{pk_p} q_{qk_q} q_{rk_r}\bar{q}_{sk_s} - 6 q_{pk_p} q_{qk_q}\bar{q}_{rk_r}\bar{q}_{sk_s}\right. \\ &\quad \left. -4i q_{pk_p}\bar{q}_{qk_q}\bar{q}_{rk_r}\bar{q}_{sk_s} + \bar{q}_{pk_p}\bar{q}_{qk_q}\bar{q}_{rk_r}\bar{q}_{sk_s}\right), \qquad (3.21) \end{aligned}$$

where the summations take into consideration the fact that the force constants (F) in the normal coordinates vanish identically unless the sum of the momenta is conserved (see below). The second equality follows from Equations (3.14) and (3.15). When the k summations are taken over the whole first BZ (as in the above equation), the factor of $2^{-1/2}$ needs to be associated with each q_{pk_p} or $\bar{q}_{pk_p}$ except q_{p0}. This exception is not made explicit for notational

simplicity unless k vectors are specifically zero.

The following analysis does not substantially depend on this particular truncation order and can thus be extended readily to a higher-order truncated Taylor expansion of V (if not to a grid-based numerical representation). As will become clear, cubic and quartic force constants give rise to leading-order anharmonic contributions to lattice structures and energies, respectively, and, in this sense, a QFF is the lowest-order truncation that is meaningful for the analysis.

In the Cartesian coordinates, the same QFF can be expressed as

$$\begin{aligned} V &= \sum_{\kappa}\sum_{m_1} F_{\kappa(m_1)} X_{\kappa(m_1)} + \frac{1}{2!}\sum_{\kappa,\lambda}\sum_{m_1,m_2} F_{\kappa(m_1)\lambda(m_2)} X_{\kappa(m_1)} X_{\lambda(m_2)} \\ &\quad + \frac{1}{3!}\sum_{\kappa,\lambda,\mu}\sum_{m_1,m_2,m_3} F_{\kappa(m_1)\lambda(m_2)\mu(m_3)} X_{\kappa(m_1)} X_{\lambda(m_2)} X_{\mu(m_3)} \\ &\quad + \frac{1}{4!}\sum_{\kappa,\lambda,\mu,\nu}\sum_{m_1,m_2,m_3,m_4} F_{\kappa(m_1)\lambda(m_2)\mu(m_3)\nu(m_4)} X_{\kappa(m_1)} X_{\lambda(m_2)} X_{\mu(m_3)} X_{\nu(m_4)} \qquad (3.22) \\ &= K\sum_{\kappa} F_{\kappa(0)} X_{\kappa(0)} + \frac{K}{2!}\sum_{\kappa,\lambda}\sum_{m_1} F_{\kappa(0)\lambda(m_1)} X_{\kappa(0)} X_{\lambda(m_1)} + \frac{K}{3!}\sum_{\kappa,\lambda,\mu}\sum_{m_1,m_2} F_{\kappa(0)\lambda(m_1)\mu(m_2)} X_{\kappa(0)} X_{\lambda(m_1)} X_{\mu(m_2)} \\ &\quad + \frac{K}{4!}\sum_{\kappa,\lambda,\mu,\nu}\sum_{m_1,m_2,m_3} F_{\kappa(0)\lambda(m_1)\mu(m_2)\nu(m_3)} X_{\kappa(0)} X_{\lambda(m_1)} X_{\mu(m_2)} X_{\nu(m_3)}, \qquad (3.23) \end{aligned}$$

where the second equality exploits the translational invariance of the force constants in the Cartesian coordinates such as

$$F_{\kappa(m_1)\lambda(m_2)\mu(m_3)\nu(m_4)} = F_{\kappa(0)\lambda(m_2-m_1)\mu(m_3-m_1)\nu(m_4-m_1)}. \qquad (3.24)$$

The factor of K that multiplies each sum in Equation (3.23) underscores the fact that the terms in V are individually size-extensive (K^1). The two sets of force constants are related to each other by the following transformations:

$$\begin{aligned} F_{pk_p} &= K^{1/2}\Delta_{k_p}\sum_{\kappa} m_\kappa^{-1/2} C^{\kappa*}_{pk_p} F_{\kappa(0)}, \qquad (3.25) \\ F_{pk_pqk_q} &= K^{0}\Delta_{k_p+k_q}\sum_{\kappa,\lambda}\sum_{m_1} m_\kappa^{-1/2} m_\lambda^{-1/2} C^{\kappa*}_{pk_p} C^{\lambda*}_{qk_q} F_{\kappa(0)\lambda(m_1)} \exp(im_1k_qa), \qquad (3.26) \\ F_{pk_pqk_qrk_r} &= K^{-1/2}\Delta_{k_p+k_q+k_r}\sum_{\kappa,\lambda,\mu}\sum_{m_1,m_2} m_\kappa^{-1/2} m_\lambda^{-1/2} m_\mu^{-1/2} \\ &\quad \times C^{\kappa*}_{pk_p} C^{\lambda*}_{qk_q} C^{\mu*}_{rk_r} F_{\kappa(0)\lambda(m_1)\mu(m_2)} \exp\left\{i(m_1k_q + m_2k_r)a\right\}, \qquad (3.27) \\ F_{pk_pqk_qrk_rsk_s} &= K^{-1}\Delta_{k_p+k_q+k_r+k_s}\sum_{\kappa,\lambda,\mu,\nu}\sum_{m_1,m_2,m_3} m_\kappa^{-1/2} m_\lambda^{-1/2} m_\mu^{-1/2} m_\nu^{-1/2} C^{\kappa*}_{pk_p} C^{\lambda*}_{qk_q} C^{\mu*}_{rk_r} C^{\nu*}_{sk_s} \\ &\quad \times F_{\kappa(0)\lambda(m_1)\mu(m_2)\nu(m_3)} \exp\left\{i(m_1k_q + m_2k_r + m_3k_s)a\right\}, \qquad (3.28) \end{aligned}$$

where Δ ensures that these force constants are nonvanishing when and only when the normal coordinates involved

satisfy the momentum conservation condition,[285] namely,

$$\Delta_k = K^{-1} \sum_m \exp(ikma) = \begin{cases} 1, & k = 2n, \{n \in \mathbb{Z}\}, \\ 0, & \text{otherwise.} \end{cases} \tag{3.29}$$

These expressions indicate that the nth-order force constants in the normal coordinates scale as $K^{1-n/2}$ (Ref. 285). Furthermore, since the normal coordinates are centered at the equilibrium lattice structure, we have

$$F_{pk_p} = 0, \tag{3.30}$$

$$F_{pk_pqk_q} = \delta_{pq}\Delta_{k_p+k_q}\omega^2_{pk_p}. \tag{3.31}$$

3.3.3 Self-consistent field theory

A VSCF wave function[67–69] of the state characterized by the string of quantum numbers $\mathbf{v}$ is the product,

$$\Phi^{\mathbf{v}}_{\mathrm{VSCF}} = \prod_p \prod_{k_p}{}' \zeta^{v_{pk_p}}_{pk_p}(q_{pk_p}) \prod_p \prod_{k_p}{}' \zeta^{\bar{v}_{pk_p}}_{pk_p}(\bar{q}_{pk_p}), \tag{3.32}$$

where $\zeta^{v_{pk_p}}_{pk_p}$ is a one-mode function (modal) of q_{pk_p} with the quantum number v_{pk_p} and the linear quasi-momentum k_p in the pth phonon branch and $\zeta^{\bar{v}_{pk_p}}_{pk_p}$ defined accordingly. It is expanded as a linear combination of the harmonic-oscillator wave functions with the same p and k_p attributes:

$$\zeta^v_{pk_p}(q_{pk_p}) = \sum_w D^{wv}_{pk_p} \eta^w_{pk_p}(q_{pk_p}), \tag{3.33}$$

where D is an expansion coefficient and some subscripts are omitted for notational simplicity. We vary ζ such that the expectation value of $\hat{H}_{\mathrm{n}}$ in the wave function $\Phi^{\mathbf{v}}_{\mathrm{VSCF}}$ becomes a minimum. This leads to coupled eigenvalue equations that need to be solved self-consistently for all p's and k_p's:

$$\sum_w G^{uw}_{pk_p} D^{wv}_{pk_p} = D^{uv}_{pk_p} E^v_{pk_p}, \tag{3.34}$$

where $E^v_{pk_p}$ is the energy of the modal $\zeta^v_{pk_p}$ and $G^{uw}_{pk_p}$ is an element of the matrix representation of $\hat{G}$ in the harmonic-oscillator basis,

$$G^{uw}_{pk_p} = \langle \eta^u_{pk_p} | \hat{G}^{\mathbf{v}}_{pk_p} | \eta^w_{pk_p} \rangle \tag{3.35}$$

with

$$\hat{G}^{\mathbf{v}}_{pk_p} = -\frac{1}{2}\frac{\partial^2}{\partial q^2_{pk_p}} + U^{\mathbf{v}}_{pk_p}(q_{pk_p}). \tag{3.36}$$

Here U is an effective one-mode (thus one-dimensional) potential for the mode pk_p and is the expectation value of V in the product of all modals except for the one in question,

$$U^{\mathbf{v}}_{pk_p}(q_{pk_p}) = \langle \Phi^{\mathbf{v}}_{pk_p} | V | \Phi^{\mathbf{v}}_{pk_p} \rangle \tag{3.37}$$

with

$$\Phi^{\mathbf{v}}_{pk_p} = \Phi^{\mathbf{v}}_{\mathrm{VSCF}} / \zeta^{v_{pk_p}}_{pk_p}(q_{pk_p}). \tag{3.38}$$

Through this potential, Equation (3.34) for one mode couples with the corresponding equations for all the other modes.

When V is a QFF, U is also a quartic function of q_{pk_p} and is written as

$$U^{\mathbf{v}}_{pk_p}(q_{pk_p}) \quad = \quad U_0 + U_1 q_{pk_p} + \frac{1}{2!}U_2 q^2_{pk_p} + \frac{1}{3!}U_3 q^3_{pk_p} + \frac{1}{4!}U_4 q^4_{pk_p}. \tag{3.39}$$

Let us first clarify what the correct dependence of U should be. Note that U is a one-dimensional potential for the mode pk_p, whose associated kinetic energy part scales as K^0. The third and subsequent terms that depend on q_{pk_p} must, therefore, scale as K^0 and determine the size-intensive (K^0) transition energies and the shapes of the modals. The first term (U_0), on the other hand, is a constant representing the sum of the energies of all the other modes and should be size-extensive (K^1). The second term ($U_1 q_{pk_p}$) should be zero for U to have the correct size dependence. We shall now show, however, that Equation (3.39) does not formally satisfy these criteria.

Substituting Equation (3.21) into Equation (3.37), we find the constant to be

$$\begin{aligned}
U_0 \quad = \quad & \sum_q F_{q0}\langle q_{q0}\rangle + \frac{1}{2!2}\sum_{q,r}\sum_{k_q} F_{qk_qrk_r}\left(\langle q_{qk_q}\rangle\langle q_{rk_r}\rangle - \langle \bar{q}_{qk_q}\rangle\langle \bar{q}_{rk_r}\rangle\right) \\
& + \frac{1}{2!2}\sum_{q}\sum_{k_q} F_{q-k_qqk_q}\left(\langle q^2_{qk_q}\rangle + \langle \bar{q}^2_{qk_q}\rangle\right) + \frac{1}{2!2}\sum_{q,r}\sum_{k_r} F_{q0r-k_rrk_r}\langle q_{q0}\rangle\left(\langle q^2_{rk_r}\rangle + \langle \bar{q}^2_{rk_r}\rangle\right) \\
& + \frac{1}{3!2^{3/2}}\sum_{q,r,s}\sum_{k_q,k_r} F_{qk_qrk_rsk_s}\left(\langle q_{qk_q}\rangle\langle q_{rk_r}\rangle\langle q_{sk_s}\rangle - 3\langle q_{qk_q}\rangle\langle \bar{q}_{rk_r}\rangle\langle \bar{q}_{sk_s}\rangle\right) \\
& + \frac{1}{2!2!2!2^2}\sum_{q,r}\sum_{k_q,k_r} F_{q-k_qqk_qr-k_rrk_r}\left(\langle q^2_{qk_q}\rangle + \langle \bar{q}^2_{qk_q}\rangle\right)\left(\langle q^2_{rk_r}\rangle + \langle \bar{q}^2_{rk_r}\rangle\right) \\
& + \frac{1}{4!2^2}\sum_{q,r,s,t}\sum_{k_q,k_r,k_s} F_{qk_qrk_rsk_stk_t}\left(\langle q_{qk_q}\rangle\langle q_{rk_r}\rangle\langle q_{sk_s}\rangle\langle q_{tk_t}\rangle + \langle \bar{q}_{qk_q}\rangle\langle \bar{q}_{rk_r}\rangle\langle \bar{q}_{sk_s}\rangle\langle \bar{q}_{tk_t}\rangle\right.
\end{aligned}$$

$$-6\langle q_{qk_q}\rangle\langle q_{rk_r}\rangle\langle \bar{q}_{sk_s}\rangle\langle \bar{q}_{tk_t}\rangle\Big) + \ldots, \tag{3.40}$$

where $\langle q_{qk_q}\rangle$ and $\langle q^2_{qk_q}\rangle$ are the short-hand notations of $\langle \zeta^{v_{qkq}}_{qk_q}|q_{qk_q}|\zeta^{v_{qkq}}_{qk_q}\rangle$ and $\langle \zeta^{v_{qkq}}_{qk_q}|q^2_{qk_q}|\zeta^{v_{qkq}}_{qk_q}\rangle$, respectively, and $\langle \bar{q}_{qk_q}\rangle$ and $\langle \bar{q}^2_{qk_q}\rangle$ are defined accordingly. It should be understood that the summations must exclude the mode pk_p because of Equation (3.38). The second term in the right-hand side also excludes $q_{qk_q} = q_{rk_r}$ as it is included in the third term. This second term involves the summation over only k_q but not k_r because $F_{qk_qrk_r}$ vanishes unless $k_q + k_r = 2n$ (n is an integer). The terms that involve odd numbers of $\bar{q}$ do not appear in this equation because it satisfies the antisymmetry relation, $\bar{q}_{q-k_q} = -\bar{q}_{qk_q}$, and the k summations are taken over the whole first BZ.

The right-hand side of Equation (3.40) does not have consistent K dependence. The first term scales as $K^{1/2}$ because F_{q0} is a $K^{1/2}$ quantity and $\langle q_{q0}\rangle = \langle \zeta^{v_{q0}}_{q0}|q_{q0}|\zeta^{v_{q0}}_{q0}\rangle$ is independent of K. The second and third terms scale as K^1 because $F_{qk_qrk_r}$ has the K^0 dependence and the summation over k_q gives rise to the factor of K^1. In the same way, we find the K dependence of the fourth and fifth terms to be $K^{1/2}$ and $K^{3/2}$, respectively. The sixth and seventh terms with the quartic force constants scale as K^1 and K^2, respectively. To summarize, only the quadratic terms and the terms with quartic force constants of the type $F_{q-k_qqk_qr-k_rrk_r}$ display the correct K^1 dependence in U_0.

The fact that U_0 is a sum of terms with varied K dependence does not immediately mean that VSCF lacks size-extensivity. This is because the terms with nonphysical K dependence may be shown to vanish in the bulk ($K = \infty$) limit. The terms whose K dependence is $K^{1/2}$ or a weaker power of K become asymptotically negligible as compared with the size-extensive (K^1) terms. It should also be noticed that the other terms with nonphysical K dependence always involve the expectation values of odd powers of the normal coordinates in ζ. Therefore, if ζ can be shown to be symmetric (i.e., even or odd) with respect to the origin as is a harmonic-oscillator wave function centered at the equilibrium lattice structure, these terms also vanish by symmetry and the entire expression remains size-extensive (K^1) in the bulk limit. That ζ is a harmonic-oscillator wave function (but with a frequency differing from ω) is indeed the case under certain circumstances to be specified below.

The gradient in Equation (3.39) is given by

$$\begin{aligned} U_1 \;=\; & \Delta_{k_p}F_{p0} + \frac{\Delta_{k_p}}{2!2}\sum_q\sum_{k_q} F_{p0q-k_qqk_q}\left(\langle q^2_{qk_q}\rangle + \langle \bar{q}^2_{qk_q}\rangle\right) \\ & + \sum_q F_{pk_pqk_q}\langle q_{qk_q}\rangle + \frac{1}{2!2^{1/2}}\sum_{q,r}\sum_{k_q} F_{pk_pqk_qrk_r}\left(\langle q_{qk_q}\rangle\langle q_{rk_r}\rangle - \langle \bar{q}_{qk_q}\rangle\langle \bar{q}_{rk_r}\rangle\right) \\ & + \frac{1}{3!2}\sum_{q,r,s}\sum_{k_q,k_r} F_{pk_pqk_qrk_rsk_s}\left(\langle q_{qk_q}\rangle\langle q_{rk_r}\rangle\langle q_{sk_s}\rangle - 3\langle q_{qk_q}\rangle\langle \bar{q}_{rk_r}\rangle\langle \bar{q}_{sk_s}\rangle\right) + \ldots, \end{aligned} \tag{3.41}$$

where q_{qk_q}, q_{rk_r}, and q_{sk_s} must differ from q_{pk_p}. The terms in the right-hand side scale as $K^{1/2}$, $K^{1/2}$, K^0, $K^{1/2}$, and K^1, respectively. Their sum, therefore, does not exhibit well-defined K dependence. The third and subsequent terms

vanish by symmetry if ζ is a harmonic-oscillator wave function for the reason described above. The first term (F_{p0}) is zero at the equilibrium lattice structure, but the second term is not; it represents the leading-order anharmonic effect on the lattice structure (see below). Note that the cubic force constants that enter this important term have the form $F_{p0q-k_qqk_q}$. The VSCF method is not size-extensive unless the sum of the first two terms ("VSCF gradient") vanishes for every in-phase coordinate (q_{p0}). This point will be expounded at the end of this subsection.

The quadratic force constant is expanded as

$$\begin{aligned}\frac{1}{2!}U_2 &= \frac{1}{2!}F_{p-k_ppk_p} + \frac{1}{2!}\sum_q F_{p-k_ppk_pq0}\langle q_{q0}\rangle + \frac{1}{2!2!}\sum_q\sum_{k_q} F_{p-k_ppk_pq-k_qqk_q}\left(\langle q^2_{qk_q}\rangle + \langle \bar{q}^2_{qk_q}\rangle\right)\\ &+\frac{1}{2!2!2}\sum_{q,r}\sum_{k_q} F_{p-k_ppk_pqk_qr-k_q}\left(\langle q_{qk_q}\rangle\langle q_{rk_q}\rangle + \langle \bar{q}_{qk_q}\rangle\langle \bar{q}_{rk_q}\rangle\right) + \ldots,\end{aligned} \tag{3.42}$$

where q_{q0}, q_{qk_q}, and q_{rk_q} must differ from q_{pk_p}. U_2 does not scale consistently, either, as the second (cubic) term scales as $K^{-1/2}$ and differently from the other terms, which are K^0 quantities. However, the second term vanishes in the bulk limit and the fourth term is also zero by symmetry if ζ is a harmonic-oscillator wave function.

The cubic and quartic force constants are given by

$$\frac{1}{3!}U_3 = \frac{1}{3!2^{1/2}}F_{pk_ppk_ppk_p} + \frac{1}{3!2}\sum_q F_{pk_ppk_ppk_pqk_q}\langle q_{qk_q}\rangle + \frac{1}{2!2}\sum_q F_{p-k_ppk_ppk_pq-k_p}\langle q_{qk_p}\rangle, \tag{3.43}$$

$$\frac{1}{4!}U_4 = \frac{1}{4!2}F_{pk_ppk_ppk_ppk_p} + \frac{1}{3!2}F_{p-k_ppk_ppk_ppk_p} + \frac{1}{2!2!2^2}F_{p-k_ppk_pp-k_ppk_p}. \tag{3.44}$$

These expressions exhibit the $K^{-1/2}$ and K^{-1} dependence, respectively, and thus vanish in the bulk limit. Generally, if we assume that ζ is a harmonic-oscillator wave function, we can show that the nth-order force constants in U decay as $K^{1-n/2}$ or more rapidly regardless of the highest order of the force constants present in V.

Let us now suppose that all VSCF gradients [the sum of the first two terms in the right-hand side of Equation (3.41)] are made to vanish by choosing an appropriate lattice structure (see the next subsection). The force constants and normal coordinates are determined at this origin. With U_3 and U_4 vanishing asymptotically, U reduces to a canonical harmonic potential (with zero off-diagonal quadratic force constants) in these normal coordinates at $K = \infty$. Each modal ($\zeta^{v}_{pk_p}$ or $\zeta^{\bar{v}}_{pk_p}$) is, therefore, a harmonic-oscillator wave function along the corresponding normal coordinate but with a different (i.e., renormalized) frequency. The change in frequency occurs because U_2 has a contribution from the quartic force constants $F_{q-k_qqk_qr-k_rrk_r}$. The modal is centered at the lattice structure with which the normal coordinates are determined and hence the expectation value of an odd power of q_{pk_p} in $\zeta^{v}_{pk_p}$ is zero by symmetry. Hence, with this choice of the lattice structure and normal coordinates, the VSCF equations become asymptotically size-extensive.

Alternatively, one can maintain the equilibrium lattice structure as the origin (where V is at minimum and $F_{p0} = 0$) and neglect cubic force constants, which also restores size-extensivity in VSCF. Under this approximation, $U^{\mathbf{v}}_{pk_p}$ again

becomes a canonical, renormalized harmonic potential. A modal in this potential must be symmetric (even or odd) with respect to the origin, erasing all nonphysical terms in $U^{\mathbf{v}}_{pk_p}$. Conversely, when nonzero VSCF gradients are retained in the equations, the size-extensivity of VSCF cannot be proven.

3.3.4 Size-extensive self-consistent field theory

The foregoing discussion reveals that the VSCF equations are plagued with terms with nonphysical K dependence, which are, however, shown to vanish under some circumstances. It is desirable to restore strict size-extensivity in the equations by retaining only the nonvanishing terms in U's that have the correct K dependence. We introduce the following restricted form of a QFF,

$$\begin{aligned} V_{\mathrm{XVSCF}} &= \frac{1}{2!2}\sum_{p}\sum_{k_p} F_{p-k_p pk_p}\left(q^2_{pk_p}+\bar{q}^2_{pk_p}\right) \\ &\quad +\frac{1}{2!2!2!2^2}\sum_{p,q}\sum_{k_p,k_q} F_{p-k_p pk_p q-k_q qk_q}\left(q^2_{pk_p}+\bar{q}^2_{pk_p}\right)\left(q^2_{qk_q}+\bar{q}^2_{qk_q}\right) \qquad (3.45) \\ &= \frac{1}{2!}\sum_{p}{\sum_{k_p}}' F_{p-k_p pk_p}\left(q^2_{pk_p}+\bar{q}^2_{pk_p}\right) \\ &\quad +\frac{1}{2!2!2!}\sum_{p,q}{\sum_{k_p,k_q}}' F_{p-k_p pk_p q-k_q qk_q}\left(q^2_{pk_p}+\bar{q}^2_{pk_p}\right)\left(q^2_{qk_q}+\bar{q}^2_{qk_q}\right), \qquad (3.46) \end{aligned}$$

where q_{pk_p} must differ from q_{qk_q} and it should understood that the factor of $2^{-1/2}$ associated with each appearance of q_{pk_p} or $\bar{q}_{pk_p}$ in Equation (3.45) is replaced by unity when $k_p = 0$. For this QFF, we can write the one-mode potential of VSCF that has the correct size-dependence as follows:

$$U^{\mathbf{v}}_{\mathrm{XVSCF}}(q_{pk_p}) = \langle\Phi^{\mathbf{v}}_{pk_p}|V_{\mathrm{XVSCF}}|\Phi^{\mathbf{v}}_{pk_p}\rangle = U_0^{\mathrm{XVSCF}} + \frac{1}{2!}U_2^{\mathrm{XVSCF}} q^2_{pk_p} \qquad (3.47)$$

with

$$\begin{aligned} U_0^{\mathrm{XVSCF}} &= \frac{1}{2!}\sum_{q}{\sum_{k_q}}' F_{q-k_q qk_q}\left(\langle q^2_{qk_q}\rangle + \langle\bar{q}^2_{qk_q}\rangle\right) \\ &\quad +\frac{1}{2!2!2!}\sum_{q,r}{\sum_{k_q,k_r}}' F_{q-k_q qk_q r-k_r rk_r}\left(\langle q^2_{qk_q}\rangle + \langle\bar{q}^2_{qk_q}\rangle\right)\left(\langle q^2_{rk_r}\rangle + \langle\bar{q}^2_{rk_r}\rangle\right), \qquad (3.48) \end{aligned}$$

and

$$\frac{1}{2!}U_2^{\mathrm{XVSCF}} = \frac{1}{2!}F_{p-k_p pk_p} + \frac{1}{2!2!}\sum_{q}{\sum_{k_q}}' F_{p-k_p pk_p q-k_q qk_q}\left(\langle q^2_{qk_q}\rangle + \langle\bar{q}^2_{qk_q}\rangle\right), \qquad (3.49)$$

where q_{qk_q} and q_{rk_r} differ from q_{pk_p} and $q_{qk_q} = q_{rk_r}$ and $\bar{q}_{qk_q} = \bar{q}_{rk_r}$ are excluded from the summation in Equation (3.48). Equation (3.47) is a sum of the size-extensive (K^1) constant and the size-intensive (K^0) quadratic function. The vibrational Schrödinger problem with this harmonic potential can be solved analytically to yield size-intensive transition energies that include the effects of anharmonicity due to $F_{p-k_p pk_p q-k_q qk_q}$. We call this method size-extensive VSCF or XVSCF (see also the methods of renormalized and self-consistent phonons).[287] The one-mode potential given above varies with all the other modals through the last term of Equation (3.47) and, therefore, the XVSCF equations [Equations (3.34)–(3.36)] must be solved self-consistently. The modal $\zeta^{v_{qk_q}}_{qk_q}$ ($\zeta^{\bar{v}_{qk_q}}_{qk_q}$) is a harmonic-oscillator wave function in q_{pk_p} ($\bar{q}_{pk_p}$) but with a different frequency than that of $\eta^{v_{qk_q}}_{qk_q}$ ($\eta^{\bar{v}_{qk_q}}_{qk_q}$). The total energy of the state $\mathbf{v}$ is the expectation value of the Hamiltonian with V_{XVSCF} in the XVSCF wave function and is written as

$$\begin{aligned} E^{\mathbf{v}}_{\mathrm{XVSCF}} &= -\frac{1}{2}\sum_p \sum_{k_p}{}' \langle \zeta^{v_{pk_p}}_{pk_p} | \frac{\partial^2}{\partial q^2_{pk_p}} | \zeta^{v_{pk_p}}_{pk_p} \rangle - \frac{1}{2}\sum_p \sum_{k_p}{}' \langle \zeta^{\bar{v}_{pk_p}}_{pk_p} | \frac{\partial^2}{\partial \bar{q}^2_{pk_p}} | \zeta^{\bar{v}_{pk_p}}_{pk_p} \rangle \\ &\quad + \frac{1}{2!}\sum_p \sum_{k_p}{}' F_{p-k_p pk_p} \left(\langle q^2_{pk_p} \rangle + \langle \bar{q}^2_{pk_p} \rangle \right) \\ &\quad + \frac{1}{2!2!2!}\sum_{p,q} \sum_{k_p,k_q}{}' F_{p-k_p pk_p q-k_q qk_q} \left(\langle q^2_{pk_p} \rangle + \langle \bar{q}^2_{pk_p} \rangle \right) \left(\langle q^2_{qk_q} \rangle + \langle \bar{q}^2_{qk_q} \rangle \right), \end{aligned} \tag{3.50}$$

where q_{pk_p} ($\bar{q}_{pk_p}$) must not coincide with q_{qk_q} ($\bar{q}_{pk_p}$). Each term in the right-hand side scales as K^1 and the sum is, therefore, strictly size-extensive. It should be evident that the sextic force constants of the type $F_{p-k_p pk_p q-k_q qk_q r-k_r rk_r}$ and analogous higher even-order force constants can also be included in a size-extensive fashion, defining sextic, octic, etc. VSCF methods.

As discussed in the previous subsection, the necessary condition for the size-extensivity of VSCF is that all VSCF gradients vanish. In XVSCF introduced above, such terms are excluded from V_{XVSCF} defined above so that the resulting equations are manifestly size-extensive. They are, however, related to an anharmonic correction to the lattice structure (more specifically, to the atomic positions but not to the lattice constants). The anharmonic correction ($\tilde{q}_{p0}$) measured in the real normal coordinates of the first kind is the one at which the VSCF gradients vanish identically:

$$\frac{\partial \tilde{U}^{\mathbf{v}}_{\mathrm{XVSCF}}(q_{p0})}{\partial q_{p0}}\Big|_{q_{p0}=\tilde{q}_{p0}} = 0 \tag{3.51}$$

with

$$\tilde{U}^{\mathbf{v}}_{\mathrm{XVSCF}}(q_{p0}) = \tilde{U}^{\mathrm{XVSCF}}_0 + \tilde{U}^{\mathrm{XVSCF}}_1 q_{p0} + \frac{1}{2!}\tilde{U}^{\mathrm{XVSCF}}_2 q^2_{p0}. \tag{3.52}$$

The gradient of $\tilde{U}^{\mathbf{v}}_{\mathrm{XVSCF}}$ is given, according to Equation (3.41), by

$$\tilde{U}^{\mathrm{XVSCF}}_{1} = F_{p0} + \frac{1}{2!}\sum_{q}{\sum_{k_q}}' F_{p0q-k_qqk_q}\left(\langle q^2_{qk_q}\rangle + \langle \bar{q}^2_{qk_q}\rangle\right), \tag{3.53}$$

whereas the expressions of $\tilde{U}^{\mathrm{XVSCF}}_{0}$ and $\tilde{U}^{\mathrm{XVSCF}}_{2}$ can be readily inferred from Equations (3.48) and (3.49), for instance,

$$\tilde{U}^{\mathrm{XVSCF}}_{2} \quad = \quad F_{p0p0} + \frac{1}{2!}\sum_{q}{\sum_{k_q}}' F_{p0p0q-k_qqk_q}\left(\langle q^2_{qk_q}\rangle + \langle \bar{q}^2_{qk_q}\rangle\right). \tag{3.54}$$

With these force constants, the anharmonic correction to the structure in the state $\mathbf{v}$ due to the cubic force constants of the type $F_{p0q-k_qqk_q}$ is

$$\tilde{q}_{p0} = -\tilde{U}^{\mathrm{XVSCF}}_{1}/\tilde{U}^{\mathrm{XVSCF}}_{2}. \tag{3.55}$$

Since $\tilde{U}^{\mathrm{XVSCF}}_{1}$ and $\tilde{U}^{\mathrm{XVSCF}}_{2}$ scale as $K^{1/2}$ and K^0, respectively, the anharmonic correction ($\tilde{q}_{p0}$) in the normal coordinate is a $K^{1/2}$ quantity. When expressed in spatially local coordinates such as the Cartesian coordinates, the correction $\tilde{X}_{\nu(0)}$ is given by

$$\tilde{X}_{\nu(0)} = K^{-1/2}m_{\nu}^{-1/2}\sum_{p} C^{\nu*}_{p0}\tilde{q}_{p0}, \tag{3.56}$$

which has the correct K^0 dependence.

Equation (3.55) can be evaluated approximately and expediently by using the harmonic-oscillator wave functions as modals, that is, $\langle q_{qk_q}\rangle \approx \langle \eta^{v_{qk_q}}_{qk_q}|q_{qk_q}|\eta^{v_{qk_q}}_{qk_q}\rangle$, and so forth. However, the fully self-consistent XVSCF procedure must simultaneously satisfy Equation (3.51) to determine the lattice structure that ensures its size-extensivity and the VSCF equations with the potential given by Equation (3.47). These two problems are coupled through the VSCF modals.

3.3.5 Perturbation theory

With a XVSCF wave function as the reference, the first- and second-order size-extensive VMP perturbation corrections to the energy ($E^{\mathbf{v}}_{\mathrm{XVSCF}}$) of the state $\mathbf{v}$ due to anharmonicity (denoted XVMP1 and XVMP2, respectively) are given by

$$E^{\mathbf{v}}_{\mathrm{XVMP1}} \quad = \quad E^{\mathbf{v}}_{\mathrm{XVSCF}} + \langle \Phi^{\mathbf{v}}_{\mathrm{VSCF}}|\tilde{V}_{\mathrm{XVSCF}}|\Phi^{\mathbf{v}}_{\mathrm{VSCF}}\rangle \tag{3.57}$$

and

$$E^{\mathbf{v}}_{\mathrm{XVMP2}} = E^{\mathbf{v}}_{\mathrm{XVMP1}} + \sum_{\mathbf{w}} \frac{|\langle\Phi^{\mathbf{v}}_{\mathrm{VSCF}}|\tilde{V}_{\mathrm{XVSCF}}|\Phi^{\mathbf{w}}_{\mathrm{VSCF}}\rangle|^2}{E^{\mathbf{v}}_{\mathrm{XVSCF}} - E^{\mathbf{w}}_{\mathrm{XVSCF}}}, \tag{3.58}$$

where the summation runs over all states **w** except for the state **v** and its degenerate states (if any). The operator $\tilde{V}_{\mathrm{XVSCF}}$ is the perturbation (the fluctuation potential) defined by the Møller–Plesset partitioning,[13,40,273]

$$\tilde{V}_{\mathrm{XVSCF}} = V - V_{\mathrm{XVSCF}}. \tag{3.59}$$

It should be recalled that, under the assumption that makes VSCF size-extensive, namely, the first two terms of Equation (3.41) are zero or neglected, ζ becomes a harmonic-oscillator wave function centered at the origin (but not corresponding to V_{HRM}). Therefore, the expectation value of an odd power of the normal coordinates in ζ vanishes by symmetry. In a QFF, therefore, we have

$$\langle\Phi^{\mathbf{v}}_{\mathrm{VSCF}}|\tilde{V}_{\mathrm{XVSCF}}|\Phi^{\mathbf{v}}_{\mathrm{VSCF}}\rangle = 0 \tag{3.60}$$

and

$$E^{\mathbf{v}}_{\mathrm{XVMP1}} = E^{\mathbf{v}}_{\mathrm{XVSCF}}, \tag{3.61}$$

which is size-extensive. That the reference modals are symmetric (even or odd) with respect to the origin ensures the disappearance of non-size-extensive terms involving F_{p0} and $F_{p0q-k_qqk_q}$.

The XVMP2 energy ($E^{\mathbf{v}}_{\mathrm{XVMP2}}$) is expressed as

$$\begin{aligned} E^{\mathbf{v}}_{\mathrm{XVMP2}} = {} & E^{\mathbf{v}}_{\mathrm{XVMP1}} + \sum_{\mathbf{p}} \frac{|V^{v_{\mathbf{p}}}_{w_{\mathbf{p}}}|^2}{E^{\mathbf{v}}_{\mathrm{XVSCF}} - E^{\mathbf{w}}_{\mathrm{XVSCF}}} + \frac{1}{2!}\sum_{\mathbf{p},\mathbf{q}}{}' \sum_{k_p} \frac{|V^{v_{\mathbf{p}}v_{\mathbf{q}}}_{w_{\mathbf{p}}w_{\mathbf{q}}}|^2}{E^{\mathbf{v}}_{\mathrm{XVSCF}} - E^{\mathbf{w}}_{\mathrm{XVSCF}}} \\ & + \frac{1}{3!}\sum_{\mathbf{p},\mathbf{q},\mathbf{r}}{}' \sum_{k_p,k_q} \frac{|V^{v_{\mathbf{p}}v_{\mathbf{q}}v_{\mathbf{r}}}_{w_{\mathbf{p}}w_{\mathbf{q}}w_{\mathbf{r}}}|^2}{E^{\mathbf{v}}_{\mathrm{XVSCF}} - E^{\mathbf{w}}_{\mathrm{XVSCF}}} + \frac{1}{4!}\sum_{\mathbf{p},\mathbf{q},\mathbf{r},\mathbf{s}}{}' \sum_{k_p,k_q,k_s} \frac{|V^{v_{\mathbf{p}}v_{\mathbf{q}}v_{\mathbf{r}}v_{\mathbf{s}}}_{w_{\mathbf{p}}w_{\mathbf{q}}w_{\mathbf{r}}w_{\mathbf{s}}}|^2}{E^{\mathbf{v}}_{\mathrm{XVSCF}} - E^{\mathbf{w}}_{\mathrm{XVSCF}}}, \end{aligned} \tag{3.62}$$

where **p** is a compound index of p and k_p and corresponds to a member of the nonredundant set of normal coordinates of the first kind, namely, the union of $\{q_{pk_p}\}$ and $\{\bar{q}_{pk_p}\}$ in the half BZ. The k summations in the above expression are redundant as the summations over **p**, **q**, etc. imply them, but they are made explicit for the sake of clarifying the K dependence. The V matrix elements are defined by

$$V^{v_{\mathbf{p}}}_{w_{\mathbf{p}}} = \langle\Phi^{\mathbf{v}}_{\mathrm{XVSCF}}|\tilde{V}_{\mathrm{XVSCF}}|\Phi^{w_{\mathbf{p}}}_{v_{\mathbf{p}}}\rangle, \tag{3.63}$$

$$V^{\nu_{\mathbf{p}}\nu_{\mathbf{q}}}_{w_{\mathbf{p}}w_{\mathbf{q}}} = \langle\Phi^{\mathbf{v}}_{\mathrm{XVSCF}}|\tilde{V}_{\mathrm{XVSCF}}|\Phi^{w_{\mathbf{p}}w_{\mathbf{q}}}_{\nu_{\mathbf{p}}\nu_{\mathbf{q}}}\rangle, \tag{3.64}$$

$$V^{\nu_{\mathbf{p}}\nu_{\mathbf{q}}\nu_{\mathbf{r}}}_{w_{\mathbf{p}}w_{\mathbf{q}}w_{\mathbf{r}}} = \langle\Phi^{\mathbf{v}}_{\mathrm{XVSCF}}|\tilde{V}_{\mathrm{XVSCF}}|\Phi^{w_{\mathbf{p}}w_{\mathbf{q}}w_{\mathbf{r}}}_{\nu_{\mathbf{p}}\nu_{\mathbf{q}}\nu_{\mathbf{r}}}\rangle, \tag{3.65}$$

and so forth, where $\Phi^{w_{\mathbf{p}}}_{\nu_{\mathbf{p}}}$ denotes a one-mode excited XVSCF wave function in which the quantum number of the mode $\mathbf{p}$ is raised from $\nu_{\mathbf{p}}$ to $w_{\mathbf{p}}$. The modes $\mathbf{p}$, $\mathbf{q}$, $\mathbf{r}$, and $\mathbf{s}$ must be distinct from one another.

Of all $\mathbf{p}$'s, only those with $k_p = 0$ can contribute to the second sum in the right-hand side of Equation (3.62), that is,

$$\sum_{\mathbf{p}} \frac{|V^{\nu_{\mathbf{p}}}_{w_{\mathbf{p}}}|^2}{E^{\mathbf{v}}_{\mathrm{XVSCF}} - E^{\mathbf{w}}_{\mathrm{XVSCF}}} = \sum_{p}\sum_{w_{pk_p}} \frac{|V^{\nu_{pk_p}}_{w_{pk_p}}|^2}{E^{\mathbf{v}}_{\mathrm{XVSCF}} - E^{\mathbf{w}}_{\mathrm{XVSCF}}} \tag{3.66}$$

with

$$\begin{aligned} V^{\nu_{pk_p}}_{w_{pk_p}} &= \Delta_{k_p} F_{p0}\langle\zeta^{\nu_{p0}}_{p0}|q_{p0}|\zeta^{w_{p0}}_{p0}\rangle \\ &\quad + \frac{\Delta_{k_p}}{2!}\sum_{q}{\sum_{k_q}}' F_{p0q-k_qqk_q}\langle\zeta^{\nu_{p0}}_{p0}|q_{p0}|\zeta^{w_{p0}}_{p0}\rangle\left(\langle\zeta^{\nu_{qk_q}}_{qk_q}|q^2_{qk_q}|\zeta^{\nu_{qk_q}}_{qk_q}\rangle + \langle\zeta^{\bar{\nu}_{qk_q}}_{qk_q}|\bar{q}^2_{qk_q}|\zeta^{\bar{\nu}_{qk_q}}_{qk_q}\rangle\right). \end{aligned} \tag{3.67}$$

The first term in the right-hand side of Equation (3.67) scales as $K^{1/2}$ because F_{p0} is a $K^{1/2}$ quantity. The other term also has the $K^{1/2}$ dependence because $F_{p0q-k_qqk_q}$ scales as $K^{-1/2}$ and the k summation gives rise to the factor of K^1. The numerator of Equation (3.66) is, therefore, a K^1 quantity. The denominator is a XVSCF transition energy and is size-intensive (K^0). Overall, Equation (3.66) scales correctly as K^1 and is size-extensive.

Remembering that $\mathbf{p}$ can stand for either q_{pk_p} or $\bar{q}_{pk_p}$, we find that the third term in the right-hand side of Equation (3.62) consists of three sums:

$$\begin{aligned} \frac{1}{2!}\sum_{\mathbf{p},\mathbf{q}}{\sum_{k_p}}' \frac{|V^{\nu_{\mathbf{p}}\nu_{\mathbf{q}}}_{w_{\mathbf{p}}w_{\mathbf{q}}}|^2}{E^{\mathbf{v}}_{\mathrm{XVSCF}} - E^{\mathbf{w}}_{\mathrm{XVSCF}}} &= \frac{1}{2!}\sum_{p,q}{\sum_{k_p}}' \sum_{w_{pk_p},w_{qk_q}} \frac{|V^{\nu_{pk_p}\nu_{qk_q}}_{w_{pk_p}w_{qk_q}}|^2}{E^{\mathbf{v}}_{\mathrm{XVSCF}} - E^{\mathbf{w}}_{\mathrm{XVSCF}}} \\ &\quad + \frac{1}{2!}\sum_{p,q}{\sum_{k_p}}' \sum_{\bar{w}_{pk_p},\bar{w}_{qk_q}} \frac{|V^{\bar{\nu}_{pk_p}\bar{\nu}_{qk_q}}_{\bar{w}_{pk_p}\bar{w}_{qk_q}}|^2}{E^{\mathbf{v}}_{\mathrm{XVSCF}} - E^{\mathbf{w}}_{\mathrm{XVSCF}}} \\ &\quad + \sum_{p,q}{\sum_{k_p}}' \sum_{w_{pk_p},\bar{w}_{qk_q}} \frac{|V^{\nu_{pk_p}\bar{\nu}_{qk_q}}_{w_{pk_p}\bar{w}_{qk_q}}|^2}{E^{\mathbf{v}}_{\mathrm{XVSCF}} - E^{\mathbf{w}}_{\mathrm{XVSCF}}}, \end{aligned} \tag{3.68}$$

where

$$\begin{aligned} V^{\nu_{pk_p}\nu_{qkq}}_{w_{pk_p}w_{qkq}} &= \frac{1}{2}F_{pk_pqk_q}\langle\zeta^{\nu_{pk_p}}_{pk_p}|q_{pk_p}|\zeta^{w_{pk_p}}_{pk_p}\rangle\langle\zeta^{\nu_{qk_q}}_{qk_q}|q_{qk_q}|\zeta^{w_{qkq}}_{qk_q}\rangle \\ &\quad + \frac{1}{2!2}\sum_{r}{\sum_{k_r}}' F_{pk_pqk_qr-k_rrk_r}\langle\zeta^{\nu_{pk_p}}_{pk_p}|q_{pk_p}|\zeta^{w_{pk_p}}_{pk_p}\rangle\langle\zeta^{\nu_{qk_q}}_{qk_q}|q_{qk_q}|\zeta^{w_{qkq}}_{qk_q}\rangle \end{aligned}$$

$$\times\Big(\langle\zeta^{v_{rk_r}}_{rk_r}|q^2_{rk_r}|\zeta^{v_{rk_r}}_{rk_r}\rangle+\langle\zeta^{\bar{v}_{rk_r}}_{rk_r}|\bar{q}^2_{rk_r}|\zeta^{\bar{v}_{rk_r}}_{rk_r}\rangle\Big), \tag{3.69}$$

$$\begin{aligned}V^{v_{pk_p}\bar{v}_{qk_q}}_{w_{pk_p}\bar{w}_{qk_q}} &= \frac{i}{2}F_{pk_pqk_q}\langle\zeta^{v_{pk_p}}_{pk_p}|q_{pk_p}|\zeta^{w_{pk_p}}_{pk_p}\rangle\langle\zeta^{v_{qk_q}}_{qk_q}|\bar{q}_{qk_q}|\zeta^{w_{qk_q}}_{qk_q}\rangle\\ &+\frac{i}{2!2}\sum_r\sum_{k_r}{}'F_{pk_pqk_qr-k_rrk_r}\langle\zeta^{v_{pk_p}}_{pk_p}|q_{pk_p}|\zeta^{w_{pk_p}}_{pk_p}\rangle\langle\zeta^{v_{qk_q}}_{qk_q}|\bar{q}_{qk_q}|\zeta^{w_{qk_q}}_{qk_q}\rangle\\ &\times\Big(\langle\zeta^{v_{rk_r}}_{rk_r}|q^2_{rk_r}|\zeta^{v_{rk_r}}_{rk_r}\rangle+\langle\zeta^{\bar{v}_{rk_r}}_{rk_r}|\bar{q}^2_{rk_r}|\zeta^{\bar{v}_{rk_r}}_{rk_r}\rangle\Big).\end{aligned} \tag{3.70}$$

The definition of $V^{\bar{v}_{pk_p}\bar{v}_{qk_q}}_{\bar{w}_{pk_p}\bar{w}_{qk_q}}$ can be obtained by interchanging v with $\bar{v}$ and w with $\bar{w}$ in Equation (3.69). Notice that $V^{v_{pk_p}\bar{v}_{qk_q}}_{w_{pk_p}\bar{w}_{qk_q}}$ contains terms with odd numbers of $\bar{q}$ and pure imaginary factors. In VMP2, these terms are squared before the k summation is taken and, therefore, can make nonvanishing contributions unlike in XVSCF. The two-mode V matrix elements scale as K^0, making Equation (3.68) a K^1 quantity and size-extensive.

Likewise, the fourth term in Equation (3.62) is an abbreviated notation of the sum of four terms:

$$\begin{aligned}\frac{1}{3!}\sum_{\mathbf{p},\mathbf{q},\mathbf{r}}\sum_{k_p,k_q}{}'\frac{|V^{v_\mathbf{p}v_\mathbf{q}v_\mathbf{r}}_{w_\mathbf{p}w_\mathbf{q}w_\mathbf{r}}|^2}{E^\mathbf{v}_{\mathrm{XVSCF}}-E^\mathbf{w}_{\mathrm{XVSCF}}} &= \frac{1}{3!}\sum_{p,q,r}\sum_{k_p,k_q}{}'\sum_{w_{pk_p},w_{qk_q},w_{rk_r}}\frac{|V^{v_{pk_p}v_{qk_q}v_{rk_r}}_{w_{pk_p}w_{qk_q}w_{rk_r}}|^2}{E^\mathbf{v}_{\mathrm{XVSCF}}-E^\mathbf{w}_{\mathrm{XVSCF}}}\\ &+\frac{1}{3!}\sum_{p,q,r}\sum_{k_p,k_q}{}'\sum_{\bar{w}_{pk_p},\bar{w}_{qk_q},\bar{w}_{rk_r}}\frac{|V^{\bar{v}_{pk_p}\bar{v}_{qk_q}\bar{v}_{rk_r}}_{\bar{w}_{pk_p}\bar{w}_{qk_q}\bar{w}_{rk_r}}|^2}{E^\mathbf{v}_{\mathrm{XVSCF}}-E^\mathbf{w}_{\mathrm{XVSCF}}}\\ &+\frac{1}{2!}\sum_{p,q,r}\sum_{k_p,k_q}{}'\sum_{w_{pk_p},\bar{w}_{qk_q},\bar{w}_{rk_r}}\frac{|V^{v_{pk_p}\bar{v}_{qk_q}\bar{v}_{rk_r}}_{w_{pk_p}\bar{w}_{qk_q}\bar{w}_{rk_r}}|^2}{E^\mathbf{v}_{\mathrm{XVSCF}}-E^\mathbf{w}_{\mathrm{XVSCF}}}\\ &+\frac{1}{2!}\sum_{p,q,r}\sum_{k_p,k_q}{}'\sum_{w_{pk_p},w_{qk_q},\bar{w}_{rk_r}}\frac{|V^{v_{pk_p}v_{qk_q}\bar{v}_{rk_r}}_{w_{pk_p}w_{qk_q}\bar{w}_{rk_r}}|^2}{E^\mathbf{v}_{\mathrm{XVSCF}}-E^\mathbf{w}_{\mathrm{XVSCF}}},\end{aligned} \tag{3.71}$$

where

$$V^{v_{pk_p}v_{qk_q}v_{rk_r}}_{w_{pk_p}w_{qk_q}w_{rk_r}} = \frac{1}{2^{3/2}}F_{pk_pqk_qrk_r}\langle\zeta^{v_{pk_p}}_{pk_p}|q_{pk_p}|\zeta^{w_{pk_p}}_{pk_p}\rangle\langle\zeta^{v_{qk_q}}_{qk_q}|q_{qk_q}|\zeta^{w_{qk_q}}_{qk_q}\rangle\langle\zeta^{v_{rk_r}}_{rk_r}|q_{rk_r}|\zeta^{w_{rk_r}}_{rk_r}\rangle, \tag{3.72}$$

$$V^{v_{pk_p}v_{qk_q}\bar{v}_{rk_r}}_{w_{pk_p}w_{qk_q}\bar{w}_{rk_r}} = \frac{i}{2^{3/2}}F_{pk_pqk_qrk_r}\langle\zeta^{v_{pk_p}}_{pk_p}|q_{pk_p}|\zeta^{w_{pk_p}}_{pk_p}\rangle\langle\zeta^{v_{qk_q}}_{qk_q}|q_{qk_q}|\zeta^{w_{qk_q}}_{qk_q}\rangle\langle\zeta^{\bar{v}_{rk_r}}_{rk_r}|\bar{q}_{rk_r}|\zeta^{\bar{w}_{rk_r}}_{rk_r}\rangle, \tag{3.73}$$

and so forth. These and other three-mode V matrix elements scale as $K^{-1/2}$. The numerators of Equation (3.71) are, therefore, invariably K^{-1} quantities. Since the two-fold k summation contributes the factor of K^2, we find Equation (3.71) size-extensive also.

Generally, an n-mode V matrix element is a $K^{1-n/2}$ quantity just as is an nth-order force constant in the normal coordinates. With this knowledge, the fifth term in Equation (3.62) with quartic force constants and thus the VMP2 correction as a whole can be shown to be size-extensive. Clearly, quintic, sextic, and all higher-order force constants can contribute to VMP2 in a size-extensive fashion, defining quintic, sextic, etc. VMP2 methods.

Alternatively, the harmonic-oscillator wave function $\Phi^\mathbf{v}_{\mathrm{HRM}}$ can be used as the reference. The first- and second-

order perturbation corrections[288,289] to $E^{\mathbf{v}}_{\mathrm{HRM}}$ of the state $\mathbf{v}$ are given by

$$E^{\mathbf{v}}_{\mathrm{VPT1}} = E^{\mathbf{v}}_{\mathrm{HRM}} + \langle \Phi^{\mathbf{v}}_{\mathrm{HRM}} | \tilde{V}_{\mathrm{HRM}} | \Phi^{\mathbf{v}}_{\mathrm{HRM}} \rangle \tag{3.74}$$

and

$$E^{\mathbf{v}}_{\mathrm{VPT2}} = E^{\mathbf{v}}_{\mathrm{VPT1}} + \sum_{\mathbf{w}} \frac{|\langle \Phi^{\mathbf{v}}_{\mathrm{HRM}} | \tilde{V}_{\mathrm{HRM}} | \Phi^{\mathbf{w}}_{\mathrm{HRM}} \rangle|^2}{E^{\mathbf{v}}_{\mathrm{HRM}} - E^{\mathbf{w}}_{\mathrm{HRM}}}, \tag{3.75}$$

where the summation runs over all states $\mathbf{w}$ except for the state $\mathbf{v}$ and its degenerate states. The operator $\tilde{V}_{\mathrm{HRM}}$ denotes the perturbation (the fluctuation potential) defined as

$$\tilde{V}_{\mathrm{HRM}} = V - V_{\mathrm{HRM}}. \tag{3.76}$$

When V is a QFF, we call this method size-extensive VPT1. Its energy, $E^{\mathbf{v}}_{\mathrm{XVPT1}}$, can be written simply as[288,289]

$$E^{\mathbf{v}}_{\mathrm{XVPT1}} = E^{\mathbf{v}}_{\mathrm{HRM}} + \frac{1}{2!2!2!} \sum_{p,q} {\sum_{k_p,k_q}}' F_{p-k_p p k_p q-k_q q k_q} \left(\langle q^2_{pk_p} \rangle + \langle \bar{q}^2_{pk_p} \rangle \right) \left(\langle q^2_{qk_q} \rangle + \langle \bar{q}^2_{qk_q} \rangle \right), \tag{3.77}$$

where q_{pk_p} ($\bar{q}_{pk_p}$) must differ from q_{qk_q} ($\bar{q}_{qk_q}$) and the integral $\langle q^2_{pk_p} \rangle$ is understood to designate $\langle \eta^{v_{pk_p}}_{pk_p} | q^2_{pk_p} | \eta^{v_{pk_p}}_{pk_p} \rangle$, which can be evaluated analytically (see Table 2.27 of Ref. 285 or Appendix III of Ref. 19). Quadratic force constants do not appear in this expression because of Equation (3.76). No expectation values of odd powers of the normal coordinates enter them, either, because of symmetry. $E^{\mathbf{v}}_{\mathrm{VPT1}}$ is size-extensive (K^1) as $F_{p-k_p p k_p q-k_q q k_q}$ is a K^{-1} quantity and the two-fold k summation gives rise to the factor of K^2. This expression is consistent with the anharmonic correction in the XVSCF energy given by Equation (3.50) and reduces to the latter exactly when the XVSCF modals (ζ's) coincide with the harmonic-oscillator wave functions (η's). As in VSCF, the sextic force constants of the type $F_{p-k_p p k_p q-k_q q k_q r-k_r r k_r}$ and higher even-order force constants can be included in VPT1 in a size-extensive fashion.

In a QFF, the second-order anharmonic correction [Equation (3.75)] is expressed as

$$\begin{aligned} E^{\mathbf{v}}_{\mathrm{XVPT2}} = {} & E^{\mathbf{v}}_{\mathrm{XVPT1}} + \sum_{\mathbf{p}} \frac{|W^{v_{\mathbf{p}}}_{w_{\mathbf{p}}}|^2}{E^{\mathbf{v}}_{\mathrm{HRM}} - E^{\mathbf{w}}_{\mathrm{HRM}}} + \frac{1}{2!} \sum_{\mathbf{p},\mathbf{q}} {\sum_{k_p}}' \frac{|W^{v_{\mathbf{p}} v_{\mathbf{q}}}_{w_{\mathbf{p}} w_{\mathbf{q}}}|^2}{E^{\mathbf{v}}_{\mathrm{HRM}} - E^{\mathbf{w}}_{\mathrm{HRM}}} \\ & + \frac{1}{3!} \sum_{\mathbf{p},\mathbf{q},\mathbf{r}} {\sum_{k_p,k_q}}' \frac{|W^{v_{\mathbf{p}} v_{\mathbf{q}} v_{\mathbf{r}}}_{w_{\mathbf{p}} w_{\mathbf{q}} w_{\mathbf{r}}}|^2}{E^{\mathbf{v}}_{\mathrm{HRM}} - E^{\mathbf{w}}_{\mathrm{HRM}}} + \frac{1}{4!} \sum_{\mathbf{p},\mathbf{q},\mathbf{r},\mathbf{s}} {\sum_{k_p,k_q,k_r}}' \frac{|W^{v_{\mathbf{p}} v_{\mathbf{q}} v_{\mathbf{r}} v_{\mathbf{s}}}_{w_{\mathbf{p}} w_{\mathbf{q}} w_{\mathbf{r}} w_{\mathbf{s}}}|^2}{E^{\mathbf{v}}_{\mathrm{HRM}} - E^{\mathbf{w}}_{\mathrm{HRM}}}, \end{aligned} \tag{3.78}$$

where the summations exclude terms with vanishing denominators. Each sum in the right-hand side can be expanded similarly as Equations (3.66), (3.68), and (3.71). Elements of the W matrices are defined by Equations (3.67), (3.69), (3.70), (3.72), (3.73), etc., in which the XVSCF modals (ζ's) are systematically replaced by the harmonic-oscillator

wave functions (η's). We call this method size-extensive VPT2 or XVPT2. Equation (3.18) can be used to simplify the denominators, which are size-intensive (K^0). It can be readily shown that each term in the right-hand side of Equation (3.78) is size-extensive (K^1) by recognizing that an n-mode W matrix element scales as $K^{1-n/2}$ and an n-fold k summation gives rise to the factor of K^n. In the second-order correction also, higher-order force constants can be included without impairing size-extensivity.

3.3.6 Configuration-interaction theory

A VCI wave function[12] of the state $\mathbf{v}$ in a QFF is a linear combination of the ground and excited XVSCF wave functions,

$$\begin{aligned}\Phi^{\mathbf{v}}_{\mathrm{XVCI}} &= \Phi^{\mathbf{v}}_{\mathrm{XVSCF}} + \sum_{\mathbf{p}} C^{w_\mathbf{p}}_{v_\mathbf{p}} \Phi^{w_\mathbf{p}}_{v_\mathbf{p}} + \frac{1}{2!}\sum_{\mathbf{p},\mathbf{q}}{\sum_{k_p}}' C^{w_\mathbf{p} w_\mathbf{q}}_{v_\mathbf{p} v_\mathbf{q}} \Phi^{w_\mathbf{p} w_\mathbf{q}}_{v_\mathbf{p} v_\mathbf{q}} \\ &\quad + \frac{1}{3!}\sum_{\mathbf{p},\mathbf{q},\mathbf{r}}{\sum_{k_p,k_q}}' C^{w_\mathbf{p} w_\mathbf{q} w_\mathbf{r}}_{v_\mathbf{p} v_\mathbf{q} v_\mathbf{r}} \Phi^{w_\mathbf{p} w_\mathbf{q} w_\mathbf{r}}_{v_\mathbf{p} v_\mathbf{q} v_\mathbf{r}} + \ldots . \end{aligned} \tag{3.79}$$

The expansion can be truncated after the n-fold excited contribution, defining n-mode XVCI or XVCI(n). Substituting this wave function into the Schrödinger equation,

$$\hat{H}_{\mathrm{n}} \Phi^{\mathbf{v}}_{\mathrm{XVCI}} = E^{\mathbf{v}}_{\mathrm{XVCI}} \Phi^{\mathbf{v}}_{\mathrm{XVCI}}, \tag{3.80}$$

and requiring that it be satisfied within the same function space spanned by the XVSCF wave functions that are used to expand the XVCI wave function, we arrive at the XVCI equations to be solved for the unknown coefficients C's:

$$E^{\mathbf{v}}_{\mathrm{XVCI}} = E^{\mathbf{v}}_{\mathrm{XVSCF}} + \sum_{\mathbf{p}} V^{v_\mathbf{p}}_{w_\mathbf{p}} C^{w_\mathbf{p}}_{v_\mathbf{p}} + \frac{1}{2!}\sum_{\mathbf{p},\mathbf{q}}{\sum_{k_p}}' V^{v_\mathbf{p} v_\mathbf{q}}_{w_\mathbf{p} w_\mathbf{q}} C^{w_\mathbf{p} w_\mathbf{q}}_{v_\mathbf{p} v_\mathbf{q}} + \ldots , \tag{3.81}$$

$$\begin{aligned} E^{\mathbf{v}}_{\mathrm{XVCI}} C^{w_\mathbf{p}}_{v_\mathbf{p}} &= V^{w_\mathbf{p}}_{v_\mathbf{p}} + E^{w_\mathbf{p}}_{\mathrm{XVSCF}} C^{w_\mathbf{p}}_{v_\mathbf{p}} + \sum_{\mathbf{q}} V^{w_\mathbf{p} v_\mathbf{q}}_{v_\mathbf{p} w_\mathbf{q}} C^{w_\mathbf{q}}_{v_\mathbf{q}} + \sum_{\mathbf{r}} V^{v_\mathbf{r}}_{w_\mathbf{r}} C^{w_\mathbf{p} w_\mathbf{r}}_{v_\mathbf{p} v_\mathbf{r}} \\ &\quad + \frac{1}{2!}\sum_{\mathbf{q},\mathbf{r}}{\sum_{k_q}}' V^{w_\mathbf{p} v_\mathbf{q} v_\mathbf{r}}_{v_\mathbf{p} w_\mathbf{q} w_\mathbf{r}} C^{w_\mathbf{q} w_\mathbf{r}}_{v_\mathbf{q} v_\mathbf{r}} + \ldots , \end{aligned} \tag{3.82}$$

$$\begin{aligned} E^{\mathbf{v}}_{\mathrm{XVCI}} C^{w_\mathbf{p} w_\mathbf{q}}_{v_\mathbf{p} v_\mathbf{q}} &= V^{w_\mathbf{p} w_\mathbf{q}}_{v_\mathbf{p} v_\mathbf{q}} + E^{w_\mathbf{p} w_\mathbf{q}}_{\mathrm{XVSCF}} C^{w_\mathbf{p} w_\mathbf{q}}_{v_\mathbf{p} v_\mathbf{q}} + \sum_{\mathbf{r}} V^{w_\mathbf{p} w_\mathbf{q} v_\mathbf{r}}_{v_\mathbf{p} v_\mathbf{q} w_\mathbf{r}} C^{w_\mathbf{r}}_{v_\mathbf{r}} + \sum_{\mathbf{r}} V^{w_\mathbf{p} v_\mathbf{r}}_{v_\mathbf{p} w_\mathbf{r}} C^{w_\mathbf{q} w_\mathbf{r}}_{v_\mathbf{q} v_\mathbf{r}} \\ &\quad + \sum_{\mathbf{r}} V^{w_\mathbf{q} v_\mathbf{r}}_{v_\mathbf{q} w_\mathbf{r}} C^{w_\mathbf{p} w_\mathbf{r}}_{v_\mathbf{p} v_\mathbf{r}} + \ldots , \end{aligned} \tag{3.83}$$

and so forth, where $\mathbf{p}$, $\mathbf{q}$, and $\mathbf{r}$ are distinct from one another and $E^{w_\mathbf{p}}_{\mathrm{XVSCF}}$ denotes the energy of the XVSCF wave function in which the quantum number of the mode $\mathbf{p}$ is raised from $v_\mathbf{p}$ to $w_\mathbf{p}$. The V matrix elements are defined by

Equations (3.63)–(3.65) as well as by

$$V^{w_\mathbf{p}}_{v_\mathbf{p}} = \langle \Phi^{w_\mathbf{p}}_{v_\mathbf{p}} | \tilde{V}_{\mathrm{XVSCF}} | \Phi^{\mathbf{v}}_{\mathrm{XVSCF}} \rangle, \tag{3.84}$$

$$V^{w_\mathbf{p} v_\mathbf{q}}_{v_\mathbf{p} w_\mathbf{q}} = \langle \Phi^{w_\mathbf{p}}_{v_\mathbf{p}} | \tilde{V}_{\mathrm{XVSCF}} | \Phi^{w_\mathbf{q}}_{v_\mathbf{q}} \rangle, \tag{3.85}$$

$$V^{w_\mathbf{p} v_\mathbf{q} v_\mathbf{r}}_{v_\mathbf{p} w_\mathbf{q} w_\mathbf{r}} = \langle \Phi^{w_\mathbf{p}}_{v_\mathbf{p}} | \tilde{V}_{\mathrm{XVSCF}} | \Phi^{w_\mathbf{q} w_\mathbf{r}}_{v_\mathbf{q} v_\mathbf{r}} \rangle, \tag{3.86}$$

and so forth. They also scale as $K^{1-n/2}$, where n is the number of modes involved.

With this, we find it impossible to assign well-defined K dependence to C's. Let us examine the K dependence of Equation (3.81). The left-hand side and the first term in the right-hand side are size-extensive (K^1) quantities. For the subsequent terms to be size-extensive, n-mode CI coefficients must scale as $K^{1-n/2}$. In this way, for instance, $V^{v_\mathbf{p} v_\mathbf{q}}_{w_\mathbf{p} w_\mathbf{q}}$ and $C^{w_\mathbf{p} w_\mathbf{q}}_{v_\mathbf{p} v_\mathbf{q}}$ in the second term both scale as K^0 and the summation over k_p gives rise to the factor of K^1, making the third term in the right-hand side overall size-extensive (K^1). Let us now consider Equation (3.82). The left-hand side is a $K^{3/2}$ quantity because, according to the preceding analysis, $E^{\mathbf{v}}_{\mathrm{XVCI}}$ and $C^{w_\mathbf{p}}_{v_\mathbf{p}}$ scale as K^1 and $K^{1/2}$, respectively. This contradicts the $K^{1/2}$ dependence of the right-hand side except for the second term, which scales as $K^{3/2}$. Therefore, XVCI is not size-extensive. An analysis of Equation (3.83) only reinforces this conclusion. Notice that the K dependence of the so-called "disconnected" terms is different and thus incompatible with that of "connected" terms; the disconnected terms, in this case, are the products of E, V, and/or C's with no common summation index such as the left-hand side of Equation (3.82) and the second term in the right-hand side of the same.

3.3.7 Coupled-cluster theory

The VCC method introduced by Christiansen[274–277] is size-extensive (see also Refs.[290–293]). An algebraic proof of this is given here on the basis of an analysis of the K dependence. A VCC wave function in a QFF (XVCC) with a XVSCF reference is written as

$$\begin{aligned}
\Phi^{\mathbf{v}}_{\mathrm{XVCC}} = {} & \Phi^{\mathbf{v}}_{\mathrm{XVSCF}} + \sum_{\mathbf{p}} T^{w_\mathbf{p}}_{v_\mathbf{p}} \Phi^{w_\mathbf{p}}_{v_\mathbf{p}} + \frac{1}{2!} \sum_{\mathbf{p},\mathbf{q}} \sum_{k_p}{}' T^{w_\mathbf{p} w_\mathbf{q}}_{v_\mathbf{p} v_\mathbf{q}} \Phi^{w_\mathbf{p} w_\mathbf{q}}_{v_\mathbf{p} v_\mathbf{q}} + \frac{1}{2!} \sum_{\mathbf{p},\mathbf{q}} T^{w_\mathbf{p}}_{v_\mathbf{p}} T^{w_\mathbf{q}}_{v_\mathbf{q}} \Phi^{w_\mathbf{p} w_\mathbf{q}}_{v_\mathbf{p} v_\mathbf{q}} \\
& + \frac{1}{3!} \sum_{\mathbf{p},\mathbf{q},\mathbf{r}} \sum_{k_p,k_q}{}' T^{w_\mathbf{p} w_\mathbf{q} w_\mathbf{r}}_{v_\mathbf{p} v_\mathbf{q} v_\mathbf{r}} \Phi^{w_\mathbf{p} w_\mathbf{q} w_\mathbf{r}}_{v_\mathbf{p} v_\mathbf{q} v_\mathbf{r}} + \frac{1}{2!} \sum_{\mathbf{p},\mathbf{q},\mathbf{r}} \sum_{k_p}{}' T^{w_\mathbf{p} w_\mathbf{q}}_{v_\mathbf{p} v_\mathbf{q}} T^{w_\mathbf{r}}_{v_\mathbf{r}} \Phi^{w_\mathbf{p} w_\mathbf{q} w_\mathbf{r}}_{v_\mathbf{p} v_\mathbf{q} v_\mathbf{r}} \\
& + \frac{1}{3!} \sum_{\mathbf{p},\mathbf{q},\mathbf{r}} T^{w_\mathbf{p}}_{v_\mathbf{p}} T^{w_\mathbf{q}}_{v_\mathbf{q}} T^{w_\mathbf{r}}_{v_\mathbf{r}} \Phi^{w_\mathbf{p} w_\mathbf{q} w_\mathbf{r}}_{v_\mathbf{p} v_\mathbf{q} v_\mathbf{r}} + \frac{1}{4!} \sum_{\mathbf{p},\mathbf{q},\mathbf{r},\mathbf{s}} \sum_{k_p,k_q,k_r}{}' T^{w_\mathbf{p} w_\mathbf{q} w_\mathbf{r} w_\mathbf{s}}_{v_\mathbf{p} v_\mathbf{q} v_\mathbf{r} v_\mathbf{s}} \Phi^{w_\mathbf{p} w_\mathbf{q} w_\mathbf{r} w_\mathbf{s}}_{v_\mathbf{p} v_\mathbf{q} v_\mathbf{r} v_\mathbf{s}} \\
& + \frac{1}{3!} \sum_{\mathbf{p},\mathbf{q},\mathbf{r},\mathbf{s}} \sum_{k_p,k_q}{}' T^{w_\mathbf{p} w_\mathbf{q} w_\mathbf{r}}_{v_\mathbf{p} v_\mathbf{q} v_\mathbf{r}} T^{w_\mathbf{s}}_{v_\mathbf{s}} \Phi^{w_\mathbf{p} w_\mathbf{q} w_\mathbf{r} w_\mathbf{s}}_{v_\mathbf{p} v_\mathbf{q} v_\mathbf{r} v_\mathbf{s}} + \ldots,
\end{aligned} \tag{3.87}$$

where T's are the unknown coefficients ("T amplitudes") determined by the equations to be discussed shortly. Again, **p**, **q**, **r**, and **s** denote compound indices of distinct modes. The number of modes in T can be limited to n, defining n-mode XVCC or XVCC(n). This equation is distinguished from the XVCI counterpart [Equation (3.79)] by the presence of the terms containing two or more T's such as the fourth term in the right-hand side. Therefore, $\Phi^{\mathbf{v}}_{\mathrm{XVCC}}$ has contributions from the XVSCF wave functions that are excited in as many modes as there are in the whole system (in this case, $3NK$).

The T amplitudes are determined by requiring that the XVCC wave function satisfy the Schrödinger equation,

$$\hat{H}_{\mathrm{n}}\Phi^{\mathbf{v}}_{\mathrm{XVCC}} = E^{\mathbf{v}}_{\mathrm{XVCC}}\Phi^{\mathbf{v}}_{\mathrm{XVCC}}, \tag{3.88}$$

within the space spanned by the XVSCF reference and its excited wave functions up to n modes. In this way, we have the same number of equations as unknowns, which includes the energy $E^{\mathbf{v}}_{\mathrm{XVCC}}$. For instance, the projections of Equation (3.88) onto the XVSCF reference ($\Phi^{\mathbf{v}}_{\mathrm{XVSCF}}$) and one-mode excited wave functions lead to the so-called energy and T_1 amplitude equations, respectively, which read

$$\begin{aligned} E^{\mathbf{v}}_{\mathrm{XVCC}} &= E^{\mathbf{v}}_{\mathrm{XVSCF}} + \sum_{\mathbf{p}} V^{v_{\mathbf{p}}}_{w_{\mathbf{p}}} T^{w_{\mathbf{p}}}_{v_{\mathbf{p}}} + \frac{1}{2!}\sum_{\mathbf{p},\mathbf{q}}\sum_{k_p}{}' V^{v_{\mathbf{p}}v_{\mathbf{q}}}_{w_{\mathbf{p}}w_{\mathbf{q}}} T^{w_{\mathbf{p}}w_{\mathbf{q}}}_{v_{\mathbf{p}}v_{\mathbf{q}}} \\ &\quad + \frac{1}{2!}\sum_{\mathbf{p},\mathbf{q}} V^{v_{\mathbf{p}}v_{\mathbf{q}}}_{w_{\mathbf{p}}w_{\mathbf{q}}} T^{w_{\mathbf{p}}}_{v_{\mathbf{p}}} T^{w_{\mathbf{q}}}_{v_{\mathbf{q}}} + \ldots, \end{aligned} \tag{3.89}$$

and

$$\begin{aligned} E^{\mathbf{v}}_{\mathrm{XVCC}} T^{w_{\mathbf{p}}}_{v_{\mathbf{p}}} &= V^{w_{\mathbf{p}}}_{v_{\mathbf{p}}} + E^{w_{\mathbf{p}}}_{\mathrm{XVSCF}} T^{w_{\mathbf{p}}}_{v_{\mathbf{p}}} + \sum_{\mathbf{q}} V^{w_{\mathbf{p}}v_{\mathbf{q}}}_{v_{\mathbf{p}}w_{\mathbf{q}}} T^{w_{\mathbf{q}}}_{v_{\mathbf{q}}} + \sum_{\mathbf{r}} V^{v_{\mathbf{r}}}_{w_{\mathbf{r}}} T^{w_{\mathbf{p}}w_{\mathbf{r}}}_{v_{\mathbf{p}}v_{\mathbf{r}}} + \sum_{\mathbf{r}} V^{v_{\mathbf{r}}}_{w_{\mathbf{r}}} T^{w_{\mathbf{p}}}_{v_{\mathbf{p}}} T^{w_{\mathbf{r}}}_{v_{\mathbf{r}}} \\ &\quad + \frac{1}{2!}\sum_{\mathbf{q},\mathbf{r}}\sum_{k_q}{}' V^{w_{\mathbf{p}}v_{\mathbf{q}}v_{\mathbf{r}}}_{v_{\mathbf{p}}w_{\mathbf{q}}w_{\mathbf{r}}} T^{w_{\mathbf{q}}w_{\mathbf{r}}}_{v_{\mathbf{q}}v_{\mathbf{r}}} + \frac{1}{2!}\sum_{\mathbf{q},\mathbf{r}} V^{w_{\mathbf{p}}v_{\mathbf{q}}v_{\mathbf{r}}}_{v_{\mathbf{p}}w_{\mathbf{q}}w_{\mathbf{r}}} T^{w_{\mathbf{q}}}_{v_{\mathbf{q}}} T^{w_{\mathbf{r}}}_{v_{\mathbf{r}}} + \ldots. \end{aligned} \tag{3.90}$$

Note that the third term in the right-hand side of Equation (3.89) has a summation over k_p while the subsequent (fourth) term does not. This is because $T^{w_{\mathbf{p}}}_{v_{\mathbf{p}}}$ vanishes unless the momentum conservation condition ($\Delta_{k_p} = 0$) is satisfied.

Equation (3.89) or the energy equation is size-extensive. Remembering that the n-mode V matrix elements scale as $K^{1-n/2}$ and assuming (as in XVCI) that the n-mode XVCC coefficients (the T_n amplitudes) are also the $K^{1-n/2}$ quantities, we find that each term in Equation (3.89) scales consistently as K^1. Therefore, the left-hand side ($E^{\mathbf{v}}_{\mathrm{XVCC}}$) is size-extensive ($K^1$).

The T_1 amplitude equation [Equation (3.90)] is not manifestly size-extensive. This can be seen by comparing the left-hand side, which is a $K^{3/2}$ quantity as $E^{\mathbf{v}}_{\mathrm{XVCC}}$ and $T^{w_{\mathbf{p}}}_{v_{\mathbf{p}}}$ scale as K^1 and $K^{1/2}$, respectively, with the first term in the right-hand side ($V^{w_{\mathbf{p}}}_{v_{\mathbf{p}}}$), which exhibits the $K^{1/2}$ dependence. However, multiplying Equation (3.89) with $T^{w_{\mathbf{p}}}_{v_{\mathbf{p}}}$ and

subtracting it from Equation (3.90), we can bring the latter in a manifestly size-extensive form as

$$\begin{aligned}\left(E^{\mathbf{v}}_{\mathrm{XVSCF}} - E^{w_\mathbf{p}}_{\mathrm{XVSCF}}\right) T^{w_\mathbf{p}}_{v_\mathbf{p}} &= V^{w_\mathbf{p}}_{v_\mathbf{p}} + \sum_{\mathbf{q}} V^{w_\mathbf{p} v_\mathbf{q}}_{v_\mathbf{p} w_\mathbf{q}} T^{w_\mathbf{q}}_{v_\mathbf{q}} + \sum_{\mathbf{r}} V^{v_\mathbf{r}}_{w_\mathbf{r}} T^{w_\mathbf{p} w_\mathbf{r}}_{v_\mathbf{p} v_\mathbf{r}} \\ &\quad + \frac{1}{2!} \sum_{\mathbf{q},\mathbf{r}} {\sum_{k_q}}' V^{w_\mathbf{p} v_\mathbf{q} v_\mathbf{r}}_{v_\mathbf{p} w_\mathbf{q} w_\mathbf{r}} T^{w_\mathbf{q} w_\mathbf{r}}_{v_\mathbf{q} v_\mathbf{r}} + \frac{1}{2!} \sum_{\mathbf{q},\mathbf{r}} V^{w_\mathbf{p} v_\mathbf{q} v_\mathbf{r}}_{v_\mathbf{p} w_\mathbf{q} w_\mathbf{r}} T^{w_\mathbf{q}}_{v_\mathbf{q}} T^{w_\mathbf{r}}_{v_\mathbf{r}} + \ldots . \end{aligned} \tag{3.91}$$

The right-hand side of this equation consists of connected terms only, that is, the sums of products of V and T's that share at least one common summation index. For instance, the fifth term in the right-hand side of Equation (3.90) is disconnected as none of the indices of $T^{w_\mathbf{p}}_{v_\mathbf{p}}$ is a summation index; this term cannot be seen in Equation (3.91). The size-extensivity of the above equation can be verified by inspection of each term. The factor in the left-hand side, $\left(E^{\mathbf{v}}_{\mathrm{XVSCF}} - E^{w_\mathbf{p}}_{\mathrm{XVSCF}}\right)$, is a transition energy and size-intensive (K^0), whereas $T^{w_\mathbf{p}}_{v_\mathbf{p}}$ is assumed to be a $K^{1/2}$ quantity. The left-hand side, therefore, scales as $K^{1/2}$. The first term in the right-hand side is a $K^{1/2}$ quantity. The second term also displays the $K^{1/2}$ dependence because $V^{w_\mathbf{p} v_\mathbf{q}}_{v_\mathbf{p} w_\mathbf{q}}$ and $T^{w_\mathbf{q}}_{v_\mathbf{q}}$ scale as K^0 and $K^{1/2}$, respectively. In this way, all terms can be shown to scale consistently as $K^{1/2}$.

The T_2 amplitude equation is obtained by the projection of Equation (3.88) on to two-mode excited XVSCF wave functions ($\Phi^{w_\mathbf{p} w_\mathbf{q}}_{v_\mathbf{p} v_\mathbf{q}}$). They can furthermore be recast into the manifestly size-extensive, connected form as

$$\begin{aligned}\left(E^{\mathbf{v}}_{\mathrm{XVSCF}} - E^{w_\mathbf{p} w_\mathbf{q}}_{\mathrm{XVSCF}}\right) T^{w_\mathbf{p} w_\mathbf{q}}_{v_\mathbf{p} v_\mathbf{q}} &= V^{w_\mathbf{p} w_\mathbf{q}}_{v_\mathbf{p} v_\mathbf{q}} + \sum_{\mathbf{r}} V^{w_\mathbf{p} w_\mathbf{q} v_\mathbf{r}}_{v_\mathbf{p} v_\mathbf{q} w_\mathbf{r}} T^{w_\mathbf{r}}_{v_\mathbf{r}} \\ &\quad + \sum_{\mathbf{r}} V^{w_\mathbf{p} v_\mathbf{r}}_{v_\mathbf{p} w_\mathbf{r}} T^{w_\mathbf{q} w_\mathbf{r}}_{v_\mathbf{q} v_\mathbf{r}} + \sum_{\mathbf{r}} V^{w_\mathbf{q} v_\mathbf{r}}_{v_\mathbf{q} w_\mathbf{r}} T^{w_\mathbf{p} w_\mathbf{r}}_{v_\mathbf{p} v_\mathbf{r}} + \ldots . \end{aligned} \tag{3.92}$$

It can be readily shown that each term in this equation consistently scales as K^0 using the fact that the n-mode V matrix elements and T_n amplitudes both scale as $K^{1-n/2}$. This procedure can be repeated for T_3 and higher-order T amplitude equations, proving the size-extensivity of XVCC.

Higher-order force constants can be included in VCC without impairing the size-extensivity or the need for adjusting the VSCF reference wave function accordingly. VCC can also be defined analogously for the harmonic-oscillator reference wave function by simply replacing the V matrix elements by the corresponding W matrix elements and $E^{\mathbf{v}}_{\mathrm{XVSCF}}$ by their harmonic counterparts. VCC remains size-extensive after these replacements.

3.4 Conclusions

The issue of size-extensivity of vibrational many-body methods has been analyzed on the basis of the dependence of terms in their formalisms on the number (K) of k vectors in the first BZ, which is a measure of the system size. The aim has been to make these methods applicable to anharmonic lattice vibrations in solids. Taking a one-dimensional

solid with a QFF PES as an example, the compact and strictly size-extensive equations of VSCF have been proposed, introducing the XVSCF method. It accounts for the effect of anharmonicity due to quartic force constants of the type $F_{p-k_p pk_p q-k_q qk_q}$ on the transition energies and that due to cubic force constants of the type $F_{p0q-k_q qk_q}$ on the lattice structures. Size-extensive VMP1, VMP2, and VCC in a QFF have been defined with the XVSCF wave function as the reference by elucidating the K scaling of integrals and excitation amplitudes. Size-extensive VPT1 and VPT2 in a QFF using the harmonic-oscillator reference wave function have also been considered. These methods and the conclusions about their size-extensivity can be readily generalized to two- and three-dimensional solids as well as to a Taylor expansion of PES truncated at any arbitrary order. This analysis, however, cannot be applied to a grid representation of PES. An algebraic proof of the lack of size-extensivity in VCI has also been given. This chapter concentrates on these formal aspects, specifically the structure of size-extensive vibrational many-body methods for anharmonic lattice vibrations.

Chapter 4

Size-extensive vibrational self-consistent field method

4.1 Introduction

In the last decades, vibrational spectroscopies have not only improved their spectral resolution but also extended their applicability to larger and more complex systems such as proteins, enzymes, and even tissues.[294,295] Parallel to these experimental advances, computational abilities to simulate high-resolution vibrational spectra from the first principles have developed, which can sometimes even challenge experimental accuracy.[26] However, such high-accuracy calculations are currently limited to small molecules (up to five or so atoms) and one needs to establish general computational methods to solve vibrational Schrödinger equations for larger molecules and solids. There are at least three issues to be addressed to achieve this goal.

The first issue is the definition of the kinetic-energy operator in the Hamiltonian. The analytical forms of the kinetic-energy operator tailored to given small molecules have been useful,[296–298] but they cannot be generalized easily to larger molecules. A widely accepted solution to this is the use of the Watson Hamiltonian[22,23] and of its various approximations, which have the simple, universal kinetic-energy operator expressed in the normal coordinates. This has proven satisfactory insofar as the vibrational modes do not involve large-amplitude motions.

The second issue is the need for a compact and accurate mathematical representation of the potential energy surface (PES) in the Hamiltonian, which is a (3N–5)- or (3N–6)-dimensional entity, if not approximated, where N is the number of nuclei. A variety of representations have been proposed.[299–302] Among them, of fundamental importance are the Taylor series expansion,[303] the grid-based representations,[34–36] and the many-body expansion or the so-called n-mode representation (nMR),[27,28] which limits the maximum number of modes to be coupled to n and can be used in conjunction with either of the first two representations.

Once the Hamiltonian is defined, the third issue arises as to how one should approximate the wave function and solve the vibrational Schrödinger equation economically. In analogy to the *ab initio* molecular orbital methods for electronic structures, there are systematic approximations for anharmonic vibrational wave functions. The mean-field approach is known as the vibrational self-consistent field (VSCF) method.[66–69] This method was applied to anharmonic vibrational density of states of a protein[304] and to thermal effects on molecular properties,[305] where it

turned out to be the most time-consuming step, leading to a search for more efficient implementations.[306] It also provides a reference wave function for vibrational "correlation" methods such as vibrational Møller–Plesset perturbation (VMP),[13,27,34,273] vibrational coupled-cluster (VCC),[15,290] and vibrational configuration interaction (VCI)[14] methods.

The single most important criterion by which to judge the validity of these approximations for larger molecules and solids is size consistency or, equivalently, size extensivity. A size-extensive method yields total energies of chemical systems that are asymptotically proportional to their volumes.[307] The mean-field method for electronic structures, the Hartree–Fock (HF) method, and correlation corrections thereof such as Møller–Plesset perturbation and coupled-cluster methods are known to be size extensive, whereas truncated configuration interaction methods are not. The size extensivity or the lack thereof can be determined unambiguously by the diagrammatic criterion or the underlying algebraic criterion that relies on the polynomial dependence of the terms in the formalisms for periodic systems on the number of wave vector sampling points in Brillouin-zone integrations.

In Chapter 3, we have investigated the size extensivity of VSCF, VMP, VCC, and VCI with these criteria and found that numerous terms in the formalism of VSCF have nonphysical size dependence. Eliminating these terms, we have defined compact and strictly size-extensive equations of VSCF on the basis of a quartic force field (QFF) in the normal coordinates.[308] It has been shown that second-order VMP and VCC methods in the QFF based on the size-extensive VSCF are also size extensive, while truncated VCI methods are not.

In this chapter*, we report the definition and programmable equations of the size-extensive VSCF (XVSCF) as well as the initial implementation and applications of XVSCF with a QFF. We shall show that not only are the equations of XVSCF drastically simplified as they retain only strictly size-extensive terms, its implementation is also considerably streamlined with no need for a matrix diagonalization unlike any implementation of VSCF. Consequently, XVSCF is three orders of magnitude faster than VSCF, when they both are implemented similarly by us, while yielding comparable results in applications for larger molecules. This implies numerically that VSCF include unnecessary, nonphysical terms that vanish in the bulk limits as our analysis of its formalism suggests. We believe that XVSCF must replace VSCF in future applications and as the basis of VMP and VCC.

4.2 Size-extensive vibrational self-consistent field theory

In Chapter 3, we revealed that the numerous terms in the one-mode function, $U_{m,\mathbf{s}}(Q_m)$, of VSCF exhibit nonphysical size dependence. This analysis was based on the polynomial dependence of terms in the corresponding formalism for periodic solids on the number of wave vector sampling points in Brillouin-zone integrations, which is equivalent to the diagrammatic criterion.[307] Eliminating these spurious terms from the formalisms, we arrived at a strictly size-extensive extension of VSCF, which is called XVSCF.

*The work in this chapter has been publshed in Ref. 309. Reprint permission is granted by American Institute of Physics.

Out of the terms in the QFF, the ones that display the correct size dependence are of the form,[308]

$$V_4 = V_{\text{ref}} + \sum_i \frac{1}{2} F_{ii} Q_i^2 + \sum_{i,j} \frac{1}{2!2^2} F_{iijj} Q_i^2 Q_j^2. \tag{4.1}$$

Hence, linear, cubic, and higher odd-order force constants cannot contribute to VSCF in a size-extensive fashion and are absent in the XVSCF formalism. Also, a small subset of quartic and higher even-order force constants can appear in XVSCF. Unlike VSCF, XVSCF requires the PES to be expanded in a Taylor series,[308] the truncation order of which is indicated as the subscript on V. While we have only implemented XVSCF(4) in this work, which uses V_4, we can readily generalize the definition of V_n for XVSCF(n) with an even truncation order, n:

$$V_6 = V_4 + \sum_{i,j,k} \frac{1}{3!2^3} F_{iijjkk} Q_i^2 Q_j^2 Q_k^2, \tag{4.2}$$

$$V_8 = V_6 + \sum_{i,j,k,l} \frac{1}{4!2^4} F_{iijjkkll} Q_i^2 Q_j^2 Q_k^2 Q_l^2, \tag{4.3}$$

and so forth.

XVSCF(n) is defined as VSCF using V_n instead of V. Thus, we solve

$$\tilde{G}_{m,\mathbf{s}} |\tilde{\phi}_{s_m}\rangle = \tilde{\epsilon}_{s_m} |\tilde{\phi}_{s_m}\rangle, \qquad m = 1, \ldots, M, \tag{4.4}$$

with

$$\tilde{G}_{m,\mathbf{s}} = -\frac{1}{2} \frac{\partial^2}{\partial Q_m^2} + \tilde{U}_{m,\mathbf{s}}(Q_m), \tag{4.5}$$

where we distinguish the XVSCF quantities from the VSCF counterparts by tildes. The one-mode function of XVSCF, $\tilde{U}_{m,\mathbf{s}}(Q_m)$, can be shown to be harmonic for V_n for any value of n,

$$\tilde{U}_{m,\mathbf{s}}(Q_m) = \tilde{U}_{m,\mathbf{s}}^{(0)} + \frac{1}{2} \tilde{U}_{m,\mathbf{s}}^{(2)} Q_m^2, \tag{4.6}$$

with

$$\begin{aligned} \tilde{U}_{m,\mathbf{s}}^{(0)} = V_{\text{ref}} &+ {\sum_i}' \left(-\frac{1}{2} \left\langle \frac{\partial^2}{\partial Q_i^2} \right\rangle + \frac{1}{2} F_{ii} \langle Q_i^2 \rangle \right) \\ &+ {\sum_{i,j}}' \frac{1}{2!2^2} F_{iijj} \langle Q_i^2 \rangle \langle Q_j^2 \rangle \\ &+ {\sum_{i,j,k}}' \frac{1}{3!2^3} F_{iijjkk} \langle Q_i^2 \rangle \langle Q_j^2 \rangle \langle Q_k^2 \rangle \end{aligned}$$

$$+\sum_{i,j,k,l}{}' \frac{1}{4!2^4} F_{iijjkkll}\langle Q_i^2\rangle\langle Q_j^2\rangle\langle Q_k^2\rangle\langle Q_l^2\rangle + \ldots, \tag{4.7}$$

$$\begin{aligned}\tilde{U}^{(2)}_{m,\mathbf{s}} &= F_{mm} + \sum_i{}' \frac{1}{2^1} F_{iimm}\langle Q_i^2\rangle \\ &+\sum_{i,j}{}' \frac{1}{2!2^2} F_{iijjmm}\langle Q_i^2\rangle\langle Q_j^2\rangle \\ &+\sum_{i,j,k}{}' \frac{1}{3!2^3} F_{iijjkkmm}\langle Q_i^2\rangle\langle Q_j^2\rangle\langle Q_k^2\rangle \\ &+\ldots,\end{aligned} \tag{4.8}$$

where the primes on the summation symbols indicate that the mth mode is excluded from the sums. XVSCF(n) truncates Equations (4.7) and (4.8) after the $(n/2)$th terms. For instance, the one-mode functions of XVSCF with a QFF or XVSCF(4) are given by

$$\begin{aligned}\tilde{U}^{(0)}_{m,\mathbf{s}} &= V_{\text{ref}} + \sum_i{}' \left(-\frac{1}{2}\left\langle\frac{\partial^2}{\partial Q_i^2}\right\rangle + \frac{1}{2}F_{ii}\langle Q_i^2\rangle\right) \\ &+\sum_{i,j}{}' \frac{1}{2!2^2} F_{iijj}\langle Q_i^2\rangle\langle Q_j^2\rangle,\end{aligned} \tag{4.9}$$

$$\tilde{U}^{(2)}_{m,\mathbf{s}} = F_{mm} + \sum_i{}' \frac{1}{2^1} F_{iimm}\langle Q_i^2\rangle. \tag{4.10}$$

In contrast to VSCF, Equation (4.4) can be solved analytically and without any need for a basis-set expansion or matrix diagonalization because the one-mode functions are effectively harmonic, which, however, include the effects of quartic and higher even-order force constants of certain types. Hence, the mth modal of XVSCF is simply a HO wave function,

$$\tilde{\phi}_{s_m}(Q_m) = \tilde{\mathcal{N}}_{s_m,m}\mathcal{H}_{s_m}(\sqrt{\tilde{\omega}_m}Q_m)\exp(-\tilde{\omega}_m Q_m^2/2), \tag{4.11}$$

with the frequencies $\tilde{\omega}_m$ being related to the one-mode functions by

$$\tilde{\omega}_m = \sqrt{\tilde{U}^{(2)}_{m,\mathbf{s}}}. \tag{4.12}$$

Because the matrix elements of various operators appearing in Equations (4.7) and (4.8) depend on the modals and their frequencies (see Table 1.1), Equation (4.12) and Equations (4.7) and (4.8) or Equations (4.9) and (4.10) must still be solved iteratively until the self consistency is achieved.

Using Table 1.1, Equations (4.7) and (4.8) can be written explicitly in terms of $\{\tilde{\omega}_i\}$, $\mathbf{s}$, and force constants as

$$\begin{aligned}
\tilde{U}^{(0)}_{m,\mathbf{s}} &= V_{\rm ref} + \sum_i{}' (\tilde{\omega}_i^2 + F_{ii}) \frac{s_i + 1/2}{2\tilde{\omega}_i} \\
&\quad + \frac{1}{2!} \sum_{i,j}{}' F_{iijj} \frac{s_i + 1/2}{2\tilde{\omega}_i} \frac{s_j + 1/2}{2\tilde{\omega}_j} \\
&\quad + \frac{1}{3!} \sum_{i,j,k}{}' F_{iijjkk} \frac{s_i + 1/2}{2\tilde{\omega}_i} \frac{s_j + 1/2}{2\tilde{\omega}_j} \frac{s_k + 1/2}{2\tilde{\omega}_k} \\
&\quad + \ldots, \qquad (4.13) \\
\tilde{U}^{(2)}_{m,\mathbf{s}} &= F_{mm} + \sum_i{}' F_{iimm} \frac{s_i + 1/2}{2\tilde{\omega}_i} \\
&\quad + \frac{1}{2!} \sum_{i,j}{}' F_{iijjmm} \frac{s_i + 1/2}{2\tilde{\omega}_i} \frac{s_j + 1/2}{2\tilde{\omega}_j} + \ldots . \qquad (4.14)
\end{aligned}$$

The total XVSCF energy of the state $\mathbf{s}$ is then written as

$$\tilde{E}_{\mathbf{s}} = (s_m + 1/2)\tilde{\omega}_m + \tilde{U}^{(0)}_{m,\mathbf{s}} \qquad (4.15)$$

or

$$\begin{aligned}
\tilde{E}_{\mathbf{s}} &= V_{\rm ref} + \sum_i (\tilde{\omega}_i^2 + F_{ii}) \frac{s_i + 1/2}{2\tilde{\omega}_i} \\
&\quad + \frac{1}{2!} \sum_{i,j} F_{iijj} \frac{s_i + 1/2}{2\tilde{\omega}_i} \frac{s_j + 1/2}{2\tilde{\omega}_j} \\
&\quad + \frac{1}{3!} \sum_{i,j,k} F_{iijjkk} \frac{s_i + 1/2}{2\tilde{\omega}_i} \frac{s_j + 1/2}{2\tilde{\omega}_j} \frac{s_k + 1/2}{2\tilde{\omega}_k} \\
&\quad + \ldots, \qquad (4.16)
\end{aligned}$$

where the summations in this equation do not exclude any particular mode.

The total XVSCF energy given by these expressions is rigorously extensive (namely, asymptotically proportional to size) in the diagrammatic sense. Figure 4.1 is a diagrammatic expression of Equation (4.16), which consists of only closed, connected diagrams. Here, the filled circle vertex with two edges represents $\tilde{\omega}_i\tilde{\omega}_j + F_{ij}$ with its two edges signifying normal modes i and j. A filled circle vertex with n edges (an nth-order vertex) with $n > 2$ corresponds to an nth-order force constant with each edge specifying a normal mode involved. A loop means two normal modes coincide and the summation must be taken of the force constant over that normal mode index (say, i) together with a factor of $(s_i + 1/2)/2\tilde{\omega}_i$. We must associate a factor of $1/m!$ for m equivalent loops. An nth-order vertex or nth-order force constant is shown to exhibit the $V^{1-n/2}$ dependence on the volume V of the system[308] and each loop gives rise to a factor of V. This is sufficient to show that each diagram in Fig. 4.1 scales as V and is extensive.

The XVSCF equations given here can be applied to an individual target state **s** to determine its wave function and total energy. However, when using this state-specific approach, one should be cautious about two issues. First, a nonlinear optimization for any state other than the ground state cannot be proved to be variational since the wave functions optimized individually for different states are not necessarily orthogonal. Second, the transition energies obtained as the energy differences between these states may not be shown to be intensive (namely, asymptotically constant with size). Therefore, we propose the XVSCF method to be used only for the ground state and the transition energies to be obtained by Equation (4.15). The fundamental transition frequency of the mth mode is thus $\tilde{\omega}_m$, which is intensive.

It may be worth clarifying precisely what we mean by the lack of size extensivity in VSCF and its practical consequences. VSCF is not size extensive in the sense that its working equations contain numerous terms that have nonphysical size dependence.[308] Under the conditions of usual calculations, these nonphysical terms decrease with size and eventually vanish in the bulk limit and the VSCF transition frequencies converge towards the ones from XVSCF. Hence, for a larger system, VSCF is a wasteful equivalent of XVSCF as the computational cost of the former scales as $O(M^n)$, where M is the number of modes and n is the truncation rank of the Taylor expansion of a PES, while the cost of the latter is only $O(M^{n/2})$. Even when only the subset of force constants used in XVSCF is retained in VSCF, the latter is considerably slower than the former, as we shall demonstrate below. Also note that VSCF with 1MR reduces to the harmonic approximation and captures no anharmonicity in the bulk limit. Therefore, the practical consequence of the difference between VSCF and XVSCF is the significant lack of efficiency in VSCF when the system is large. Furthermore, the terms that involve cubic force constants of the F_{ijj} type and higher odd-order force constants of certain types have the effect of shifting the minima of the mean-field potentials of VSCF away from the equilibrium geometry,[308] making the expansion of wave functions by basis functions centered at the equilibrium geometry less effective for larger systems. Another potential practical consequence is, therefore, the lack of stability in the algorithm to solve the working equations of VSCF when the system is large. The numerical proof of these assertions is given in the Appendix.

When the system is relatively small, VSCF is generally more accurate than XVSCF since the former takes into account $O(M^n)$ force constants while the latter does only $O(M^{n/2})$ force constants. Furthermore, VSCF can be used in conjunction with virtually any mathematical representation of a PES including grid-based ones, which may be more suitable for large-amplitude motions. XVSCF, on the other hand, is defined only for a PES expanded in a Taylor series, although the truncation rank can be arbitrary. This limitation arises because a Taylor series expansion in the normal coordinates has well-defined size dependence (see above), which is essential for our purpose of constructing size-extensive vibrational methods.

4.3 Implementations

The XVSCF method with a QFF [XVSCF(4)] as well as VSCF with a QFF have been implemented as a part of the general vibrational many-body program package MaVi.[310] All calculations described below have been performed with MaVi except the PES scan and the generation of QFF's. The latter have been done with the Sindo code written by Yagi.[70]

4.3.1 VSCF

Among the terms of Equation (1.17), $U^{(0)}_{m,\mathbf{s}}$ is the most time-consuming to evaluate as it involves a four-fold summation. However, since it is just a constant, it can be neglected during the iterative solution of VSCF. It is evaluated only once and included in the total energy after the iterative solutions converge. The VSCF algorithm implemented by us is summarized in Fig. 4.2.

The operational cost associated with the diagonalization of the G matrix (Step 6 of Fig. 4.2) is $O(N_{\mathrm{it}}MN_m^3)$, where N_{it} is the number of iterations (typically, not exceeding 10), M is the number of modes, and N_m is the number of HO basis functions of the mth mode. We have used $N_m = 20$ in all the calculations discussed below. The costs of building $U^{(0)}_{m,\mathbf{s}}$ (Step 9) and $U^{(1)}_{m,\mathbf{s}}$ (Step 4) increase as $O(N_{\mathrm{it}}M^4)$ and $O(M^3)$, respectively. Obtaining all necessary force constants in a QFF (Step 0) may require $O(M^4)$ single-point electronic structure calculations. The overall scaling of the cost of VSCF with a QFF is, therefore, M^4. The nMR approximation can reduce it to M^n.

4.3.2 XVSCF

Not only is XVSCF size extensive and theoretically more sound than VSCF, its algorithm is considerably streamlined than that of the latter. The algorithm of XVSCF is outlined in Fig. 4.3. The calculation of $\tilde{U}^{(2)}_{m,\mathbf{s}}$ scales linearly with the number of modes for XVSCF(4), hence a single iteration involves only $O(M^2)$ operations. Unlike VSCF, XVSCF does not require basis-set expansion or matrix diagonalization. Consequently, XVSCF is nearly three orders of magnitude faster than VSCF, which are implemented similarly by us, even when the latter takes into account only the quadratic and quartic force constants of F_{iijj} type (see Fig. 4.4). A VSCF calculation that takes into account a whole QFF costs even more and the cost also increases much more rapidly (as M^4) with M. One iteration of the self-consistent solution (Steps 2–6 of Fig. 4.3) of the XVSCF equation takes less than one second on a single 1.3-GHz processor for a molecule with 6,600 modes. The convergence of the self-consistent iterations is also observed to be rapid. The errors in $\tilde{\omega}$'s become less than 10^{-10} cm^{-1} after seven iterations.

VSCF with the quadratic and quartic force constants of F_{iijj} type is in fact an alternative way to perform a XVSCF(4) calculation, although the former involves diagonalization of the G matrix and is thus not an efficient

implementation (see Fig. 4.4). We have compared the result of this calculation with that of XVSCF(4) to verify our XVSCF(4) implementation.

4.4 Numerical Applications

We applied XVSCF(4) and VSCF with QFF's implemented in MAVI to H_2O as well as benzene and polyacenes of increasing sizes, namely, naphthalene, anthracene, and tetracene. The QFF of H_2O was computed at the MP2/aug-cc-pVTZ level and those of benzene and polyacenes at the MP2/STO-3G level using NWCHEM[311] and SINDO,[70,303] The focus of these applications in this chapter is to elucidate the comparative performance of XVSCF(4) and VSCF and its size dependence and, therefore, the accuracy of the PES and QFF's is not our primary concern.

Tables 4.1 lists the fundamental frequencies of H_2O computed by the harmonic approximation, XVSCF(4), and VSCF as well as vibrational full configuration interaction (VCI) using either V in Equation (1.10) or V_4 in Equation (4.1). Generally, the XVSCF(4) frequencies are in much worse agreement with the exact, VCI(V) results than the VSCF ones simply because XVSCF(4) takes into account only a small subset of the QFF and no cubic force constants, in particular. In some cases, XVSCF(4) even gives the wrong sign in the anharmonic corrections to the harmonic frequencies. For the bending mode (ν_1) of H_2O, in which cubic force constants do not play a significant role, XVSCF(4) captures almost as much anharmonic effects as VSCF.

XVSCF(4) agrees excellently with VCI(V_4) for all modes examined here. This supports our assertion that the poor agreement between XVSCF(4) and VCI(V) is traced almost entirely to the difference in the force constants included in these two methods. We note, furthermore, that the effects of these additional force constants in VSCF, while unquestionably important in small molecules, are to be washed out with increasing molecular size (see below). Neither VCI(V_4) nor VCI(V) is size extensive.

Figure 4.5 compares the anharmonic corrections to the harmonic fundamental frequencies of benzene and polyacenes obtained by XVSCF(4), VSCF with the QFF in the 1MR approximation, and VSCF with the QFF in the 2MR approximation. In benzene, XVSCF(4) systematically underestimates the anharmonic corrections as compared with VSCF(2MR) or even with VSCF(1MR) in some instances. This is traced, again, to the fact that XVSCF(4) excludes all cubic and many quartic force constants, which are considered in VSCF(2MR) or even in VSCF(1MR). However, VSCF(1MR) turns out to be extremely poor in describing the C–H stretching vibrations (modes 25–30), in which anharmonic mode-mode couplings must be significant.

As we increase the size of the polyacenes, XVSCF(4) and VSCF(2MR) become closer to each other, while VSCF(1MR) is in worse agreement with VSCF(2MR) than XVSCF(4). The mean absolute devitations between XVSCF(4) and VSCF(2MR) decrease from 12.4 (benzene) to 9.8 (naphthalene), 9.3 (anthracene), and 8.9 cm^{-1}

(tetracene) as we increase the size of the molecules. This is the numerical manifestation of the fact that the cubic and quartic force constants included in VSCF but excluded in XVSCF(4) have nonphysical size dependence and their contributions vanish gradually with increasing size. In other words, VSCF(2MR) is nearly three orders of magnitude more expensive than XVSCF(4) with no additional benefit in accuracy of their results for large molecules and solids. This is particularly evident in the C–H stretching vibrations of each molecule which can be discerned from the rest by their large anharmonic corrections. For these modes, the mean absolute devitations between XVSCF(4) and VSCF(2MR) decrease from 21.4 (benzene) to 17.0 (naphthalene), 14.0 (anthracene), and 12.0 cm^{-1} (tetracene), moreover this gradual convergence can also be inferred from the figure. It is also clear that VSCF(1MR) captures inadequately small portions of anharmonic corrections in larger molecules. In fact, VSCF(1MR) reduces to the harmonic approximation in the bulk limit, while VSCF(2MR) to XVSCF(4) in the same limit.

4.5 Size-extensivity analysis

Here we analyze the size dependence of the mean-field potentials and frequencies of VSCF and XVSCF using a one-dimensional colinear chain of $N + 1$ unit masses experiencing a nearest-neighbor QFF of the form,

$$\begin{aligned} V(x_1, \ldots, x_{N+1}) &= \sum_{\kappa=1}^{N} \frac{1}{2!}(x_{\kappa+1} - x_\kappa)^2 \\ &\quad + \sum_{\kappa=1}^{N} \frac{1}{3!}(x_{\kappa+1} - x_\kappa)^3 \\ &\quad + \sum_{\kappa=1}^{N} \frac{1}{4!}(x_{\kappa+1} - x_\kappa)^4, \end{aligned} \tag{4.17}$$

where x_κ denotes the signed displacement from the equilibrium position of the κth mass. There are N vibrational degrees of freedom in this system. The corresponding QFF in the normal coordinates can be obtained through the following transformations,

$$F_i = \sum_{\kappa} C_i^\kappa F_\kappa = 0, \tag{4.18}$$

$$F_{ij} = \sum_{\kappa,\lambda} C_i^\kappa C_j^\lambda F_{\kappa\lambda} = \delta_{ij}\omega_i^2, \tag{4.19}$$

$$F_{ijk} = \sum_{\kappa,\lambda,\mu} C_i^\kappa C_j^\lambda C_k^\mu F_{\kappa\lambda\mu}, \tag{4.20}$$

and

$$F_{ijkl} = \sum_{\kappa,\lambda,\mu,\nu} C_i^\kappa C_j^\lambda C_k^\mu C_l^\nu F_{\kappa\lambda\mu\nu}, \tag{4.21}$$

where ω_i and C_i^κ denote the square root of the eigenvalue (harmonic frequency) and the κth element of the eigenvector, respectively, of the mass-weighted Hessian matrix corresponding to the ith normal coordinate. The force constants with the Greek subscripts are the original QFF in the Cartesian coordinates such as

$$F_{\kappa\lambda\mu\nu} = \frac{\partial^4 V}{\partial x_\kappa \partial x_\lambda \partial x_\mu \partial x_\nu}. \tag{4.22}$$

The force constants in the normal coordinates can be used to carry out VSCF-QFF and XVSCF(4) calculations for the chains with various lengths (simply referred to as VSCF and XVSCF in this section). The units are arbitrary.

First, let us consider VSCF in the 1MR approximation for this system. Figure 4.6 shows that the mean and maximum deviations in the frequencies between the VSCF and harmonic approximations decrease exponentially with N (the number of modes or the measure of system size). This numerically demonstrates that VSCF-1MR, while being an exact anharmonic treatment of diatomic molecules, reduces to the harmonic approximation in the bulk limit, capturing no anharmonicity whatsoever. In other words, VSCF-1MR is not size extensive. The situation is analogous to a truncated CI for electronic structures, which is not size extensive and yields vanishing correlation energies in the bulk limit, reducing to a wasteful equivalent of HF.[307]

When we retain the full QFF, we encounter a convergence problem with VSCF (but not with XVSCF) as N is increased, which is another manifestation of the lack of size extensivity in VSCF. With increasing N, we find that more and more basis functions per mode are needed to expand even the lowest-lying modals of VSCF. This is because these modals acquire greater contributions from higher-lying excited HO basis functions in their expansions as N increases. The source of this rather puzzling convergence problem can be understood by inspecting the VSCF mean-field potentials, $U_{m,\mathbf{s}}(Q_m)$, for different values of N. Figures 4.7 and 4.8 plot $U_{2,\mathbf{0}}(Q_2)$ as a function of Q_2, which is the lowest-lying breathing vibration ($m = 2$) of the chain, at two different chain lengths, $N = 4$ and 16, respectively. The XVSCF mean-field potentials, $\tilde{U}_{2,\mathbf{0}}(Q_2)$, are also superimposed for comparison. As seen, the minimum of the VSCF mean-field potential shifts away from $Q_2 = 0$ as N is increased, while that of the XVSCF mean-field potential remains at the origin (the equilibrium geometry). This explains the decreased effectiveness in expanding modals of the VSCF mean-field potentials by the HO basis functions centered at the equilibrium geometry.

This observed shift of the minimum is anticipated in our prior analysis[308] and is due to the cubic force constants of the F_{ijj} type. These force constants lower the VSCF mean-field potentials by amounts that do not scale correctly with size.[308] In other words, both the vertical and horizontal shifts of the mean-field potentials by the F_{ijj} force constants are the direct evidence of the lack of size extensivity of VSCF. While the shapes of the mean-field potentials and thus the transition frequencies are unchanged by these force constants, the total energies and the stability of the algorithm of VSCF are negatively affected. In the expressions of the XVSCF frequencies, these and other cubic force constants

are, therefore, not present. We did not encounter the convergence problem in the VSCF calculations of polyacenes with such severity. This was probably because most of the contributions from F_{ijj} vanished due to symmetry and the size of the system was not too large.

If we exclude the cubic force constants of the F_{ijj} type from the QFF, VSCF no longer experiences the aforementioned convergence problem because it restores the minimum of the mean-field potentials at the equilibrium geometry. However, VSCF in this approximation still differs from XVSCF because VSCF involves other cubic and quartic force constants not included in XVSCF. These extra force constants vanish in the bulk limit. Figure 4.9 compares the mean-field potentials of VSCF (with no F_{ijj}) and XVSCF at $N = 64$. The two mean-field potentials are indistinguishable from each other, indicating that the force constants included only in VSCF at an enormously increased computational cost indeed play no role in the final computational results in the bulk limit. Furthermore, the figure supports our claim that the VSCF mean-field potentials become quadratic in the bulk limit. XVSCF utilizes this fact at the formalism level and its mean-field potentials are quadratic by definition. This must not to be taken to mean that XVSCF reduces to the harmonic approximation; the effectively quadratic mean-field potentials of XVSCF include the effect of F_{iijj}.

Finally, the deviations between the VSCF (with no F_{ijj}) and XVSCF frequencies are plotted as a function of N in Fig. 4.10. The VSCF results rapidly approach those of the XVSCF ones with increasing N in spite of numerous more contributions considered in the former. This numerically proves that these contributions in VSCF are not size extensive and vanish in the bulk limit, making VSCF a wasteful equivalent of diagrammatically size-extensive XVSCF.

4.6 Conclusion

This chapter has introduced the theory, programmable equations, algorithms, and initial implementation as well as numerical applications of XVSCF using a QFF [XVSCF(4)] in normal coordinates. Note that XVSCF is *not* an approximation to VSCF; Being a size-extensive mean-field theory for vibrations, XVSCF replaces VSCF. XVSCF is thus built on the diagrammatic size-extensivity criteria[307,308] with its definitions expressed by connected diagrams only [Fig. 4.1]. It is, therefore, expected to maintain uniform accuracy across different molecular sizes from small molecules to solids. Although a decisive numerical proof is hard to achieve (the analytical, diagrammatic proof is given in this chapter and elsewhere[307,308]), we have demonstrated the gradual convergence of XVSCF(4) and VSCF(2MR). Since XVSCF(4) includes only a small subset of quartic force constants, which makes the one-mode function always effectively harmonic, the XVSCF equations can be solved without a need for an expansion of modals with basis functions or matrix diagonalization. Consequently, our XVSCF(4) code is nearly three orders of magnitude faster than the VSCF code implemented by us similarly including just the same set of force constants. VSCF with a full set of QFF scales as M^4 where M is the number of modes and is even more expensive than XVSCF(4), which scales as

M^2.

It should be noted that XVSCF(4) is the lowest member of a systematic hierarchy of the XVSCF(n) approximations defined by various truncation orders of a Taylor series expansion of a PES. For instance, with sextic force constants of F_{iijjkk} type, we can define XVSCF(6). XVSCF(n) also forms the basis of size-extensive correlated anharmonic vibrational methods such as size-extensive VMP (XVMP2) and size-extensive VCC (XVCC), which can restore the effects of force constants excluded in XVSCF in a size-extensive fashion.[308] Implementations of these methods are underway in our laboratory and will be reported separately.

After the publication of this study, we have been notified by Makri about earlier work on quantum dissipative dynamics that have similar conclusions to ours.[312–314]

4.7 Figures

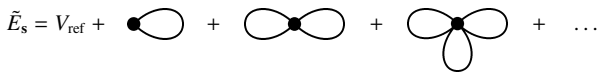

Figure 4.1: Diagrammatic expression of Equation (4.16).

```
0:  Input M, s, F_ii, F_ijk, F_ijkl, etc.
1:  Construct an initial guess for C_{n,s_m}
2:  Repeat
3:     For m = 1 to M do
4:        Calculate U^(1)_{m,s}, U^(2)_{m,s}, U^(3)_{m,s}, and U^(4)_{m,s}
5:        Form the G matrix
6:        Diagonalize the G matrix to determine ε_{s_m} and C_{n,s_m}
7:     End for
8:  Until all ε_{s_m} cease to change more than a threshold
9:  Calculate U^(0)_{m,s} and E_s
```

Figure 4.2: The algorithm of VSCF.

```
0:  Input M, s, F_ii, F_iijj (i ≠ j), etc.
1:  Construct an initial guess for ω̃_m
2:  Repeat
3:     For m = 1 to M do
4:        Calculate Ũ^(2)_{m,s} and ω̃_m
5:     End for
6:  Until all ω̃_m cease to change more than a threshold
7:  Calculate Ũ^(0)_{m,s} and Ẽ_s
```

Figure 4.3: The algorithm of XVSCF.

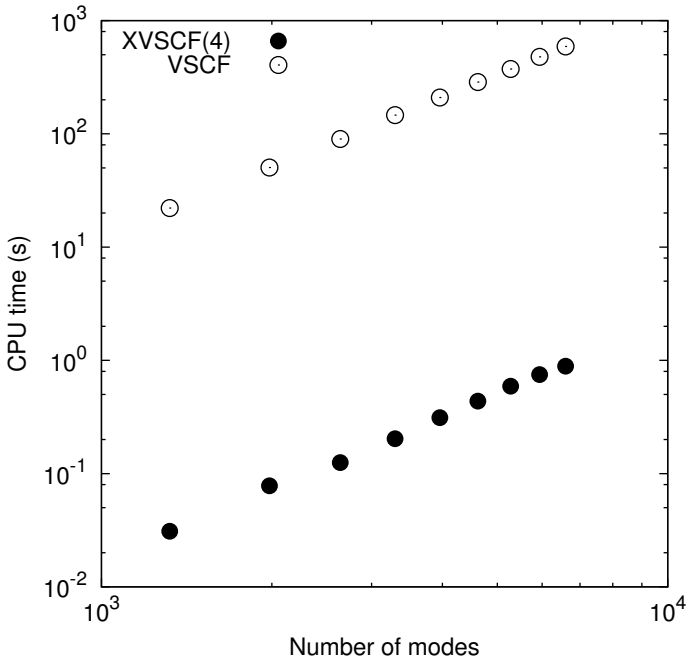

Figure 4.4: The CPU time (in seconds) required in one iteration of VSCF and XVSCF with a QFF as a function of the number of modes (M). The systems used consist of up to 100 noninteracting anthracene molecules. In VSCF, only the quadratic force constants and quartic force constants of F_{iijj} type are included, resulting in quadratic overall scaling of CPU time as a function of M in both VSCF and XVSCF. A VSCF calculation with a full QFF involves $O(M^4)$ operations.

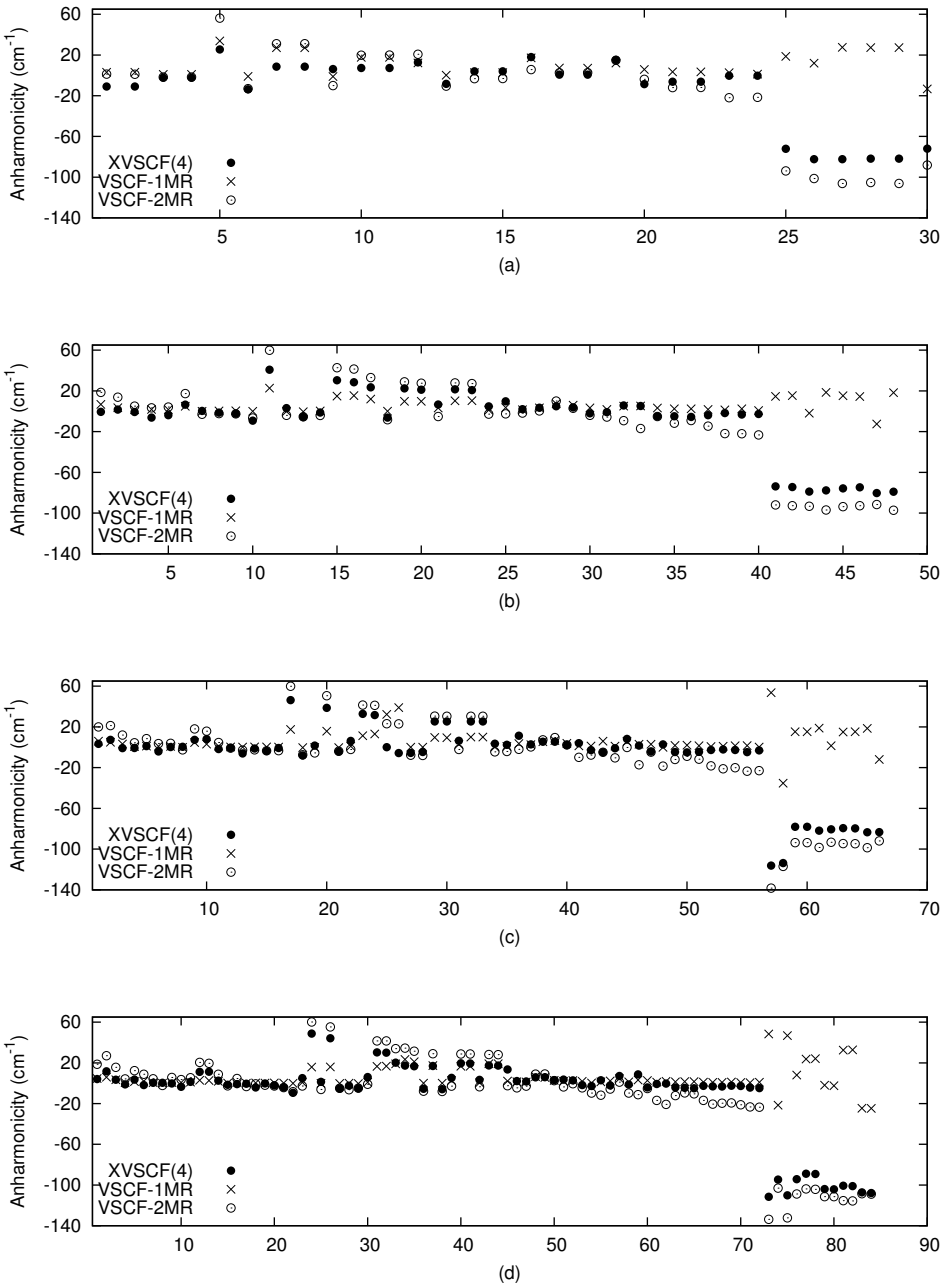

Figure 4.5: The anharmonic corrections (in cm^{-1}) to the fundamental frequencies of (a) benzene, (b) naphthalene, (c) anthracene, and (d) tetracene obtained by XVSCF(4), VSCF(1MR), and VSCF(2MR). The modes (the horizontal axes) are numbered for each molecule in the increasing order of their harmonic frequencies.

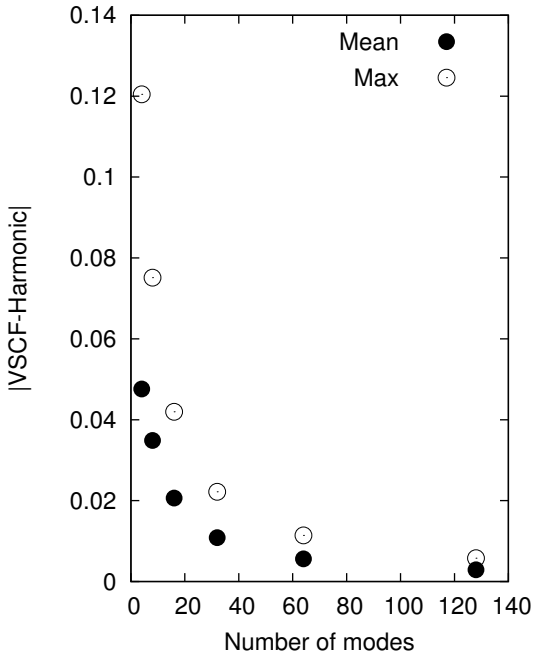

Figure 4.6: The mean and maximum deviations in the frequencies between of the VSCF-1MR and harmonic approximations as a function of the number of modes (N). The dataset includes the zero-point energies per mode and the fundamental transition frequencies.

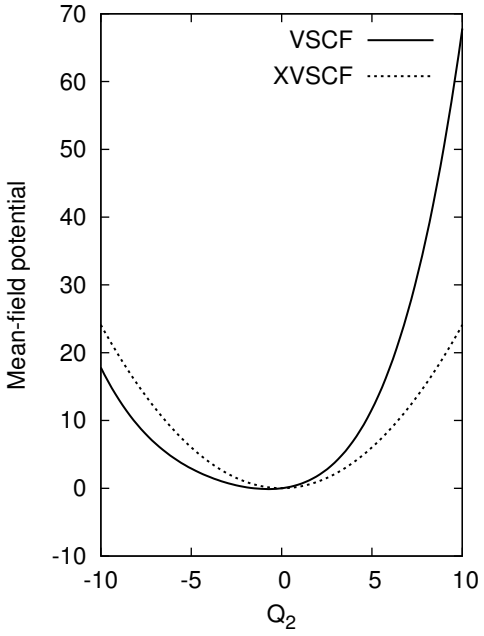

Figure 4.7: The VSCF ($U_{2,\mathbf{0}}$) and XVSCF ($\tilde{U}_{2,\mathbf{0}}$) mean-field potentials along the breathing mode in the chain with $N = 4$.

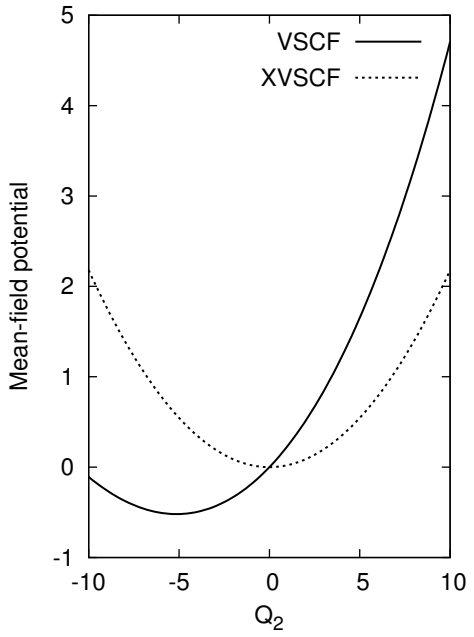

Figure 4.8: The VSCF ($U_{2,\mathbf{0}}$) and XVSCF ($\tilde{U}_{2,\mathbf{0}}$) mean-field potentials along the breathing mode in the chain with $N = 16$.

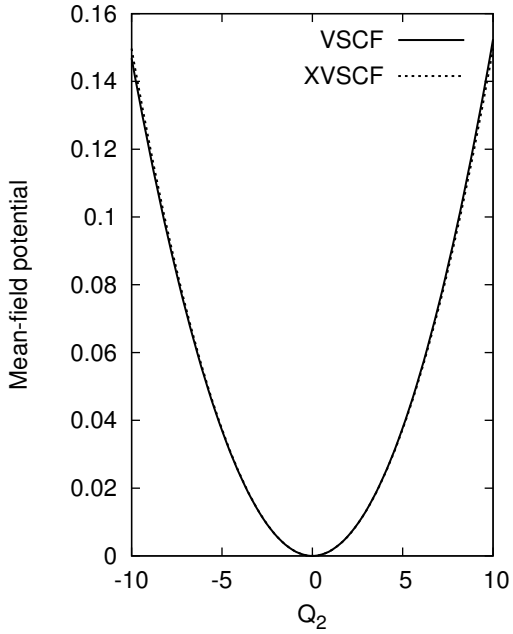

Figure 4.9: The VSCF ($U_{2,\mathbf{0}}$) and XVSCF ($\tilde{U}_{2,\mathbf{0}}$) mean-field potentials along the breathing mode in the chain with $N = 64$. The QFF excludes the force constants of the F_{ijj} type (see text for details).

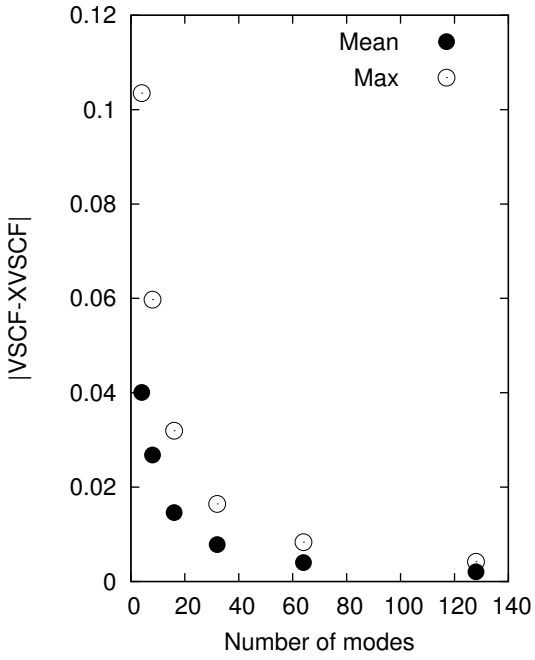

Figure 4.10: The mean and maximum deviations in the frequencies between of VSCF and XVSCF as a function of the number of modes (N). The dataset includes the zero-point energies per mode and the fundamental transition frequencies. The QFF excludes the force constants of the F_{ijj} type (see text for details).

4.8 Tables

Table 4.1: The fundamental frequencies (in cm^{-1}) of H_2O obtained by the harmonic approximation, XVSCF(4), VCI with V_4 [Equation (4.1)], VSCF, and VCI with V [Equation (1.10)].

Mode	Harmonic	XVSCF(4)	VCI(V_4)	VSCF	VCI(V)
ν_1	1628	1543	1542	1562	1557
ν_2	3822	3875	3871	3727	3682
ν_3	3948	3993	3988	3815	3792

Table 4.2: The fundamental frequencies (in cm^{-1}) of CO_2 obtained by the harmonic approximation, XVSCF(4), VCI with V_4 [Equation (4.1)], VSCF, and VCI with V [Equation (1.10)].

Mode	Harmonic	XVSCF(4)	VCI(V_4)	VSCF	VCI(V)
ν_1	656	641	641	652	651
ν_2	1305	1305	1305	1297	1252
ν_3	2379	2365	2365	2348	2344

Chapter 5

Anharmonic frequencies of polyethylene and polyacetylene in the Γ approximation

5.1 Introduction

The vibrational configuration-interaction (VCI) method[12] and even the vibrational self-consistent field (VSCF) method[67–69] under certain circumstances are not size-extensive and cannot, therefore, be applied to anharmonic lattice vibrations.[281] One straightforward way of restoring size-extensivity in these methods is to invoke the Γ approximation.[315–318] It restricts the wave vectors (k vectors) included in the Brillouin zone (BZ) integrations to those that correspond to the in-phase ones, namely, those occurring at the Γ point ($k = 0$) in the phonon dispersion curves. In addition to rendering virtually any vibrational method size-extensive, it has the following three important advantages: (1) While the Γ approximation can yield the energies of the in-phase ($k = 0$) vibrations only, such vibrations are of particular interest as they are the only ones observable by infrared and/or Raman spectroscopies according to their selection rules. The approximation, therefore, constitutes one of the most efficient ways of probing these important modes selectively. (2) The approximation requires only those force constants with respect to in-phase ($k = 0$) and real normal coordinates, which can be obtained without having to lift periodic symmetry in electronic structure calculations. The crystal orbital (CO) methods[260,261,319] based on the periodic boundary conditions can thus be used to obtain these force constants adopting the most compact unit cell, namely, without the so-called supercell or frozen phonon approach. (3) It is efficient and also accurate as demonstrated in this work, although it neglects anharmonic phonon-phonon coupling across different linear quasi-momenta (k vectors).

In this chapter*, we study the validity of the Γ approximation in quantitative, anharmonic treatments[8,269–271] of the in-phase lattice vibrations of polyethylene and polyacetylene, the frequencies of which have been measured by infrared and Raman spectroscopies.[321–326] The individual effects of electron correlation and anharmonicity are quantified by using the Gaussian-basis-set CO methods[260,261,319] at the Hartree–Fock (HF)[263–265] and second-order Møller–Plesset perturbation (MP2) levels[266,327] for electrons and VSCF, VCI, and vibrational MP2 (VMP2)[13] methods in the Γ approximation for vibrations. We show that the VCI and VMP2 calculations based on the potential energy surface (PES) obtained by MP2 can reproduce the observed frequencies of infrared and Raman bands of polyethylene and

*The work in this chapter has been published in Ref. 320. Reprint permission is granted by American Institute of Physics.

polyacetylene with remarkable accuracy, suggesting that the anharmonic phonon-phonon coupling across different k vectors may indeed be weak. It is also shown numerically that electron correlation enhances anharmonicity in the PES significantly. Fermi resonances in polyethylene have also been identified and semi-quantitatively explained by our calculations.

5.2 Computational methods

5.2.1 Electronic part

The equilibrium structures of the infinite chains of all-*trans* polyethylene (the C_2H_4 unit cell) and polyacetylene (the C_2H_2 unit cell) were determined by the HF CO method with the 6-31G* basis set using the analytical gradients[328] implemented in the POLYMER program.[319] The structural parameters thus obtained are compiled in Table 5.1. The harmonic force constants along in-phase ($k = 0$) collective atomic coordinates were obtained by numerical differentiation of the analytical gradients. With these, the normal coordinates and associated harmonic frequencies of the $k = 0$ phonons were determined. There are 14 and 8 nonzero frequencies at $k = 0$ in polyethylene and polyacetylene, respectively.

The PES's of these polymers are, therefore, 14- and 8-dimensional quantities even in the Γ approximation. They were approximated by quartic force fields (QFF's)[56,303] in the n-mode coupling (nMR) scheme[28] with $n = 3$. Furthermore, one-, two-, and three-mode coupling contributions (V_1, V_2, and V_3, respectively) were computed by different electronic structure methods, which is an example of the multiresolution PES scheme.[30,273,329–331] Note that the geometries and normal coordinates used were no longer those of the multiresolution PES's thus defined.

The electronic structure methods employed for polyethylene were MP2/6-31G* for V_1 and V_2 and HF/6-31G* for V_3. These calculations included the 6 and 10 nearest neighbor cells in the lattice sums for the short- and long-range interactions ($S = 6$ and $L = 10$), respectively, and 20 k points in the first BZ ($K = 20$).[308,332] The Namur cutoff criterion[333] was used. For polyacetylene, we used MP2/6-31G** for V_1 and V_2 and HF/6-31G* for V_3. The values of lattice sum parameters were $S = 6$, $L = 12$ and $K = 24$ for polyacetylene. The values of L and K were increased to 20 and 40, respectively, in the 2MR HF/6-31G* calculations for both polymers to verify that the results obtained were within 1 cm^{-1} of the converged.

The CO calculations, being completely independent of one another, were executed in parallel on a supercomputer at the University of Florida High-Performance Computing Center.

5.2.2 Vibrational part

The Γ approximation[315–318] reduces the vibrational Hamiltonian to

$$\hat{H} = -\frac{1}{2}\sum_{p=1}^{3N-4}\frac{\partial^2}{\partial Q_p^2} + V(Q_1,\ldots,Q_{3N-4}), \tag{5.1}$$

where N is the number of atoms in the unit cell, Q_p is an in-phase normal coordinate, and superfluous k indices are omitted. The anharmonic vibrational problem of a polymer in the Γ approximation resembles that for an isolated molecule and thus the SINDO program[70] designed for molecules was used to solve the VSCF, VMP2, and VCI equations of polymers by simply adjusting the number of vibrational degrees of freedom to $3N-4$. Rovibrational couplings are nonexistent in solids.[285]

The VSCF equation was solved for each of the $k = 0$ vibrational states in the basis of 21 lowest-energy harmonic-oscillator wave functions. The VMP2 correction was made, using the same basis, to each of these states using as the reference a product of the VSCF modals determined for the ground (zero-point) state.[31] The VCI calculations were performed using as a basis up to quadruply excited VSCF states of which the sums of their vibrational quantum numbers were less or equal to 5 in polyethylene or 7 in polyacetylene. These VSCF wave functions were, in turn, expanded by the 11 lowest-energy harmonic-oscillator wave functions. The results were found to change no more than a few cm^{-1} upon increasing these parameters.

Approximate MP2 harmonic frequencies of polyethylene (6-31G*) and polyacetylene (6-31G**) were obtained by retaining only the quadratic force constants in the PES's and carrying out VCI calculations. They were approximate because the geometries at which these force constants were obtained were not the equilibrium ones. Since a normal coordinate analysis does not depend on the origin of the coordinates, the correct harmonic frequencies should be obtained regardless of the origin insofar as the PES is strictly harmonic. The very presence of anharmonicity, however, makes these frequencies differ from those obtained at the equilibrium geometries.

5.3 Results and discussion

5.3.1 Polyethylene

The vibrations in polyethylene have been well characterized[283,334–336] except for $\nu_3(\pi)$ (see below) and are, therefore, an ideal basis on which to assess the validity and accuracy of the approximations employed. An infinite all-*trans* chain of polyethylene belongs to a factor group isomorphous to the point group D_{2h} and it has 14 $k = 0$ vibrations that are either infrared- or Raman-active with the C_2H_4 translational repeat unit. infrared- or Raman-active, where the phase refers to that between two adjacent CH_2 oscillators. See Ref. 334 for the labeling convention of the modes.

Table 5.2 lists the harmonic and anharmonic frequencies of $k = 0$ phonons obtained with the HF/6-31G* PES. Since electron correlation is neglected, accurate results cannot be expected. This table illustrates how the results converge as we include higher-dimensional slices of the anharmonic PES, namely, V_1, V_2, and V_3. Surprisingly, the inclusion of anharmonicity at the 1MR level (V_1) does not improve upon the harmonic results and in fact slightly deteriorates them. Among the four highest-lying modes, only one [$\nu_1(0)$] of them, which is the symmetric stretch (a_g) of four C–H bonds and whose potential is Morse-like, is improved by the 1MR treatment. The inclusion of 2MR (V_2) noticeably reduces both the maximum and mean absolute deviations by ≈ 40 %, although the deviations are still in excess of 140 cm^{-1}. The 3MR results are only a marginal improvement upon the 2MR ones, indicating that the simultaneous interactions of three distinct phonons are negligible in polyethylene, whereas those of two distinct phonons are not.

Table 5.3 compiles the frequencies of the $k = 0$ phonons obtained with the PES's that are at least partly evaluated by MP2 and include up to 3MR. The inclusion of electron correlation reduces the mean absolute deviation in harmonic frequencies by one third, but the remaining errors are still substantial, underscoring the equal significance of anharmonicity and electron correlation in this example. When the effects of anharmonicity are included by VCI, the computed frequencies agree well with the observed with the mean absolute deviation of 50 cm^{-1}. Equally or even more accurate agreement was obtained by one of the authors[334] by harmonic frequencies evaluated by density-functional calculations and scaled by a single empirical factor. The present first-principles calculations indicate that the anharmonic corrections are not always positive [see, e.g., $\nu_8(\pi)$] and, therefore, that the agreement in this previous work[334] is partly due to the cancellation of errors between the empirical scaling and inevitable approximations in the density functionals used.

The VSCF results are distinctly less accurate by a few tens of cm^{-1} on average than the VMP2 and VCI results. This indicates that phonon-phonon couplings, which tend not to be included adequately by VSCF, are significant and yet treatable as perturbation. Also, the good agreement between VCI and experiments suggests that the couplings across different k vectors neglected in the Γ approximation are indeed not large. However, a definitive and quantitative conclusion about this issue warrants a comparison with a calculation without the Γ approximation. The results obtained with the two PES's (A and B) are comparable with each other, indicating that essential electron-correlation effects are in 1MR (V_1). The greatest anharmonic effects (in excess of 200 cm^{-1}) are in the frequencies of the C–H stretch (ν_1 and ν_6). These are also the modes with the largest remaining errors as a QFF is inadequate for such strong anharmonicity.

Nielsen and Holland[337] assigned a Raman band at 1415 cm^{-1} to $\nu_3(\pi)$ (see also Ref. 338), whereas Snyder[339,340] suggested a revised assignment to a weaker Raman band at 1370 cm^{-1}. However, the latter band was not observed in a subsequent study[325,326] performed at low temperatures for high-density polyethylene. Our calculation predicts the frequency of $\nu_3(\pi)$ to fall in the range of 1421–1438 cm^{-1} and clearly favors the original assignment by Nielsen and

Holland.[337]

An inspection of the VCI wave functions reveals the presence of Fermi resonance[10] between the fundamental of $\nu_2(0)$ and the first overtone of $\nu_8(\pi)$, whose transition energies nearly coincide. The VCI calculation (PES A) predicts two a_g states at 1498 and 1542 cm^{-1} above zero point with the contributions of the $\nu_2(0)$ harmonic-oscillator wave function being approximately 60 and 30 %, respectively. The Fermi doublet has been observed in Raman spectra,[325,341,342] which display two peaks at *ca.* 1442 and 1468 cm^{-1} with 2:1 intensity ratio. Our calculation can thus reproduce, albeit only semi-quantitatively, the frequency difference between the Fermi doublet peaks as well as their intensity ratio from the first principles.[47] The VCI calculation also predicts Fermi resonances in the C–H stretching region.

5.3.2 Polyacetylene

All-*trans* polyacetylene[343] is a prototypical Peierls insulator with alternating C=C and C–C bonds. The structure with the C=C and C–C bonds reversed can be superimposed on the original structure and, in this sense, polyacetylene is said to have a doubly degenerate ground state.[344] In other words, the PES of polyacetylene along the coordinate connecting these two equivalent structures ("the dimerization coordinate") is a highly anharmonic double well. The normal coordinates of the in-phase C=C stretch (ν_2) and the in-phase C–C stretch (ν_4) are largely parallel to this dimerization coordinate.[345] Furthermore there is strong electron correlation involving the highest-occupied (C=C bonding and C–C antibonding) and the lowest-unoccupied (C=C antibonding and C–C bonding) CO's.[345] Therefore, both electron correlation and anharmonicity are expected to affect the frequencies of the phonons in polyacetylene, particularly, those of ν_2 and ν_4.

Polyacetylene has 8 optical phonon branches and their $k = 0$ modes can be classified according to the factor group isomorphous to the point group C_{2h}. Table 5.4 compares the anharmonic frequencies obtained with the 1MR, 2MR, and 3MR representations of the HF/6-31G* QFF as well as the harmonic frequencies. At 1MR level, only the frequencies of the a_g modes are improved over the harmonic approximation, while the inclusion of the phonon-phonon coupling in 2MR leads to considerable reductions in the maximum and mean absolute deviations in all modes. The 3MR results are close to the 2MR ones except for ν_5 for which the difference is 71 cm^{-1}. This large difference is a result of the mixing (*ca.* 20%) of this mode with the combination tone of ν_2 and ν_6, which is accounted for only at the 3MR level and higher. The deviations from the observed values are large particularly for ν_2 ($\approx$ 350 cm^{-1}) and ν_4 ($\approx$ 200 cm^{-1}), substantiating the assertion made previously that electron correlation influences these two modes especially strongly.[345]

Table 5.5 summarizes the results obtained with 3MR PES's that are partially electron correlated at MP2/6-31G**. The MP2 harmonic frequencies deviate particularly severely from the observed for ν_2 ($\approx$ 270 cm^{-1}) and ν_4 ($\approx$ 120

cm^{-1}), which underscores the fact that the lack of electron correlation alone does not cause the large errors; electron correlation and anharmonicity are equally significant. In fact, there is evidence that these two effects are not only individually important, but they enhance each other. The decreases in frequencies of ν_2 and ν_4 by the inclusion of anharmonicity are only 53 and 23 cm^{-1} according to VCI with HF/6-31G* QFF (Table 5.4). The harmonic frequencies of the same modes drop by 131 and 101 cm^{-1} upon the inclusion of electron correlation. The sums of these individual reductions in frequencies account for merely half of the errors in the HF harmonic frequencies, which are 397 and 220 cm^{-1}. The electron-correlated calculations lowers the barrier of the double well potential to a greater extent than their minima, making the potential not only softer but also more anharmonic. In this sense, the good agreement between uniformly scaled harmonic frequencies obtained by a density-functional method[346] and the observed is again to some extent fortuitous.

The two multiresolution PES's differ in the electronic structure theory to evaluate V_2; PES A uses MP2/6-31G** for $V_1 + V_2$, whereas V_2 in PES B is based on HF/6-31G**. The VSCF, VMP2, and VCI results for PES A do not constitute an improvement over those for PES B. This indicates, as in the case of polyethylene, that the essential electron-correlation effects are in 1MR (V_1) and the higher-dimensional slices of the PES can be treated by HF, justifying the use of multiresolution PES's. With PES A, we have encountered some difficulties achieving convergence in the VSCF and VCI solutions for some a_g modes, which are traced to the instability of MP2/6-31G** in evaluating V_2. If we assume that the aforementioned observation that the effect of electron correlation is largely confined in 1MR (V_1) holds true for these a_g modes, the results obtained with PES B for all modes should be reliable. However, such an assumption may well be invalid and the convergence of the calculated frequencies of the a_g modes (ν_2 and ν_4, in particular) should be viewed with some caution. VMP2 is more robust, yielding sensible results for all states. This is because our VMP2 calculations use a VSCF reference configuration that is composed of modals determined for the ground (zero-point) state, of which a VSCF iterative solution converges rapidly.

The calculated frequencies obtained with VCI and PES B agree excellently with the observed with the mean absolute deviation of 36 cm^{-1}. A similar degree of agreement can be seen in the results of VMP2 with PES A. The inclusion of both anharmonicity and electron correlation is essential to achieve the agreement. Hirata[345] proposed attributing the infrared band at 1170 cm^{-1} to ν_6. The calculated frequency of the same mode is 1195 cm^{-1} in excellent agreement with this observed value (1170 cm^{-1}). The present calculation is without empirical scaling of force constants contrarily to the one adopted in Ref. 345 and the accurate agreement between theory and experiment renders an independent and strong support of the assignment. The fact that the frequencies of ν_2 (the C=C stretch) and ν_4 (the C–C stretch) calculated with QFF's agree well with the observed implies either that the corresponding $v = 1$ states lie below the barrier in the double-well potential or that the states experience a single-well diabatic potential owing to strong electron-phonon coupling regardless of whether the states lie below or above the barrier. This issue warrants a

quantitative, coupled electron-phonon treatment, which is beyond the scope of this work.

5.4 Conclusions

The key findings of this chapter can be summarized as follows: (1) the VSCF, VMP2, and VCI methods in normal coordinates can be usefully applied to extended systems with the Γ approximation, providing anharmonic corrections to frequencies of $k = 0$ phonons. (2) The anharmonic phonon-phonon coupling across different k vectors seems rather insignificant for the polymers studied, although a definitive conclusion requires a comparison with calculations without the Γ approximation. (3) In polyethylene and polyacetylene, electron correlation and anharmonicity are equally significant and the inclusion of both is essential in achieving accurate frequencies. (4) The effect of electron correlation is largely confined in the 1MR. (5) The VCI calculations have reproduced the observed frequency separation and intensity ratio of the Fermi doublet of polyethylene involving the $\nu_2(0)$ fundamental and the $\nu_8(\pi)$ first overtone. They also predicted the presence of Fermi resonances in the C–H stretching region. (6) The good agreement has been obtained between the calculated and observed frequencies of ν_2 and ν_4 of polyacetylene with the multiresolution QFF. This may suggest either that the corresponding states lie below the barrier in the dimerization potential or that they experience diabatic single-well potential owing to strong electron-phonon coupling.

5.5 Tables

Table 5.1: The structural parameters (in Å and degrees) of polyethylene and polyacetylene obtained with HF/6-31G*.

Polymer	r_{C-C}	$r_{C=C}$	r_{C-H}	a_{CCC}	a_{HCH}	$a_{C=CH}$
Polyethylene	1.530	...	1.089	113.3	106.2	...
Polyacetylene	1.455	1.333	1.079	124.1	...	119.2

Table 5.2: Harmonic (HRM) and anharmonic (VCI) frequencies (in cm^{-1}) of the $k = 0$ phonons in polyethylene obtained with the HF/6-31G* PES.

Mode	Sym.	HRM	1MR	2MR	3MR	Obs.[a]
$\nu_6(\pi)$	b_{1u}	3244	3282	3116	3115	2920
$\nu_6(0)$	b_{3g}	3191	3231	3060	3083	2881
$\nu_1(\pi)$	b_{2u}	3192	3226	3076	3060	2850
$\nu_1(0)$	a_g	3185	3158	3018	3008	2846
$\nu_2(\pi)$	b_{2u}	1661	1662	1631	1619	1475
$\nu_2(0)$	a_g	1638	1639	1597	1616	1442
$\nu_3(\pi)$	b_{1g}	1571	1575	1558	1546	1412
$\nu_7(\pi)$	b_{2g}	1444	1449	1423	1413	1295
$\nu_3(0)$	b_{3u}	1315	1329	1309	1297	1173
$\nu_7(0)$	b_{3g}	1318	1320	1306	1294	1172
$\nu_4(0)$	a_g	1236	1231	1223	1222	1134
$\nu_4(\pi)$	b_{1g}	1138	1140	1130	1128	1062
$\nu_8(0)$	a_u	1162	1177	1159	1147	1050
$\nu_8(\pi)$	b_{1u}	781	832	804	788	722
max[b]		342	376	226	210	
mad[b]		189	201	141	136	

[a] References 325, 326.

[b] The maximum and mean absolute deviations from the observed.

Table 5.3: Harmonic (HRM) and anharmonic (VSCF, VMP2, and VCI) frequencies (in cm^{-1}) of the $k = 0$ phonons in polyethylene obtained with the multiresolution 3MR PES's computed by MP2/6-31G* and HF/6-31G*.

Mode	Sym.	PES A[a]				PES B[b]			Obs.[c]
		HRM[d]	VSCF	VMP2	VCI	VSCF	VMP2	VCI	
$\nu_6(\pi)$	b_{1u}	3244	3020	2995	2997	3023	2998	3000	2920
$\nu_6(0)$	b_{3g}	3204	2977	2958	2963	2979	2959	2964	2881
$\nu_1(\pi)$	b_{2u}	3177	2968	2906	2927	2971	2905	2929	2850
$\nu_1(0)$	a_g	3164	2963	2946	2925	2964	2945	2925	2846
$\nu_2(\pi)$	b_{2u}	1566	1546	1532	1530	1544	1530	1528	1475
$\nu_2(0)$	a_g	1543	1525	1507	1498	1523	1505	1494	1442
$\nu_3(\pi)$	b_{1g}	1430	1439	1424	1423	1438	1422	1421	1412
$\nu_7(\pi)$	b_{2g}	1337	1333	1320	1318	1331	1318	1317	1295
$\nu_3(0)$	b_{3u}	1201	1224	1207	1206	1223	1206	1205	1173
$\nu_7(0)$	b_{3g}	1235	1238	1224	1223	1236	1222	1221	1172
$\nu_4(0)$	a_g	1180	1169	1162	1163	1169	1162	1163	1134
$\nu_4(\pi)$	b_{1g}	1107	1103	1098	1099	1104	1098	1099	1062
$\nu_8(0)$	a_u	1071	1098	1081	1080	1098	1081	1080	1050
$\nu_8(\pi)$	b_{1u}	693	781	757	753	780	756	752	722
max[e]		327	118	100	82	121	99	83	
mad[e]		127	68	49	48	68	48	47	

[a] $V_1 + V_2$ computed by MP2/6-31G* and V_3 by HF/6-31G*.

[b] V_1 computed by MP2/6-31G* and $V_2 + V_3$ by HF/6-31G*.

[c] References 325, 326.

[d] Approximate values (see text).

[e] The maximum and mean absolute deviations from the observed.

Table 5.4: Harmonic (HRM) and anharmonic (VCI) frequencies (in cm^{-1}) of the $k = 0$ phonons in polyacetylene obtained with the HF/6-31G* PES.

Mode	Sym.	HRM	1MR	2MR	3MR	Obs.[a]
ν_5	b_u	3342	3408	3174	3245	3013
ν_1	a_g	3335	3283	3194	3177	2990
ν_2	a_g	1854	1834	1806	1801	1457
ν_3	a_g	1450	1448	1432	1427	1294
ν_6	b_u	1300	1327	1298	1290	1170
ν_4	a_g	1286	1282	1268	1263	1066
ν_7	a_u	1160	1186	1143	1128	1012
ν_8	b_g	1034	1054	1025	1011	884
max[b]		397	395	349	344	
mad[b]		234	242	182	182	

[a] References 322–324.

[b] The maximum and mean absolute deviations from the observed.

Table 5.5: Harmonic (HRM) and anharmonic (VSCF, VMP2, and VCI) frequencies (in cm^{-1}) of the $k = 0$ phonons in polyacetylene obtained with the multiresolution 3MR PES's computed by MP2/6-31G**, HF/6-31G**, and HF/6-31G*.

Mode	Sym.	PES A[a]				PES B[b]			Obs.[c]
		HRM[d]	VSCF	VMP2	VCI	VSCF	VMP2	VCI	
ν_5	b_u	3304	3052	3076	3093	3061	3085	3099	3013
ν_1	a_g	3297	3066	3059	3052	3076	3070	3069	2990
ν_2	a_g	1723	—[e]	1441	—[e]	1411	1513	1463	1457
ν_3	a_g	1359	1342	1266	1347	1339	1225	1292	1294
ν_6	b_u	1199	1209	1195	1193	1212	1198	1195	1170
ν_4	a_g	1185	1155	1053	—[e]	1181	1146	1106	1066
ν_7	a_u	1031	1060	1036	1032	1050	1026	1020	1012
ν_8	b_g	831	884	862	857	871	850	844	884
max[f]		307	89	69	80	115	80	86	
mad[f]		144	48	33	44	54	54	36	

[a] $V_1 + V_2$ computed by MP2/6-31G** and V_3 by HF/6-31G*.

[b] V_1 computed by MP2/6-31G**, V_2 by HF/6-31G**, and V_3 by HF/6-31G*.

[c] References 322–324.

[d] Approximate values (see text).

[e] No convergence.

[f] The maximum and mean absolute deviations from the observed.

Chapter 6

Conclusions

In Chapter 2, we proposed an accurate and predictive scheme to compute low-lying vibrational wave functions and energies of polyatomic molecules with applications to the seven key species of hydrocarbon combustion: HCO^+, HCO, HNO, HOO, HOO^-, CH_3^+, and CH_3. A combination of coupled-cluster singles and doubles (CCSD), CCSD with a second-order perturbation correction in the space of triples [CCSD(2)$_T$] and in the space of triples and quadruples [CCSD(2)$_{TQ}$], and a correlation-consistent basis set series has been employed to achieve the complete-correlation, complete-basis-set limits of the potential energy surfaces (PESs) of these species near equilibrium geometries. A new, compact representation of PESs that combines two existing representations, namely, a fourth-order Taylor expansion and numerical values on a rectilinear grid, has been proposed and shown to yield accurate frequencies, when combined with vibrational general-order configuration-interaction method. The mean absolute deviation in the predicted frequencies is 11 cm^{-1}.

In Chapter 3, we derived size-extensive generalizations of the vibrational self-consistent field (VSCF), vibrational Møller–Plesset perturbation (VMP), and vibrational coupled-cluster (VCC) methods for anharmonic lattice vibrations of extended periodic systems on the basis of a quartic force field (QFF) in delocalized normal coordinates. Copious terms in the formalisms of VSCF that have nonphysical size dependence are identified algebraically and eliminated, leading to compact and strictly size-extensive equations. This size-extensive VSCF method (XVSCF) thus defined has no contributions from cubic force constants and alters only the transition energies of the underlying harmonic-oscillator reference from a subset of quartic force constants. It also provides a way to evaluate an anharmonic correction to the lattice structure due to cubic force constants of a certain type. The second-order VMP (VMP2) and VCC methods in the QFF based on the XVSCF reference are shown to account for anharmonic effects due to all cubic and quartic force constants in a size-extensive fashion. These methods can be readily extended to a higher-order truncated Taylor expansion of a potential energy surface in normal coordinates. An algebraic proof of the lack of size-extensivity in the vibrational configuration-interaction (VCI) method is also presented.

In Chapter 4, we report the definition, programmable equations, and corresponding initial implementation of the size-extensive modification of VSCF, from which numerous terms with nonphysical size dependence in the original VSCF equations have been eliminated. When combined with a quartic force field, this compact and strictly size-

extensive VSCF (XVSCF) method requires only quartic force constants of the $\partial^4 V/\partial Q_i^2 \partial Q_j^2$ type, where V is the electronic energy and Q_i is the ith normal coordinate. The effective (mean-field) potential of XVSCF felt by each mode is shown to be harmonic, making the XVSCF equations subject to a self-consistent analytical solution without matrix diagonalization or a basis-set expansion, which are necessary in VSCF. Consequently, XVSCF is nearly three orders of magnitude faster than VSCF implemented similarly. Yet, XVSCF and VSCF are shown to yield comparable results for larger molecules, implying numerically the inclusion of unnecessary, nonphysical terms in VSCF.

In Chapter 5, we computed the frequencies of the infrared- and/or Raman-active ($k = 0$) vibrations of polyethylene and polyacetylene by taking account of the anharmonicity in the potential energy surfaces (PES) and the resulting phonon-phonon couplings explicitly. The electronic part of the calculations is based on Gaussian-basis-set crystalline orbital theory at the Hartree–Fock and MP2 levels, providing one-, two-, and/or three-dimensional slices of the PES (namely, using the so-called n-mode coupling approximation with $n = 3$), which are in turn expanded in the fourth-order Taylor series with respect to the normal coordinates. The vibrational part uses the VSCF, VMP2, and truncated VCI methods within the Γ approximation, which amounts to including only $k = 0$ phonons. It is shown that accounting for both electron correlation and anharmonicity is essential in achieving good agreement (the mean and maximum absolute deviations less than 50, and 90 cm^{-1}, respectively, for polyethylene and polyacetylene) between computed and observed frequencies. The corresponding values for the calculations including only one of such effects are in excess of 120 and 300 cm^{-1}, respectively. The VCI calculations also reproduce semi-quantitatively the frequency separation and intensity ratio of the Fermi doublet involving the $\nu_2(0)$ fundamental and $\nu_8(\pi)$ first overtone in polyethylene.

References

[1] D. M. Dennison. Rev. Mod. Phys. **3**, 280 (1931).

[2] S. Hirata and K. Yagi. Chem. Phys. Lett. **464**, 123 (2008).

[3] M. Born and R. Oppenheimer. Ann. Phys. **84**, 457–484 (1927).

[4] A. Tajti, P. G. Szalay, A. G. Császár, M. Kállay, J. Gauss, E. F. Valeev, B. A. Flowers, J. Vázquez, and J. F. Stanton. J. Chem. Phys. **121**, 11599 (2004).

[5] T. Shiozaki, M. Kamiya, S. Hirata, and E. F. Valeev. J. Chem. Phys. **130**, 054101 (2009).

[6] J. M. Bowman, S. Carter, and X. Huang. Int. Rev. Phys. Chem. **22**, 533 (2003).

[7] G. Czakó, T. Furtenbacher, A. G. Császár, and V. Szalay. Mol. Phys. **102**, 2411 (2004).

[8] O. Christiansen. Phys. Chem. Chem. Phys. **9**, 2942 (2007).

[9] A. G. Császár, C. Fábri, T. Szidarovszky, E. Mátyus, T. Furtenbacher, and G. Czakó. Phys. Chem. Chem. Phys. **14**, 1085 (2011).

[10] E. Fermi. Z. Phys. (Munich) **71**, 250 (1931).

[11] N. W. Ashcroft and N. D. Mermin. *Solid state physics* (Holt, Rinehart and Winston, 1976).

[12] J. M. Bowman, K. Christoffel, and F. Tobin. J. Phys. Chem. **83**, 905 (1979).

[13] L. S. Norris, M. A. Ratner, A. E. Roitberg, and R. B. Gerber. J. Chem. Phys. **105**, 11261 (1996).

[14] F. L. Tobin and J. M. Bowman. Chem. Phys. **47**, 151 (1980).

[15] O. Christiansen. J. Chem. Phys. **120**, 2140 (2004).

[16] H. Meyer. Annu. Rev. Phys. Chem. **53**, 141 (2002).

[17] C. Eckart. Phys. Rev. **47**, 552 (1935).

[18] R. G. Littlejohn and M. Reinsch. Rev. Mod. Phys. **69**, 213 (1997).

[19] E. B. Wilson Jr., J. C. Decius, and P. C. Cross. *Molecular Vibrations* (McGraw-Hill, New York, 1955).

[20] E. B. Wilson and J. B. Howard. J. Chem. Phys. **4**, 260 (1936).

[21] B. T. Darling and D. M. Dennison. Phys. Rev. **57**, 128 (1940).

[22] J. K. G. Watson. Mol. Phys. **15**, 479 (1968).

[23] J. K. G. Watson. Mol. Phys. **19**, 465 (1970).

[24] P. Carbonniere and V. Barone. Chem. Phys. Lett. **392**, 365 (2004).

[25] E. Mátyus, G. Czakó, B. T. Sutcliffe, and A. G. Császár. J. Chem. Phys. **127**, 084102 (2007).

[26] O. L. Polyansky, A. G. Császár, S. V. Shirin, N. F. Zobov, P. Barletta, J. Tennyson, D. W. Schwenke, and P. J. Knowles. Science **299**, 539 (2003).

[27] J. O. Jung and R. B. Gerber. J. Chem. Phys. **105**, 10332 (1996).

[28] S. Carter, S. J. Culik, and J. M. Bowman. J. Chem. Phys. **107**, 10458 (1997).

[29] J. Wu, X. Huang, S. Carter, and J. M. Bowman. Chem. Phys. Lett. **426**, 285 (2006).

[30] G. Rauhut. J. Chem. Phys. **121**, 9313 (2004).

[31] K. Yagi, S. Hirata, and K. Hirao. Theor. Chem. Acc. **118**, 681 (2007).

[32] R. J. Whitehead and N. C. Handy. J. Mol. Spectrosc. **55**, 356 (1975).

[33] R. J. Whitehead and N. C. Handy. J. Mol. Spectrosc. **59**, 459 (1976).

[34] G. M. Chaban, J. O. Jung, and R. B. Gerber. J. Chem. Phys. **111**, 1823 (1999).

[35] K. Yagi, T. Taketsugu, K. Hirao, and M. S. Gordon. J. Chem. Phys. **113**, 1005 (2000).

[36] S. Irle and J. M. Bowman. J. Chem. Phys. **113**, 8401 (2000).

[37] R. Burcl, S. Carter, and N. C. Handy. Chem. Phys. Lett. **380**, 237 (2003).

[38] C. Møller and M. S. Plesset. Phys. Rev. **46**, 618 (1934).

[39] K. Yagi, S. Hirata, and K. Hirao. Phys. Chem. Chem. Phys. **10**, 1781 (2008).

[40] O. Christiansen. J. Chem. Phys. **119**, 5773 (2003).

[41] A. Szabo and N. S. Ostlund. *Modern Quantum Chemistry: Introduction to Advanced Electronic Structure Theory* (MacMillan, New York, 1982).

[42] Y. Scribano, D. M. Lauvergnat, and D. M. Benoit. J. Chem. Phys. **133**, 094103 (2010).

[43] T. H. Dunning Jr. J. Chem. Phys. **90**, 1007 (1989).

[44] R. A. Kendall, T. H. Dunning Jr., and R. J. Harrison. J. Chem. Phys. **96**, 6796 (1992).

[45] M. Keçeli, T. Shiozaki, K. Yagi, and S. Hirata. Mol. Phys. **107**, 1283 (2009).

[46] V. Rodriguez-Garcia, K. Yagi, K. Hirao, S. Iwata, and S. Hirata. J. Chem. Phys. **125**, 014109 (2006).

[47] V. Rodriguez-Garcia, S. Hirata, K. Yagi, K. Hirao, T. Taketsugu, I. Schweigert, and M. Tasumi. J. Chem. Phys. **126**, 124303 (2007).

[48] S. Hirata, K. Yagi, S. A. Perera, S. Yamazaki, and K. Hirao. J. Chem. Phys. **128**, 214305 (2008).

[49] G. D. Purvis III and R. J. Bartlett. J. Chem. Phys. **76**, 1910 (1982).

[50] G. E. Scuseria, T. J. Lee, and H. F. Schaefer III. Chem. Phys. Lett. **130**, 236 (1986).

[51] S. Hirata. J. Chem. Phys. **121**, 51 (2004).

[52] T. H. Dunning Jr. and K. A. Peterson. J. Chem. Phys. **113**, 7799 (2000).

[53] J. Rychlewski. *Explicitly Correlated Wave Functions in Chemistry and Physics* (Kluwer Academic Publishers, Dordrecht, 2003).

[54] T. Shiozaki, M. Kamiya, S. Hirata, and E. F. Valeev. Phys. Chem. Chem. Phys. **10**, 3358 (2008).

[55] T. Shiozaki, M. Kamiya, S. Hirata, and E. F. Valeev. J. Chem. Phys. **129**, 071101 (2008).

[56] K. Yagi, T. Taketsugu, and K. Hirao. J. Chem. Phys. **116**, 3963 (2002).

[57] K. Yagi, K. Hirao, T. Taketsugu, M. W. Schmidt, and M. S. Gordon. J. Chem. Phys. **121**, 1383 (2004).

[58] M. S. Schuurman, W. D. Allen, P. v. R. Schleyer, and H. F. Schaefer III. J. Chem. Phys. **122**, 104302 (2005).

[59] M. S. Schuurman, W. D. Allen, and H. F. Schaefer III. J. Comput. Chem. **26**, 1106 (2005).

[60] A. C. Simmonett, F. A. Evangelista, W. D. Allen, and H. F. Schaefer III. J. Chem. Phys. **127**, 014306 (2007).

[61] X. Huang and T. J. Lee. J. Chem. Phys. **129**, 044312 (2008).

[62] A. C. Simmonett, H. F. Schaefer III, and W. D. Allen. J. Chem. Phys. **130**, 044301 (2009).

[63] W. Meyer, P. Botschwina, and P. Burton. J. Chem. Phys. **84**, 891 (1986).

[64] G. M. Chaban and M. S. Gordon. J. Phys. Chem. A **103**, 185 (1999).

[65] I. M. Mills and A. G. Robiette. Mol. Phys. **56**, 743 (1985).

[66] G. D. Carney, L. L. Sprandel, and C. W. Kern. Adv. Chem. Phys **37**, 305–379 (1978).

[67] J. M. Bowman. J. Chem. Phys. **68**, 608 (1978).

[68] J. M. Bowman, J. S. Bittman, and L. B. Harding. J. Chem. Phys. **85**, 911 (1986).

[69] M. A. Ratner and R. B. Gerber. J. Phys. Chem. **90**, 20 (1986).

[70] K. Yagi. SINDO, version 2.0 (2006).

[71] T. J. Lee and C. E. Dateo. J. Chem. Phys. **103**, 9110 (1995).

[72] A. Császár, W. D. Allen, Y. Yamaguchi, and H. F. Schaefer III. In P. Jensen and P. R. Bunker, editors, *Computational Molecular Spectroscopy* (John Wiley & Sons, Chichester, 2000).

[73] J. A. Pople, M. Head-Gordon, D. J. Fox, K. Raghavachari, and L. A. Curtiss. J. Chem. Phys. **90**, 5622 (1989).

[74] K. A. Peterson, D. E. Woon, and T. H. Dunning Jr. J. Chem. Phys. **100**, 7410 (1994).

[75] J. M. L. Martin and T. J. Lee. Chem. Phys. Lett. **258**, 136 (1996).

[76] T. Helgaker, J. Gauss, P. Jørgensen, and J. Olsen. J. Chem. Phys. **106**, 6430 (1997).

[77] S. Hirata, T. Yanai, W. A. de Jong, T. Nakajima, and K. Hirao. J. Chem. Phys. **120**, 3297 (2004).

[78] T. P. Straatsma, E. Aprà, T. L. Windus, E. J. Bylaska, W. A. de Jong, S. Hirata, M. Valiev, M. T. Hackler, L. Pollack, R. J. Harrison, M. Dupuis, D. M. A. Smith, J. Nieplocha, V. Tipparaju, M. Krishnan, A. A. Auer, E. Brown, G. Cisneros, G. I. Fann, H. Früchtl, J. Garza, K. Hirao, R. Kendall, J. A. Nichols, K. Tsemekhman, K. Wolinski, J. Anchell, D. Bernholdt, P. Borowski, T. Clark, D. Clerc, H. Dachsel, M. Deegan, K. Dyall, D. Elwood, E. Glendening, M. Gutowski, A. Hess, J. Jaffe, B. Johnson, J. Ju, R. Kobayashi, R. Kutteh, Z. Lin, R. Littlefield, X. Long, B. Meng, T. Nakajima, S. Niu, M. Rosing, G. Sandrone, M. Stave, H. Taylor, G. Thomas, J. v. Lenthe, A. Wong, and Z. Zhang. NWChem, a computational chemistry package for parallel computers, version 4.7 (2005).

[79] J. F. Stanton, J. Gauss, J. D. Watts, M. Nooijen, N. Oliphant, S. A. Perera, P. G. Szalay, W. J. Lauderdale, S. A. Kucharski, S. R. Gwaltney, S. Beck, A. Balková, D. E. Bernhold, K. K. Baeck, P. Rozyczko, H.Sekino, C. Hober, and R. J. Bartlett. ACES II, a program product of the Quantum Theory Project.

[80] L. J. Allamandola. J. Mol. Struct. **157**, 255 (1987).

[81] J. Warnatz. In W. C. Gardiner Jr., editor, *Combustion Chemistry* (Springer-Verlag, Berlin, 1984).

[82] D. Buhl and L. E. Snyder. Nature **228**, 267 (1970).

[83] W. Klemperer. Nature **227**, 1230 (1970).

[84] U. Wahlgren, B. Liu, P. K. Pearson, and H. F. Schaefer III. Nature (London) Phys. Sci. **246**, 4 (1973).

[85] L. E. Snyder, J. M. Hollis, B. L. Ulich, F. J. Lovas, and D. Buhl. Bull. Am. Astron. Soc. **7**, 497 (1975).

[86] R. C. Woods, T. A. Dixon, R. J. Saykally, and P. G. Szanto. Phys. Rev. Lett. **35**, 1269 (1975).

[87] M. Bogey, C. Demuynck, and J. L. Destombes. Mol. Phys. **43**, 1043 (1981).

[88] K. V. L. N. Sastry, E. Herbst, and F. C. De Lucia. J. Chem. Phys. **75**, 4169 (1981).

[89] R. C. Woods, R. J. Saykally, T. G. Anderson, T. A. Dixon, and P. G. Szanto. J. Chem. Phys. **75**, 4256 (1981).

[90] E. Hirota and Y. Endo. J. Mol. Spectrosc. **127**, 527 (1988).

[91] R. C. Woods. Philosophical Transactions of the Royal Society of London. Series A, Mathematical and Physical Sciences (1934-1990) **324**, 141 (1988).

[92] V. Lattanzi, A. Walters, B. J. Drouin, and J. C. Pearson. The Astrophysical Journal **662**, 771 (2007).

[93] F. Tinti, L. Bizzocchi, C. Degli Esposti, and L. Dore. Astrophysical Journal Letters **669**, L113 (2007).

[94] T. Hirao, S. Yu, and T. Amano. J. Mol. Spectrosc. **248**, 26 (2008).

[95] C. S. Gudeman, M. H. Begemann, J. Pfaff, and R. J. Saykally. Phys. Rev. Lett. **50**, 727 (1983).

[96] T. Amano. J. Chem. Phys. **79**, 3595 (1983).

[97] P. B. Davies and W. J. Rothwell. J. Chem. Phys. **81**, 5239 (1984).

[98] P. B. Davies, P. A. Hamilton, and W. J. Rothwell. J. Chem. Phys. **81**, 1598 (1984).

[99] S. C. Foster, A. R. W. McKellar, and T. J. Sears. J. Chem. Phys. **81**, 578 (1984).

[100] K. Kawaguchi, C. Yamada, S. Saito, and E. Hirota. J. Chem. Phys. **82**, 1750 (1985).

[101] D. Liu, S. Lee, and T. Oka. J. Mol. Spectrosc. **128**, 236 (1988).

[102] J. C. Owrutsky, E. R. Keim, J. V. Coe, and R. J. Saykally. J. Phys. Chem. **93**, 5960 (1989).

[103] E. R. Keim, M. L. Polak, J. C. Owrutsky, J. V. Coe, and R. J. Saykally. J. Chem. Phys. **93**, 3111 (1990).

[104] R. J. Foltynowicz, J. D. Robinson, E. J. Zückerman, H. G. Hedderich, and E. R. Grant. J. Mol. Spectrosc. **199**, 147 (2000).

[105] H. B. Jansen and P. Ros. Chem. Phys. Lett. **3**, 140 (1969).

[106] P. J. Bruna, S. D. Peyerimhoff, and R. J. Buenker. Chem. Phys. **10**, 323 (1975).

[107] F. A. Gianturco, U. T. Lamanna, and D. Ignazzi. Chem. Phys. **48**, 387 (1980).

[108] D. J. DeFrees, J. S. Binkley, and A. D. McLean. J. Chem. Phys. **80**, 3720 (1984).

[109] N. L. Ma, B. J. Smith, and L. Radom. Chem. Phys. Lett. **197**, 573 (1992).

[110] Y. Yamaguchi, C. A. Richards Jr., and H. F. Schaefer III. J. Chem. Phys. **101**, 8945 (1994).

[111] J. M. L. Martin, P. R. Taylor, and T. J. Lee. J. Chem. Phys. **99**, 286 (1993).

[112] C. Puzzarini, R. Tarroni, P. Palmieri, S. Carter, and L. Dore. Mol. Phys. **87**, 879 (1996).

[113] M. Mladenović, P. Botschwina, P. Sebald, and S. Carter. Theor. Chem. Acc. **100**, 134 (1998).

[114] T. van Mourik, T. H. Dunning Jr., and K. A. Peterson. J. Phys. Chem. A **104**, 2287 (2000).

[115] W. M. Vaidya. Proceedings of the Royal Society of London. Series A, Mathematical and Physical Sciences **147**, 513 (1934).

[116] D. A. Ramsay. J. Chem. Phys. **21**, 960 (1953).

[117] G. Herzberg and D. A. Ramsay. Proceedings of the Royal Society of London. Series A, Mathematical and Physical Sciences **233**, 34 (1955).

[118] B. M. Stone, M. Noble, and E. K. C. Lee. Chem. Phys. Lett. **118**, 83 (1985).

[119] K. K. Murray, T. M. Miller, D. G. Leopold, and W. C. Lineberger. J. Chem. Phys. **84**, 2520 (1986).

[120] C. B. Dane, D. R. Lander, R. F. Curl, F. K. Tittel, Y. Guo, M. I. F. Ochsner, and C. B. Moore. J. Chem. Phys. **88**, 2121 (1988).

[121] A. R. W. McKellar, J. B. Burkholder, J. J. Orlando, and C. J. Howard. J. Mol. Spectrosc. **130**, 445 (1988).

[122] G. Rumbles, E. K. C. Lee, and J. J. Valentini. J. Chem. Soc.-Faraday Trans. **86**, 3837 (1990).

[123] J. M. Brown and D. A. Ramsay. Can. J. Phys. **53**, 2232 (1975).

[124] J. W. C. Johns and A. R. W. McKellar. J. Chem. Phys. **66**, 1217 (1977).

[125] B. M. Landsberg, A. J. Merer, and T. Oka. J. Mol. Spectrosc. **67**, 459 (1977).

[126] A. D. Sappey and D. R. Crosley. J. Chem. Phys. **93**, 7601 (1990).

[127] J. P. Reilly, J. H. Clark, C. B. Moore, and G. C. Pimentel. J. Chem. Phys. **69**, 4381 (1978).

[128] J. M. Brown, J. Buttenshaw, A. Carrington, K. Dumper, and C. R. Parent. J. Mol. Spectrosc. **79**, 47 (1980).

[129] P. Botschwina. Chem. Phys. Lett. **29**, 98 (1974).

[130] K. Tanaka and E. R. Davidson. J. Chem. Phys. **70**, 2904 (1979).

[131] T. H. Dunning Jr. J. Chem. Phys. **73**, 2304 (1980).

[132] J. M. Bowman. Acc. Chem. Res. **19**, 202 (1986).

[133] F. Pauzat, S. Chekir, and Y. Ellinger. J. Chem. Phys. **85**, 2861 (1986).

[134] D. A. Clabo Jr., W. D. Allen, R. B. Remington, Y. Yamaguchi, and H. F. Schaefer III. Chem. Phys. **123**, 187 (1988).

[135] Q. Sun, J. M. Bowman, and B. Gazdy. J. Chem. Phys. **89**, 3124 (1988).

[136] J. M. Bowman and B. Gazdy. J. Chem. Phys. **94**, 816 (1991).

[137] J. M. Bowman and B. Gazdy. Chem. Phys. Lett. **200**, 311 (1992).

[138] H. Lorenzen-Schmidt, M. Perić, and S. D. Peyerimhoff. J. Chem. Phys. **98**, 525 (1993).

[139] M. Perić, C. M. Marian, and S. D. Peyerimhoff. J. Mol. Spectrosc. **166**, 406 (1994).

[140] M. Bittererová, H. Lischka, and S. Biskupic. Int. J. Quantum Chem. **55**, 261 (1995).

[141] J. Qi, J. M. Bowman, and M. R. Manaa. J. Chem. Phys. **103**, 7664 (1995).

[142] V. Ryaboy and N. Moiseyev. J. Chem. Phys. **103**, 4061 (1995).

[143] D. Wang and J. M. Bowman. Chem. Phys. Lett. **235**, 277 (1995).

[144] H. Werner, C. Bauer, P. Rosmus, H. Keller, M. Stumpf, and R. Schinke. J. Chem. Phys. **102**, 3593 (1995).

[145] H. Keller, H. Flöthmann, A. J. Dobbyn, R. Schinke, H. Werner, C. Bauer, and P. Rosmus. J. Chem. Phys. **105**, 4983 (1996).

[146] J. Qi and J. M. Bowman. J. Chem. Phys. **105**, 9884 (1996).

[147] G. S. Whittier and J. C. Light. J. Chem. Phys. **107**, 1816 (1997).

[148] L. Serrano-Andres, N. Forsberg, and P.-r. Malmqvist. J. Chem. Phys. **108**, 7202 (1998).

[149] B. Poirier and J. C. Light. J. Chem. Phys. **114**, 6562 (2001).

[150] A. V. Marenich and J. E. Boggs. J. Phys. Chem. A **107**, 2343 (2003).

[151] A. V. Marenich and J. E. Boggs. J. Phys. Chem. A **108**, 5431 (2004).

[152] J. M. Brown, H. E. Radford, and T. J. Sears. J. Mol. Spectrosc. **148**, 20 (1991).

[153] E. Hirota. J. Mol. Struct. **146**, 237 (1986).

[154] J. F. Ogilvie. J. Mol. Struct. **31**, 407 (1976).

[155] J. A. Miller and C. T. Bowman. Prog. Energy Combust. Sci. **15**, 287 (1989).

[156] J. M. Fukuto, A. S. Dutton, and K. N. Houk. ChemBioChem **6**, 612 (2005).

[157] J. M. Fukuto, C. H. Switzer, K. M. Miranda, and D. A. Wink. Annual Review of Pharmacology & Toxicology **45**, 335 (2005).

[158] F. W. Dalby. Can. J. Phys. **36**, 1336 (1958).

[159] H. W. Brown and G. C. Pimentel. J. Chem. Phys. **29**, 883 (1958).

[160] B. L. Ulich, J. M. Hollis, and L. E. Snyder. Astrophysical Journal **217**, L105 (1977).

[161] M. J. Y. Clement and D. A. Ramsay. Can. J. Phys. **39**, 205 (1961).

[162] J. L. Bancroft, J. M. Hollas, and D. A. Ramsay. Can. J. Phys. **40**, 322 (1962).

[163] P. N. Clough, B. A. Thrush, D. A. Ramsay, and J. G. Stamper. Chem. Phys. Lett. **23**, 155 (1973).

[164] M. E. Jacox and D. E. Milligan. J. Mol. Spectrosc. **48**, 536 (1973).

[165] J. W. C. Johns and A. R. W. McKellar. J. Chem. Phys. **66**, 1217 (1977).

[166] J. W. C. Johns, A. R. W. McKellar, and E. Weinberger. Can. J. Phys. **61**, 1106 (1983).

[167] J. C. Petersen and M. Vervloet. Chem. Phys. Lett. **141**, 499 (1987).

[168] S. Saito and K. Takagi. Astrophys. J. **175**, L47 (1972).

[169] S. Saito and K. Takagi. J. Mol. Spectrosc. **47**, 99 (1973).

[170] A. W. Salotto and L. Burnelle. Chem. Phys. Lett. **3**, 80 (1969).

[171] P. Botschwina. Mol. Phys. **32**, 729 (1976).

[172] P. Botschwina. Chem. Phys. **40**, 33 (1979).

[173] O. Nomura and S. Iwata. Chem. Phys. Lett. **66**, 523 (1979).

[174] O. Nomura. Int. J. Quantum Chem. **18**, 143 (1980).

[175] R. N. Dixon, M. Noble, C. A. Taylor, and M. Delhoume. Faraday Discuss. 125–142 (1981).

[176] A. Heiberg and J. Almlöf. Chem. Phys. Lett. **85**, 542 (1982).

[177] C. E. Dateo, T. J. Lee, and D. W. Schwenke. J. Chem. Phys. **101**, 5853 (1994).

[178] R. Guadagnini, G. C. Schatz, and S. P. Walch. J. Chem. Phys. **102**, 774 (1995).

[179] D. H. Mordaunt, H. Flöthmann, M. Stumpf, H. Keller, C. Beck, R. Schinke, and K. Yamashita. J. Chem. Phys. **107**, 6603 (1997).

[180] T. J. Lee. J. Chem. Phys. **99**, 9783 (1993).

[181] J. Demaison, L. Margulès, and J. E. Boggs. Chem. Phys. **260**, 65 (2000).

[182] J. Demaison, A. G. Császár, and A. Dehayem-Kamadjeu. J. Phys. Chem. A **110**, 13609 (2006).

[183] J. A. Miller. J. Chem. Phys. **84**, 6170 (1986).

[184] M. E. Summers, R. R. Conway, D. E. Siskind, M. H. Stevens, D. Offermann, M. Riese, P. Preusse, D. F. Strobel, and J. M. Russell III. Science **277**, 1967 (1997).

[185] D. Xie, C. Xu, T. Ho, H. Rabitz, G. Lendvay, S. Y. Lin, and H. Guo. J. Chem. Phys. **126**, 074315 (2007).

[186] C. Yamada, Y. Endo, and E. Hirota. J. Chem. Phys. **78**, 4379 (1983).

[187] J. B. Burkholder, P. D. Hammer, C. J. Howard, J. P. Towle, and J. M. Brown. J. Mol. Spectrosc. **151**, 493 (1992).

[188] K. Nagai, Y. Endo, and E. Hirota. J. Mol. Spectrosc. **89**, 520 (1981).

[189] J. W. Buchanan, B. A. Thrush, and G. S. Tyndall. Chem. Phys. Lett. **103**, 167 (1983).

[190] J. W. C. Johns, A. R. W. McKellar, and M. Riggin. J. Chem. Phys. **68**, 3957 (1978).

[191] D. D. Nelson Jr. and M. S. Zahniser. J. Mol. Spectrosc. **150**, 527 (1991).

[192] C. E. Barnes, J. M. Brown, A. Carrington, J. Pinkstone, T. J. Sears, and P. J. Thistlethwaite. J. Mol. Spectrosc. **72**, 86 (1978).

[193] C. E. Barnes, J. M. Brown, and H. E. Radford. J. Mol. Spectrosc. **84**, 179 (1980).

[194] S. P. Walch and R. J. Duchovic. J. Chem. Phys. **94**, 7068 (1991).

[195] Y. Xu, N. Blinov, W. Jäger, and P. Roy. J. Chem. Phys. **124**, 081101 (2006).

[196] C. Lanczos. J. Res. Nat. Bur. Stand. **45**, 255 (1950).

[197] C. Xu, B. Jiang, D. Xie, S. C. Farantos, S. Y. Lin, and H. Guo. J. Phys. Chem. A **111**, 10353 (2007).

[198] S. Y. Lin, H. Guo, P. Honvault, C. Xu, and D. Xie. J. Chem. Phys. **128**, 014303 (2008).

[199] C. F. Melius and R. J. Blint. Chem. Phys. Lett. **64**, 183 (1979).

[200] A. Komornicki and R. L. Jaffe. J. Chem. Phys. **71**, 2150 (1979).

[201] M. R. Pastrana, L. A. M. Quintales, J. Brãndao, and A. J. C. Varandas. J. Phys. Chem. **94**, 8073 (1990).

[202] P. R. Bunker, I. P. Hamilton, and P. Jensen. J. Mol. Spectrosc. **155**, 44 (1992).

[203] V. Barone. J. Chem. Phys. **101**, 10666 (1994).

[204] V. J. Barclay and I. P. Hamilton. J. Chem. Phys. **103**, 2834 (1995).

[205] V. A. Mandelshtam, T. P. Grozdanov, and H. S. Taylor. J. Chem. Phys. **103**, 10074 (1995).

[206] P. Botschwina and M. Horn. J. Mol. Spectrosc. **181**, 452 (1997).

[207] P. Jensen, R. J. Buenker, J. Gu, G. Osmann, and P. R. Bunker. Can. J. Phys. **79**, 641 (2001).

[208] J. Troe and V. G. Ushakov. Chem. Phys. **346**, 186 (2008).

[209] J. Troe and V. G. Ushakov. Chem. Phys. **346**, 193 (2008).

[210] J. M. Oakes, L. B. Harding, and G. B. Ellison. J. Chem. Phys. **83**, 5400 (1985).

[211] M. Horn, S. Seeger, R. Oswald, and P. Botschwina. Zeitschrift für Physik D Atoms, Molecules and Clusters **36**, 293 (1996).

[212] W. Chan and I. P. Hamilton. J. Chem. Phys. **105**, 5907 (1996).

[213] G. J. Vazquez, R. J. Buenker, and S. D. Peyerimhoff. J. Chem. Phys. **90**, 7229 (1989).

[214] W. Z. Liang and M. Head-Gordon. J. Phys. Chem. A **108**, 3206 (2004).

[215] R. Li, X. Zhang, H. Zheng, J. Liang, and Z. Cui. Journal of Molecular Structure: THEOCHEM **860**, 106 (2008).

[216] M. W. Crofton, M. Jagod, B. D. Rehfuss, W. A. Kreiner, and T. Oka. J. Chem. Phys. **88**, 666 (1988).

[217] M. W. Crofton, W. A. Kreiner, M. Jagod, B. D. Rehfuss, and T. Oka. J. Chem. Phys. **83**, 3702 (1985).

[218] M. Jagod, C. M. Gabrys, M. Rösslein, D. Uy, and T. Oka. Can. J. Phys. **72**, 1192 (1994).

[219] J. Dyke, N. Jonathan, E. Lee, and A. Morris. Journal of the Chemical Society-Faraday Transactions II **72**, 1385 (1976).

[220] T. Koenig, T. Balle, and J. C. Chang. Spectrosc. Lett. **9**, 755 (1976).

[221] T. Koenig, T. Balle, and W. Snell. J. Am. Chem. Soc. **97**, 662 (1975).

[222] X. H. Liu, R. L. Gross, and A. G. Suits. Science **294**, 2527 (2001).

[223] W. A. Lathan, W. J. Hehre, L. A. Curtiss, and J. A. Pople. J. Am. Chem. Soc. **93**, 6377 (1971).

[224] G. T. Surratt and W. A. Goddard III. Chem. Phys. **23**, 39 (1977).

[225] F. T. Chau. Journal of Molecular Structure: THEOCHEM **119**, 281 (1985).

[226] D. J. DeFrees and A. D. McLean. J. Chem. Phys. **82**, 333 (1985).

[227] W. P. Kraemer and V. Špirko. J. Mol. Spectrosc. **149**, 235 (1991).

[228] P. Pracna, V. Špirko, and W. P. Kraemer. J. Mol. Spectrosc. **158**, 433 (1993).

[229] H. Yu and T. J. Sears. J. Chem. Phys. **117**, 666 (2002).

[230] A. Halkier, T. Helgaker, P. Jørgensen, W. Klopper, H. Koch, J. Olsen, and A. K. Wilson. Chem. Phys. Lett. **286**, 243 (1998).

[231] C. Yamada, E. Hirota, and K. Kawaguchi. J. Chem. Phys. **75**, 5256 (1981).

[232] P. L. Holt, K. E. McCurdy, R. B. Weisman, J. S. Adams, and P. S. Engel. J. Chem. Phys. **81**, 3349 (1984).

[233] P. B. Kelly and S. G. Westre. Chem. Phys. Lett. **151**, 253 (1988).

[234] N. E. Triggs, M. Zahedi, J. W. Nibler, P. DeBarber, and J. J. Valentini. J. Chem. Phys. **96**, 1822 (1992).

[235] M. Zahedi, J. A. Harrison, and J. W. Nibler. J. Chem. Phys. **100**, 4043 (1994).

[236] S. Hädrich, S. Hefter, B. Pfelzer, T. Doerk, P. Jauernik, and J. Uhlenbusch. Chem. Phys. Lett. **256**, 83 (1996).

[237] L. Y. Tan, A. M. Winer, and G. C. Pimentel. J. Chem. Phys. **57**, 4028 (1972).

[238] J. Wormhoudt and K. E. McCurdy. Chem. Phys. Lett. **156**, 47 (1989).

[239] T. Amano, P. F. Bernath, C. Yamada, Y. Endo, and E. Hirota. J. Chem. Phys. **77**, 5284 (1982).

[240] I. Tanarro, M. M. Sanz, D. Bermejo, C. Domingo, and J. Santos. J. Chem. Phys. **100**, 238 (1994).

[241] I. Tanarro, M. M. Sanz, C. Domingo, D. Bermejo, J. Santos, and J. L. Domenech. J. Phys. Chem. **98**, 5862 (1994).

[242] G. A. Bethardy and R. G. Macdonald. J. Chem. Phys. **103**, 2863 (1995).

[243] S. Davis, D. T. Anderson, G. Duxbury, and D. J. Nesbitt. J. Chem. Phys. **107**, 5661 (1997).

[244] K. Kawaguchi. Can. J. Phys. **79**, 449 (2001).

[245] A. Snelson. J. Phys. Chem. **74**, 537 (1970).

[246] M. E. Jacox. J. Mol. Spectrosc. **66**, 272 (1977).

[247] T. Momose, M. Miki, M. Uchida, T. Shimizu, I. Yoshizawa, and T. Shida. J. Chem. Phys. **103**, 1400 (1995).

[248] S. Tam, M. Macler, and M. E. Fajardo. J. Chem. Phys. **106**, 8955 (1997).

[249] D. S. Marynick and D. A. Dixon. Proc. Nat. Acad. Sci. U.S.A. **74**, 410 (1977).

[250] K. Raghavachari, R. A. Whiteside, J. A. Pople, and P. v. R. Schleyer. J. Am. Chem. Soc. **103**, 5649 (1981).

[251] V. Špirko and P. R. Bunker. J. Mol. Spectrosc. **95**, 381 (1982).

[252] P. Botschwina, J. Flesch, and W. Meyer. Chem. Phys. **74**, 321 (1983).

[253] D. M. Chipman. J. Chem. Phys. **78**, 3112 (1983).

[254] F. T. Chau. J. Electron Spectrosc. Relat. Phenom. **40**, 59 (1986).

[255] U. Salzner and P. v. R. Schleyer. Chem. Phys. Lett. **199**, 267 (1992).

[256] D. A. Dixon, D. Feller, and K. A. Peterson. J. Phys. Chem. A **101**, 9405 (1997).

[257] O. Roberto-Neto, S. Chakravorty, and F. B. C. Machado. Int. J. Quantum Chem. **103**, 649 (2005).

[258] J. Burdett. J. Chem. Phys. **52**, 2983 (1970).

[259] P. Carbonniere, D. Begue, A. Dargelos, and C. Pouchan. Chem. Phys. **300**, 41 (2004).

[260] J. Sun and R. J. Bartlett. Topics Current Chem. **203**, 121 (1999).

[261] B. Champagne. In V. Galiatsatos, editor, *Molecular Simulation Methods for Predicting Polymer Properties*, 1–46 (Wiley, New York, 2005).

[262] S. Hirata and T. Shimazaki. Phys. Rev. B **80**, 085118 (2009).

[263] G. Del Re, J. Ladik, and G. Biczó. Phys. Rev. **155**, 997 (1967).

[264] J. André, L. Gouverneur, and G. Leroy. Int. J. Quantum Chem. **1**, 427 (1967).

[265] J. André, L. Gouverneur, and G. Leroy. Int. J. Quantum Chem. **1**, 451 (1967).

[266] A. B. Kunz. Phys. Rev. B **6**, 606 (1972).

[267] S. Suhai. Chem. Phys. Lett. **96**, 619 (1983).

[268] S. Hirata, S. Ivanov, I. Grabowski, R. J. Bartlett, K. Burke, and J. D. Talman. J. Chem. Phys. **115**, 1635 (2001).

[269] J. M. Bowman, T. Carrington, and H. D. Meyer. Mol. Phys. **106**, 2145 (2008).

[270] R. B. Gerber, G. M. Chaban, B. Bauer, and Y. Miller. In C. E. Dykstra, G. Frenking, K. S. Kim, and G. E. Scuseria, editors, *Theory and Applications of Computational Chemistry: The First Forty Years*, 165 (Elsevier, Amsterdam, 2005).

[271] J. M. Bowman. Chem. Phys. **308**, 255 (2005).

[272] R. B. Gerber and M. A. Ratner. Adv. Chem. Phys. **70**, 97 (1988).

[273] K. Yagi, S. Hirata, and K. Hirao. J. Chem. Phys. **127**, 034111 (2007).

[274] O. Christiansen. J. Chem. Phys. **120**, 2149 (2004).

[275] P. Seidler and O. Christiansen. J. Chem. Phys. **126**, 204101 (2007).

[276] P. Seidler, M. B. Hansen, and O. Christiansen. J. Chem. Phys. **128**, 154113 (2008).

[277] P. Seidler, E. Matito, and O. Christiansen. J. Chem. Phys. **131**, 034115 (2009).

[278] A. Wierzbicki and J. M. Bowman. J. Chem. Phys. **87**, 2363 (1987).

[279] A. Wierzbicki and J. M. Bowman. Surf. Sci. **191**, 518 (1987).

[280] I. Scivetti, N. Gidopoulos, and J. Kohanoff. Phys. Rev. B **78**, 224108 (2008). Copyright (C) 2010 The American Physical Society; Please report any problems to prola@aps.org.

[281] S. Hirata, M. Keçeli, and K. Yagi. J. Chem. Phys. **133**, 034109 (2010).

[282] N. H. March, W. H. Young, and S. Sampanthar. *The Many-Body Problem in Quantum Mechanics* (Cambridge University Press, Cambridge, 1967).

[283] M. Tasumi and T. Shimanouchi. J. Chem. Phys. **43**, 1245 (1965).

[284] L. Piseri and G. Zerbi. J. Mol. Spectrosc. **26**, 254 (1968).

[285] M. Born and K. Huang. *Dynamical Theory of Crystal Lattices* (Oxford University Press, New York, 1954).

[286] B. J. Braams and J. M. Bowman. Int. Rev. Phys. Chem. **28**, 577 (2009).

[287] D. C. Wallace. *Thermodynamics of Crystals* (Wiley, New York, 1972).

[288] A. A. Maradudin and A. E. Fein. Phys. Rev. **1**, 2589 (1962).

[289] R. A. Cowley. Rep. Prog. Phys. **31**, 123 (1968).

[290] V. Nagalakshmi, V. Lakshminarayana, G. Sumithra, and M. D. Prasad. Chem. Phys. Lett. **217**, 279 (1994).

[291] S. Banik, S. Pal, and M. D. Prasad. J. Chem. Phys. **129**, 134111 (2008).

[292] R. F. Bishop and M. F. Flynn. Phys. Rev. A **38**, 2211 (1988).

[293] R. F. Bishop, M. C. Bosca, and M. F. Flynn. Phys. Rev. A **40**, 3484 (1989).

[294] F. Siebert and P. Hildebrandt. *Vibrational spectroscopy in life science* (Wiley-VCH, 2008).

[295] P. Lasch and J. Kneipp. *Biomedical vibrational spectroscopy* (John Wiley and Sons, 2008).

[296] N. C. Handy. Mol. Phys. **61**, 207 (1987).

[297] B. T. Sutcliffe and J. Tennyson. Int. J. Quantum Chem. **39**, 183 (1991).

[298] A. G. Császár and N. C. Handy. J. Chem. Phys. **102**, 3962 (1995).

[299] D. Toffoli, J. Kongsted, and O. Christiansen. J. Chem. Phys. **127**, 204106 (2007).

[300] S. Manzhos and T. Carrington. J. Chem. Phys. **129**, 224104 (2008).

[301] M. Malshe, R. Narulkar, L. M. Raff, M. Hagan, S. Bukkapatnam, P. M. Agrawal, and R. Komanduri. J. Chem. Phys. **130**, 184102 (2009).

[302] E. Matito, D. Toffoli, and O. Christiansen. J. Chem. Phys. **130**, 134104 (2009).

[303] K. Yagi, K. Hirao, T. Taketsugu, M. W. Schmidt, and M. S. Gordon. J. Chem. Phys. **121**, 1383 (2004).

[304] A. Roitberg, R. Gerber, R. Elber, and M. Ratner. Science **268**, 1319 (1995).

[305] M. B. Hansen, O. Christiansen, D. Toffoli, and J. Kongsted. J. Chem. Phys. **128**, 174106 (2008).

[306] M. B. Hansen, M. Sparta, P. Seidler, D. Toffoli, and O. Christiansen. J. Chem. Theory Comput. **6**, 235 (2010).

[307] S. Hirata. Theoretical Chemistry Accounts: Theory, Computation, and Modeling (Theoretica Chimica Acta) 1–20 (2011).

[308] S. Hirata. Mol. Phys. **108**, 3113 (2010).

[309] M. Keçeli and S. Hirata. J. Chem. Phys. **135**, 134108 (2011).

[310] M. Keçeli. MaVi (2011).

[311] E. Aprà, E. J. Bylaska, W. A. de Jong, M. T. Hackler, S. Hirata, L. Pollack, D. Smith, T. P. Straatsma, T. L. Windus, R. J. Harrison, J. Nieplocha, V. Tipparaju, M. Kumar, E. Brown, G. Cisneros, M. Dupuis, G. I. Fann, H. Fruchtl, J. Garza, K. Hirao, R. Kendall, J. A. Nichols, K. Tsemekhman, M. Valiev, K. Wolinski, J. Anchell, D. Bernholdt, P. Borowski, T. Clark, D. Clerc, H. Dachsel, M. Deegan, K. Dyall, D. Elwood, E. Glendening, M. Gutowski, A. Hess, J. Jaffe, B. Johnson, J. Ju, R. Kobayashi, R. Kutteh, Z. Lin, R. Littlefield, X. Long, B. Meng, T. Nakajima, S. Niu, M. Rosing, G. Sandrone, M. Stave, H. Taylor, G. Thomas, J. van Lenthe, A. Wong, and Z. Zhang. NWChem, a computational chemistry package for parallel computers (2003).

[312] A. Suárez and R. Silbey. J. Chem. Phys. **95**, 9115 (1991).

[313] J. Cao and G. A. Voth. J. Chem. Phys. **102**, 3337 (1995).

[314] N. Makri. J. Phys. Chem. B **103**, 2823 (1999).

[315] O. Sode, M. Keçeli, S. Hirata, and K. Yagi. Int. J. Quantum Chem. **109**, 1928 (2009).

[316] T. Shimazaki and S. Hirata. Int. J. Quantum Chem. **109**, 2953 (2009).

[317] S. Hirata, M. Tobita, T. Shimazaki, R. Podeszwa, M. Tasumi, H. Torii, S. Iwata, M. Head-Gordon, and R. J. Bartlett. POLYMER (2009).

[318] A. Warshel. J. Chem. Phys. **54**, 5324 (1971).

[319] S. Hirata and T. Shimazaki. Phys. Rev. B **80**, 085118 (2009).

[320] M. Keçeli, S. Hirata, and K. Yagi. J. Chem. Phys. **133**, 034110 (2010).

[321] R. G. Brown. J. Chem. Phys. **38**, 221 (1963).

[322] H. Shirakawa and S. Ikeda. Polym. J. (Tokyo) **2**, 231 (1971).

[323] H. Kuzmany. Phys. Status Solidi B **97**, 521 (1980).

[324] H. Takeuchi, T. Arakawa, Y. Furukawa, I. Harada, and H. Shirakawa. J. Mol. Struct. **158**, 179 (1987).

[325] Y. Takahashi. Macromolecules **34**, 7836 (2001).

[326] M. Takahashi, Y. Watanabe, T. Taketsugu, and D. J. Wales. J. Chem. Phys. **123**, 044302 (2005).

[327] S. Suhai. Phys. Rev. B **27**, 3506 (1983).

[328] H. Teramae, T. Yamabe, and A. Imamura. J. Chem. Phys. **81**, 3564 (1984).

[329] S. Carter, J. M. Bowman, and B. J. Braams. Chem. Phys. Lett. **342**, 636 (2001).

[330] S. Carter and N. C. Handy. Mol. Phys. **100**, 681 (2002).

[331] T. Hrenar, H. J. Werner, and G. Rauhut. Phys. Chem. Chem. Phys. **7**, 3123 (2005).

[332] S. Hirata, P. Fan, A. A. Auer, M. Nooijen, and P. Piecuch. J. Chem. Phys. **121**, 12197 (2004).

[333] J. Delhalle, L. Piela, J. Brédas, and J. André. Phys. Rev. B **22**, 6254 (1980).

[334] S. Hirata and S. Iwata. J. Phys. Chem. A **102**, 8426 (1998).

[335] M. Tasumi, T. Shimanouchi, and T. Miyazawa. J. Mol. Spectrosc. **9**, 261 (1962).

[336] M. Tasumi, T. Shimanouchi, and T. Miyazawa. J. Mol. Spectrosc. **11**, 422 (1963).

[337] J. R. Nielsen and R. F. Holland. J. Mol. Spectrosc. **6**, 394 (1961).

[338] D. Bower and W. Maddams. *The Vibrational Spectroscopy of Polymers*. Cambridge Solid State Science Series (Cambridge University Press, Cambridge, 1989).

[339] R. G. Snyder. J. Mol. Spectrosc. **23**, 224 (1967).

[340] R. G. Snyder. J. Mol. Spectrosc. **31**, 464 (1969).

[341] R. G. Snyder, S. L. Hsu, and S. Krimm. Spectrochim. Acta A **34**, 395 (1978).

[342] S. Abbate, G. Zerbi, and S. L. Wunder. J. Phys. Chem. **86**, 3140 (1982).

[343] J. C. W. Chien. *Polyacetylene: Chemistry, Physics, and Material Science* (Academic, Orlando, 1984).

[344] A. J. Heeger, S. Kivelson, J. R. Schrieffer, and W. P. Su. Rev. Mod. Phys. **60**, 781 (1988).

[345] S. Hirata, H. Yoshida, H. Torii, and M. Tasumi. J. Chem. Phys. **103**, 8955 (1995).

[346] S. Hirata and S. Iwata. J. Chem. Phys. **107**, 10075 (1997).